Title
The Context Dependent Function of Transcriptional Regulator Rap1 in Gene silencing and Activation

Author
Bondra, Eliana Rose

Publication Date
2023

Peer reviewed|Thesis/dissertation

The Context Dependent Function of Transcriptional Regulator Rap1 in Gene Silencing and Activation

By

Eliana Rose Bondra

A dissertation submitted in partial satisfaction of the

requirements for the degree of

Doctor of Philosophy

in

Molecular and Cell Biology

in the

Graduate Division

of the

University of California, Berkeley

Committee in charge:

Professor Jasper Rine, Chair
Professor Elçin Ünal
Professor Xavier Darzacq
Professor Kathleen Ryan

Spring 2023

Abstract

The Context Dependent Function of Transcriptional Regulator Rap1 in Gene Silencing and Activation

by

Eliana Rose Bondra

Doctor of Philosophy in Molecular and Cell Biology

University of California, Berkeley

Professor Jasper Rine, Chair

Compaction of the eukaryotic genome into regions of open euchromatin and dense heterochromatin serves as a fundamental regulator of gene expression in cells. In the budding yeast *Saccharomyces cerevisiae*, the Silent information regulator (Sir) protein complex regulates a heterochromatin-like structure at the silent mating type loci, *HML* and *HMR,* and at the telomeres. In addition to the Sir proteins, Repressor activator protein 1 (Rap1) functions in establishing and maintaining silent chromatin at *HML* and *HMR* by binding to nucleation sites known as silencers (silent enhancers) and recruiting silencing machinery. As its name suggests, Rap1 is simultaneously an essential transcription factor that activates hundreds of genes across the genome, including many ribosomal protein genes and the *MATα1* and *α2* genes whose expression determine the mating-type of α cells.

Sequence identity between the mating-type locus *MAT* and the auxiliary *HML* allows a unique opportunity to study the role of Rap1 in both silent and expressed contexts, and how local chromatin state affects function. Chapter two focuses on discerning the context-dependent functions of Rap1. Using ChIP-seq I established that Rap1 accessed its binding site at the promoter of *HML*, even in the silent context. My findings supported and extended the view that pre-initiation complex machinery is unable to act in silent chromatin, thus narrowing the mechanism of silencing to a step between recruitment of the native activator, Rap1, and occlusion of the pre-initiation complex. Surprisingly, Rap1 enrichment at its three binding sites across the silent locus was enhanced by the presence of Sir proteins, despite binding of this transcription factor preceding Sir protein recruitment. As Rap1 was bound in the silent locus but was not functionally recruiting transcription machinery, I tested whether the presence of this enigmatic protein could instead be enhancing silencing. Utilizing a highly sensitive assay that monitors loss-of-silencing events, I established a novel and specific contribution of promoter-bound Rap1, which was previously seen as having potential only for activation,

to silencing. Furthermore, I investigated the mechanism by which Rap1 promotes transcription when acting as an activator and have evidence that it may be aiding in the transition from transcription initiation to elongation.

ChIP offers a static view of protein-DNA interactions rather than a dynamic readout. To assess whether *in vivo* dwell time of Rap1 might contribute to its function as an activator or repressor, I coupled a nuclear depletion strategy with a ChIP-seq time course to measure enrichment at and decay of Rap1 from its binding sites genome wide. The apparent Rap1 dwell time did not differ between silenced *HML* and expressed *MAT*. However, genome-wide Rap1 residence time correlated with transcriptional output and nucleosome positioning. These results point toward a model in which the duality of Rap1 function is mediated by local chromatin environment rather than binding-site availability. I have conducted a number of experiments attempting to pinpoint the mechanism by which Rap1 switches function, following up mainly on post-translational modifications. Some of this work is described in the appendix.

While study of Sir silencing at the *HM* loci has been integral in understanding the establishment and maintenance of heterochromatin in eukaryotes, the effects of these same proteins at telomeres has been less clear. Chapter three focuses on an incomplete set of experiments designed to better understand the functional similarities and differences in Sir-mediated silencing at telomeres and the *HM* loci. Early studies of telomere position effect in yeast led to a hypothesis that distance from telomere dictated the amount of gene repression imparted by Sir proteins in a gradated manner. At the time I began working on the project, there was mounting evidence against this hypothesis. I designed and performed preliminary experiments testing whether silencing was a function of distance from telomere utilizing fluorescent reporters for high throughput analysis. Furthermore, I investigated whether telomere length affected silencing of *HML* and *HMR* by titrating available Sir proteins away from these loci. I also pioneered usage of a novel form of single molecule RNA FISH in our lab and I planned to use this technique to assess whether subtelomeric genes, which are enriched for metabolic function, were spatially co-regulated in response to environmental stimuli.

Table of Contents

List of Figures

List of Tables

Acknowledgments

The journey towards earning my PhD has been transformative and filled with some of the highest highs and lowest lows. I owe many people a great deal of thanks in helping me learn, grow, and succeed as both a scientist and a person over the years.

I must start by thanking my adviser, Jasper Rine, for his perpetual optimism, for his generosity, and for allowing me independence in my project. By entrusting me to succeed on my own, I have learned more, thought more critically, and become a much better scientist. Perhaps most importantly, I am thankful to Jasper for fostering a lab environment that allowed people to be creative and brought together some wonderful scientists.

I also want to thank my committee, Elçin Ünal, Xavier Darzacq, and Kathleen Ryan, for their helpful suggestions and support over the years. I have appreciated knowing that I have three other faculty members with my best interest in mind. I am particularly thankful for their encouragement when I felt my project would never amount to anything.

I truly don't think I would be where I am today had I not had the distinct pleasure of starting my scientific career in Rick Harrison's lab. Rick was immensely generous, even to an undergraduate in his lab; I am honored to be part of his academic legacy. He cared deeply about his trainees and recruited likeminded individuals who served as my direct mentors. I want to thank Erica Larson for being my first scientific mentor - for teaching me to pipette and helping me see that I had a place in research. Findley Ransler Finseth played an integral part in fostering my scientific curiosity and encouraging me to follow a path in academic research. Both women treated me with a level of kindness and respect that I think is rare as an undergrad, and for that I am eternally grateful. They showed me that you could be a great scientist without sacrificing your character and generosity and inspired me to strive to do the same.

Importantly, I would not have ended up in Melissa Harrison's lab without first being in Rick's. On top of vastly expanding my research experience from a technical and educational standpoint, my time in Melissa's lab prepared me for grad school better than I even appreciated at the time. I am lucky and proud to have worked with her. Science almost never works the way we think it will, and the constant failures can be debilitatingly bleak. Melissa instilled in me the idea that we should always celebrate the small victories, because the big ones are few and far between. I am so thankful for the continued support, both personal and professional, that I've received from Melissa over the years. I'd also like to thank Danielle Hamm for being a generous source of guidance and realism over the years. Both Rick and Melissa were proponents of the idea that we should make decisions that better our lives holistically; that there might not be a perfect time for something but that doesn't mean you shouldn't do it. I've tried to hold onto that wisdom, and I think it has informed many of my decisions.

I knew when I was choosing a lab that I was making an important choice about how I was going to spend my time for the next 6 years, both in terms of science and work environment. The Rine lab was a truly wonderful workplace and that was due entirely to the people in the lab. I am extremely lucky to have spent years enjoying being at work because I was laughing so much. Collectively, the Rine lab embodied the idea that you could do good work without sacrificing your happiness. That is not to say they didn't work hard, they absolutely did, but they managed to have and be fun while doing it.

There are a few members in particular of whom I am particularly appreciative. I am forever grateful to my rotation mentor, Ryan Janke, for making me feel valued as a scientist even as a first year. Ryan is endlessly patient and generous, the epitome of a good mentor, game for (and the instigator of) many silly antics, and when he left I and the rest of the lab certainly felt the loss. I also have Ryan to thank for taking me on my first California backpacking trip which sparked a whole set of adventures for me. Katie Sieverman is such a force, and I am lucky to have gotten to know and be friends with her. Katie's steadfastness in her beliefs and standards is inspiring and made a huge impact on how rigorously I think and talk about science. She also has a fantastic sense of humor and continues to make me laugh. On top of being a wonderful cook and great person, Gavin Schlissel is a passionate and impressive scientist. I will never cease to be amazed by the creativity Gavin brings to science, and the seemingly endless stream of ideas he has. Marc Fouet is one of the kindest and most generous people I have met. He is perpetually helpful; our lab would not function without him. I am very grateful to have had his company and optimism, particularly for the last year and a half when the lab has been much emptier. I easily could have given up without him trying to cheer me up and telling me I could do it. I owe a huge thanks to Davis Goodnight. In reflecting on my time in the lab, Davis is the defining character of the Rine lab. He is a hilarious, smart, impressive, and thoughtful person. He is a fantastic scientist and amazing individual; I will always be grateful to have worked with him. Thank you, Davis, for always being willing to answer my questions, even if they were in fact bad questions, and for never making me feel stupid about it. Thank you for always making me laugh, even when I was in the hospital. Thank you for continuing to be a source of scientific and emotional support even after moving away; for taking a zoom call to help me figure out my paper and editing said paper. Thank you for being a wonderful friend. Finally, I am so happy that I was able to recruit Delaney Farris to the Rine lab and am fortunate to have become friends with her. Seeing her, thriving in her own research, at a conference this past year was a joy and made me realize that I will miss being a part of the academic world, if only for the people that science has brought into my life. On top of those mentioned above, being a part of the Rine lab has given me a tremendous wealth of good colleagues and I am thankful to everyone I overlapped with including: Nick Marini, Jean Yan, Katya Yamamoto, Victoria Blake, Daniel Saxton, and Molly Brothers.

The greater MCB community is a special one and has made this journey so much more enjoyable. MCB is full of smart, creative, and caring people who support each other

and enact change for the betterment of the community. The amount of altruistic organizing that graduate students and postdocs do on top of all their research is astonishing. A big thank you to the Follies Committees who convinced me, as someone who has never had team spirit, to buy into the whole thing. And a particularly special thank you to the entering class of 2016; I couldn't have asked for a better cohort and am lucky to have learned from and alongside all of you.

Graduate school would not have been possible without the friends who supported me through it and have become my chosen family. Thank you to Blue House *et al*., Maya Emmons-Bell, Josh Cofsky, Justin Roncaioli, Tess Linden, Perri Callaway, and Arik Shams for seeing me through the best and worst times of grad school. Thank you for being adventure buddies, party planners, movie-night watchers, and incredible sources of support and fun throughout this journey. Thank you to the Emmons-Bell's for welcoming us into your home for Thanksgiving each year. A special thank you to Josh for getting up every day in Spring 2020 to do Insanity™ and, ironically, keeping me from going insane. I have missed them all as they've left, but I am lucky to have these people in my life and so proud to watch them all thrive post-graduation. Thank you to Hayley McCausland for showing me that you *can* make a life outside of MCB, and always being up for whatever hike I find for us to do. Thank you to Shally Margolis for being a constant source of emotional support since the very beginning and an overall terrific friend. Shally brings passion and energy to everything she does. She has encouraged me, commiserated with me, celebrated with me, and been there for me at every step, including many many steps along a ~220 mile long hike through the Sierras. I also must give huge thanks to Helen Vander Wende. Helen is thoughtful, deeply caring, and unapologetically herself. Thank you for being a perpetual source of encouragement, wry humor, and understanding. I am so lucky to call you a friend, and to know that I never have to pretend to be anything I am not in your presence. Finally, thank you to the people who have supported me from afar. Thank you to my sister, Rachel Bondra, for being proud of me when I couldn't be proud of myself. Thank you to Katie White for always checking in on me.

Finally, I owe massive amounts of gratitude to my partner, Paige Diamond. I am indescribably lucky to have Paige in my life. She impresses me every day with what she can accomplish and inspires me to strive to do and be my very best. She is the perfect trip planner, adventure buddy, and co-dog mom. Thank you for showing me the same love when I am at my lowest as when I am thriving. Thank you for bringing so much joy to my life and always trying to make me laugh. Thank you for celebrating the achievements with me and understanding, better than anyone else could, the setbacks. Without your endless encouragement, your patience, your love and support, I would not be the person or scientist that I am today.

Chapter 1:

Introduction to gene silencing and activation as a feature of cell-fate specification

Almost every cell in a eukaryotic organism contains the same genetic material. Despite this fact, there exist a plethora of distinct cell types, each with its own gene expression profile. Recent advances in single-cell RNA sequencing, characterizing unique expression profiles for thousands of individual cells from an adult human, have put estimates of the number of different cell types, each with a dedicated task(s), upwards of 250 and will continue to shed light on novel expression profiles heretofore unappreciated (He *et al.* 2020). Beyond the sheer diversity in functions, it is incredible the degree to which fidelity of expression profiles is maintained among cells of the same type at such a large scale. When there *is* breakdown of this finely tuned system, it often results in disease or cell death.

It is perhaps easiest to imagine different cell types through their diverse functions and physiologies. A dendritic neuron imparts a completely different function, and takes a different form, than a red blood cell. But at the core, they contain the same genetic information – the same DNA. We are indoctrinated with the central dogma early in our educations; that DNA encodes RNA, which in turn is used as the blueprint for proteins. That DNA is the basis for genetic diversity, and yet is effectively the same in every cell, has led to interest in and investigation of how cell-type specific expression patterns are established and maintained for the better part of a century.

1.1 Fine tuning of gene expression patterns gives rise to different and stable cell types

In 1957, Conrad Hal Waddington published his now infamous drawing depicting the process of cell fate and differentiation (**figure 1.1**) (reviewed in Ferrell 2012). In this simple model, a ball starts at the top of a hill that resembles many of the rolling hills that border Berkeley (**figure 1.1**). Further down the hill there are valleys and ridges which create different paths the ball could follow. Each valley is subsequently bifurcated by a ridge, and in this way, we end up with many different paths. Each path leads to a different outcome and, importantly, the slope of the initial hill dictates that the ball cannot roll backwards and change direction. Notably, the idea that the flow of information regarding differentiation goes only one way may be too simplistic. The discovery of critical transcription factors that can induce de-differentiation in somatic cells forces a rethinking of this paradigm (Takahashi and Yamanaka 2006). However, the model presented in Waddington's sketch is a way to think about cell fate and gene expression. If we imagine the top of the hill as the totipotent state of a fertilized embryo, each juncture represents a pruning of the expression profile with multipotent stem cells being higher up on the hill and terminally differentiated states represented at the bottom. In reality, it would be a much hillier and intricate map, but the idea remains sound. To achieve the differentiated states at the bottom of the hill, there must be changes to the gene expression profiles at each node along the way.

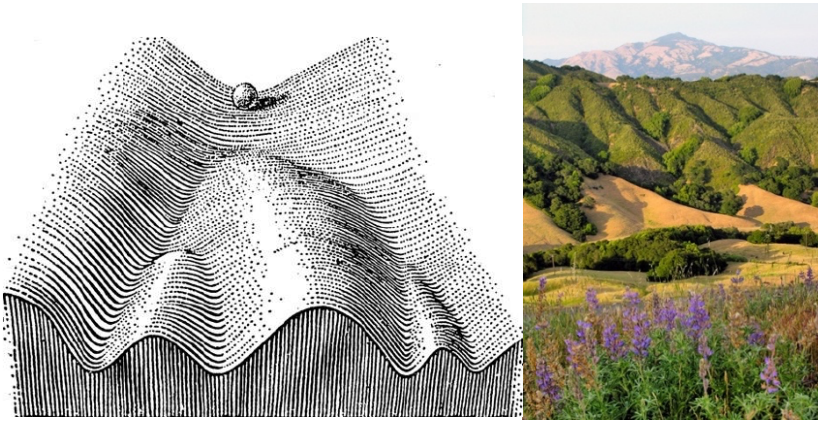

Figure 1.1: Waddington's epigenetic landscape and cell fate determinism. (Left) Waddington's original sketch of the epigenetic landscape. (Right) A picture of the hills east of Berkeley, with many ridges and valleys. Mount Diablo in the background.

Cells utilize many forms of regulation to achieve this daunting diversity of gene expression. One of the most basic in concept of these modes is the compaction of DNA into the nucleus (reviewed in Rando and Winston 2012; Talbert *et al.* 2019; Gaskill and Harrison 2022). Cells are faced with the problem of containing 6 feet of DNA in a 10μm nucleus. The wrapping of DNA around histone octamers is an integral solution to this problem. Compaction of DNA into chromatin also allows for the coarse partitioning of the genome into areas of active, and relatively "open" euchromatin, and more compact, generally silenced heterochromatin. These DNA states were first defined by Emil Heitz in the 1920's and 30's based on cytological evidence that parts of different mitotic chromosomes were more densely stained than others (Passarge 1979; Berger 2019). Even within this general class of regulation, however, there are nuances. There is a distinction between "facultative" heterochromatin, which forms over disparate, sometimes euchromatic chromosomal regions. The most well-studied form of facultative heterochromatin is the inactive X chromosome in mammals, wherein one copy of the X chromosome in females is stochastically silenced in somatic cells (Ohno *et al.* 1959; Lyon 1961; reviewed in Chadwick and Willard 2004). Facultative heterochromatin is often implicated in differentiating developmental lineages, and is also common at the Hox gene clusters (Brown 1966; Endoh *et al.* 2008). The other flavor of heterochromatin is "constitutive". As its name suggests, this mode of regulation is characterized by the omnipresence of the compacted and "off" state over a genomic locus, most often telomeres and pericentric regions (reviewed in Grunstein and Gasser 2013). Common to both types of heterochromatin is the marked absence of acetylation at specific residues of histone tails and the presence of other repressive epigenetic marks. Additionally, heterochromatin is defined by the DNA-protein complexes that form the macromolecular structure comprising these cytologically dense domains (Rando and Winston 2012). The machinery for reading and writing these cues, as well as the proteins that are recruited

by them (i.e. HP1, polycomb group proteins) were likely present in the last common ancestor of metazoans and fungi (Talbert *et al.* 2019). The machinery for RNA interference (RNAi) and DNA methylation, both of which play major roles in heterochromatin-mediated gene repression in diverse organisms, was also present in this ancestral lineage but has been lost in multiple evolutionary clades (Iyer *et al.* 2011; Martienssen and Moazed 2015). Strikingly, many of these programs have been lost in the fungal lineage that gave rise to *Saccharomyces*. In their place, *Saccharomyces* have developed an orthogonal, and functionally analogous, system for silencing genes in a domain-specific, sequence-independent manner.

Tuning the level of transcriptional activation is a fundamental source of gene expression differences. Other, locus specific, forms of gene regulation include *cis*-regulatory sequence elements that act to enhance or repress transcription. These can be in close proximity (promoters and terminators), or at a distance (enhancers and topologically associated domains). The differences between these elements are perhaps less distinct than once thought (reviewed in Andersson and Sandelin 2020). Both regulatory elements are characterized by generally open chromatin structures that exhibit high DNA accessibility and are nucleosome depleted. Promoters inherently have strong core promoter elements that lead to stronger recruitment of RNA Pol II machinery including many transcription factor binding sites per region, and high transcription factor binding coverage of the nucleosome depleted region. Meanwhile, enhancers, which can act at a distance of up to 1Mb from their target promoter element, may have minimal, low promoter activity on their own, with few transcription factor binding sites encoded in the region. Varying in basal activity, promoters and enhancers may work together to increase local concentrations of transcription factors, co-activators, and ultimately RNA pol II, to increase the probability of target gene activation (Andersson and Sandelin 2020).

Much research has gone into understanding the dynamic interactions between enhancers and promoters and identifying these regulatory elements genome-wide. Beyond “promoter bashing” and reporter assays, researchers have characterized the local chromatin landscape surrounding promoters and enhancers to aid in their identification and to better understand their putative functions. These studies have led to the formulation of the “histone code”, a form of epigenetic regulation whose study has gained immense popularity over the last three decades (Jenuwein and Allis 2001). Building on the knowledge that the packaging of DNA into euchromatin and heterochromatin plays important roles in transcriptional regulation, the histone code hypothesizes that transcription is regulated primarily by post-translational modifications to the tails of the histones around which DNA is wrapped. “Readers and writers” of epigenetic marks act to limit or enhance the accessibility of transcription factors and machinery to histone-wrapped DNA. Generally, acetylation of histone tails is associated with regions of active transcription, and thus enzymes that remove these marks (HDACs), and chromatin-associated proteins that would block transcription machinery (HP1, Sir proteins, polycomb group proteins) act negatively on expression (Eissenberg *et al.* 1990; Strahl and Allis 2000; Jenuwein and Allis 2001; Grunstein and Gasser 2013). Conversely, gene activation is associated with histone tail methylation (and sometimes acetylation) by

a myriad of epigenetic writers. These modified tails may lessen the affinity of DNA for histones, thus allowing more labile nucleosome architecture and increasing frequent interactions with transcription machinery. These generalizations bely the massive complexity of the histone code hypothesis but hopefully highlight the myriad of regulatory mechanisms controlling gene expression in eukaryotes.

1.2 Epigenetic regulation of gene expression

More than 150 years after Mendel's studies that laid the foundation of the field of genetics, the field of epigenetics in its modern connotation was born. With the advent and advancement of affordable next-generation sequencing came a whole area of study on genome-wide association screening revealing that the inheritance of most traits are complex and pleiotropic, and that only a small amount of variation in any given trait can be explained entirely by a particular variation in genetic code. Instead, complex traits are often an amalgamation of small effects by each of many genes (reviewed in Kruglyak 2008). In the intervening years, the term "epigenetics" evolved to be used as a catch-all for non-DNA encoded changes to hereditary material (Waddington 2012; Berger 2019). Meaning "above" or "beyond" genetics, Waddington originally coined the term as an appraisal of the causal mechanisms of how genotype informs phenotype, particularly with regards to development rather than heredity. However, the phrase was re-termed to something closer to its current meaning; that cells with the same genotype can exhibit different phenotypes, and that these phenotypes can be triggered by environmental cues, but that the differences in expression may persist indefinitely (Metz 1938; Nanney 1958; Berger *et al.* 2009; Haig 2012). Based on these criteria, the field of epigenetics expanded our views of gene expression and heredity as the "primary genetic material" was not enough to explain all variation in cell type.

Today, the term epigenetics is often used to describe the stable, heritable changes to chromatin that do not involve mutation of DNA itself. By definition, gene silencing is an epigenetic phenomenon; it is heritable and imparts repression on the underlying genes in a sequence-agnostic manner (Rusche *et al.* 2003; Grunstein and Gasser 2013). Generally, current research in this field focuses primarily on DNA methylation and histone modifications. As discussed in the above section, histone modifications may influence the association of certain proteins with chromatin (Phillips 1963; Murray 1964) and these interactions could increase or decrease gene expression *in vitro* (Allfrey *et al.* 1964) and *in vivo* (Clark-Adams *et al.* 1988; Kayne *et al.* 1988; Johnson *et al.* 1990). The semiconservative replication model posits that new and old histones are equally incorporated into the daughter strand in genome replication (Watson and Crick 1953), and much research over many decades has worked to uncover the mechanisms of nucleosome deposition following DNA replication (Jackson and Chalkley 1985; Jackson 1988; Zhang *et al.* 2000; Radman-Livaja *et al.* 2011b; Reverón-Gómez *et al.* 2018). Since epigenetic modifications are inherently not encoded in DNA, many studies have investigated whether nucleosomes themselves could be the carriers of epigenetic information (Audergon *et al.* 2015; Ragunathan *et al.* 2015), including several papers from the Rine lab during my tenure in graduate school (Schlissel and Rine 2019; Saxton and Rine 2019). It appears that assigning a single mode of

transmission to epigenetic inheritance is too elementary and the underlying biology is, as always, more complicated.

1.3 Yeast as a model for heterochromatin

Despite the fact that yeast are single-cell organisms, they maintain 23% of the same genes as humans (Kachroo *et al.* 2015; Liu *et al.* 2017). While it is easier to understand the ways that turning genes on or off in combinatorial ways leads to a diversity of cell types in metazoans, why a single-celled organism would need this mechanism of gene silencing might be less apparent. Although though they do not undergo vast differentiation, yeast display two distinct cell types, the mating types **a** and **α**, which each have their own suite of cell-type specific gene expression (Herskowitz *et al.* 1992). To maintain these programs, *S. cerevisiae* chromosome III encodes not only the mating type information *MATa* or *MATα* but also two auxiliary mating cassettes, *HMLα* and *HMRa* which are constitutively silenced by the Silent information regulator (Sir) proteins (Hicks *et al.* 1979; Rine *et al.* 1979; Rine and Herskowitz 1987). Functionally, these copies of the expressed *MAT* locus exist for yeast to use as templates in homology directed repair when *MAT* is cleaved by the endonuclease *HO* for the end result of switching mating types (Strathern *et al.* 1982; Haber 2012). Additionally, yeast chromosomes are organized in a similar manner to those in metazoans; their telomeres are compacted to protect chromosome ends from degradation and recombination, and are important for nuclear architecture (Taddei and Gasser 2012; Grunstein and Gasser 2013). The silent chromatin in *S. cerevisiae* bears many of the hallmarks of classically defined heterochromatin, such as being gene poor and refractory to *Dam* methyltransferases, yet achieves these features with no contribution from noncoding RNAs in contrast to silencing mechanisms in *S. pombe, D. melanogaster*, and mammals (Gartenberg and Smith, 2016). Thus, this context offers the opportunity to address fundamental questions regarding the mechanism of silencing and epigenetic inheritance with one fewer layers of complexity than other common model organisms used in genetics.

Repression of *HML, HMR,* and the telomeres depends on four silencing proteins, Sir1-4. These genes were identified several times through monitoring defects in mating but were characterized for their role in repressing the silent mating loci through a genetic screen specifically for de-repression of *HML* and *HMR* (Rine and Herskowitz 1987). *SIR2, SIR3,* and *SIR4* were identified as integral to the maintenance of silent chromatin, whereas deletion of *SIR1* resulted in bistable epigenetic states where some portion of the population expressed the *HM* loci while others maintained silencing (Pillus and Rine 1989). How Sir proteins are site-specifically recruited and spread to silence genes in the domain to which they bind has been the area of much research over the past decades and has resulted in a well-established system to study heterochromatin formation and maintenance. In addition to the Sir proteins, important components of silent chromatin include *cis*-regulatory elements termed “silencers” to which site-specific DNA binding proteins, and Sir proteins in turn, are recruited (Abraham *et al.* 1984; Feldman *et al.* 1984). *HML* and *HMR* are flanked by these silencers named E for **e**ssential and I for **i**mportant. The silencer binding proteins are Repressor activator protein 1 (Rap1), ARS-binding

factor 1 (Abf1), and the Origin recognition complex (ORC) and are present in different combinations at all four silencers (Brand *et al.* 1985; Shore *et al.* 1987; Laurenson and Rine 1992; Sjöstrand *et al.* 2002). Silencers act in a position and orientation independent manner and are able to silence genes in some other chromosomal contexts (Mahoney and Broach 1989).

It is well-established that interactions between ORC and Sir1 are the impetus for the establishment of silencing (Bell *et al.* 1993; Foss *et al.* 1993; Fox *et al.* 1997; Gardner *et al.* 1999). Further protein-protein interactions between the C-terminal domain of Rap1 and both Sir3 and Sir4 work to recruit the rest of the complex to the *HM* loci (Shore *et al.* 1987; Moretti *et al.* 1994; Moretti and Shore 2001). Mechanistically, Sir2 is an H4K16 histone deacetylase and the only catalytic subunit of the complex (Imai *et al.* 2000; Landry *et al.* 2000; Smith *et al.* 2000). As Sir2 and Sir4 exist in complex with one another (Moazed *et al.* 1997), interactions between the silencer-binding proteins and Sir4 also leads to the recruitment of Sir2 to the locus. In the establishment of silencing, Sir2 deacetylates nearby histone tails thus creating a higher affinity interaction domain for Sir3, which in turn leads to further recruitment of Sir2/4 and so on and so forth until Sir proteins fully cover the domain (Hecht *et al.* 1995; Carmen *et al.* 2002; Liou *et al.* 2005). At telomeres, Sir proteins are recruited independent of the action of Sir1. Instead, Rap1 bound to the telomerase generated repeats acts as the primary scaffold upon which the silent domain is established (Buchman *et al.* 1988a; b; Lustig *et al.* 1990; Kyrion *et al.* 1993; Moretti *et al.* 1994; Moretti and Shore 2001).

The composition of the silencers is curious for a couple of reasons. First, both Rap1 and Abf1 are essential and prolific transcriptional activators at other loci genome-wide, including some of the most highly transcribed regions of the genome (Shore and Nasmyth 1987a; Mager and Planta 1990; Knight *et al.* 2014; Reja *et al.* 2015; Azad and Tomar 2016). Second, both transcription factors display nucleosome displacement capabilities (Yan *et al.* 2018). Therefore, the silencers are paradoxically nucleosome-depleted regions (a hallmark of active promoters) and comprise transcriptional activators yet act to establish silencing rather than activation. It is this contradiction, in the context of cell-type fidelity, that drew me to studying the dual functions of Rap1.

1.4 Telomeric and subtelomeric silencing

Silent chromatin imparts repression, in an epigenetic and metastable manner, on genes inserted within and adjacent to heterochromatin. The general term for this phenomenon is position-effect variegation (PEV) and was first discovered in *Drosophila melanogaster* (Muller 1930; Eissenberg *et al.* 1990; Reuter and Spierer 1992). The study of PEV in the *Drosophila* eye led to the discovery of two classes of the major readers and writers of epigenetic regulation: suppressors of variegation, *Su(var),* which results in increased silencing, and enhancers of variegation, *E(var)* which antagonize silencing machinery (Elgin and Reuter 2013). At telomeres, this phenomenon it is termed “telomere position effect” (TPE). In addition to their role in nucleating silencing at the silencers that flank *HML* and *HMR,* binding sites for Rap1 and Abf1 are also found at subtleomeric elements and are proposed to dictate the recruitment of Sir proteins to these domains as

well (Lebrun *et al.* 2001; Fourel *et al.* 2002; Rehman *et al.* 2006; Power *et al.* 2011). Relevant telomeric elements include: 1) telomeric repeats, which are tracts of C1-3A repeats approximately 300bp in length to which approximately 25 Rap1 proteins bind; and 2) X-elements, which are further subdivided into Core-X, comprised of ARS consensus sequences (potential ORC binding sites) and Abf1 binding sequences, and Tbf1 binding sites in the form of STARs (subtelomeric anti-silencing regions) (reviewed in Wellinger and Zakian 2012).

Research beginning with Gottschling and colleagues in 1990 asserted that four conserved principles of TPE apply to *S. cerevisiae* telomeric silencing (Gottschling *et al.* 1990; Gottschling 1992). First, heterochromatic proteins, Sir2/3/4 in the case of yeast, are necessary for telomeric silencing (Buchman *et al.* 1988b; Kyrion *et al.* 1993; Moretti *et al.* 1994; Cockell *et al.* 1995; Liu and Lustig 1996; Lustig *et al.* 1996; Moretti and Shore 2001). Second, the strength of silencing is reported to vary as a function of distance from the telomeric repeats. Third, either RNA Pol II- or Pol III-transcribed genes can be silenced, demonstrating that silencing is independent of a specific promoter architecture. And finally, the heritability of the expression state indicates that the effect of silencing on transcription is epigenetic. These experiments were conducted by inserting *URA3* and *ADE2* reporter genes adjacent to an artificially truncated telomere (Aparicio *et al.* 1991; Gottschling 1992; Renauld *et al.* 1993; Rossmann *et al.* 2011; Takahashi *et al.* 2011). Results from these early experiments informed a prevailing model positing strong repression of genes at or very near telomeres, with a decreasing gradient of repression of genes from telomere-proximal to telomere-distal, reflecting variation in the extent of spreading of Sir proteins from telomeres. Further investigation revealed that TPE is varied in strength and occurrence at natural telomeres, calling into question this model (Pryde and Louis 1999; Takahashi *et al.* 2011; Ellahi *et al.* 2015).The mechanism by which subtelomeric silencing occurs and its similarity or difference from constitutive heterochromatin found at loci such as *HML* and *HMR* remains elusive.

While constitutive silencing of the *HM* loci and facultative heterochromatin formation in other contexts makes sense conceptually as a form of expression regulation and cell-type specificity, why subtelomeric genes are silenced may be less clear. The function of telomeres is often described as end-protecting (reviewed in Bonnell *et al.* 2021). Replicative lifespan of cells, in many organisms, is dictated by the length of telomeres. This is due to the end-replication problem, wherein the protruding 3' nature of the ends of linear chromosomes proves difficult to replicate with each cell division. Therefore, as cells continue to divide their telomeres become iteratively shorter. Multicellular eukaryotes exhibit delayed replication forks at telomeres due to their silenced nature (Ivessa *et al.* 2002; Makovets *et al.* 2004; Moser and Nakamura 2009). The heterochromatic formation of telomeres also acts as a barrier to promiscuous recombination and chromosomal rearrangements (Wellinger and Zakian 2012; de Lange 2018). In summary, the heterochromatin at telomeres plays an important structural role that aids in maintaining genome stability by ensuring proper chromosome segregation during mitosis and regulating repeat sequences of transposable elements. Subtelomeric

silencing is a byproduct of this structural role and there is evidence that the genomic architecture associated with these regions, characterizes by being gene poor but the genes that do reside in these domains are enriched for metabolic processes, acts as a bet-hedging mechanism for stochastic gene expression (Brown *et al.* 2010; Andreev *et al.* 2023). Chapter 3 of this dissertation discusses the ways in which I attempted to understand better the role of Sir proteins in *cerevisiae* subtelomeric silencing.

1.5 The mechanism of Sir-based silencing

Study of the nucleation and spread of Sir proteins has served as an integral model for heterochromatin establishment and maintenance. Despite the wealth of knowledge this system has produced, the fundamental question regarding the mechanism of Sir-based silencing has remained inadequately answered. Early studies of the *HM* loci revealed them to be refractory to the endonuclease responsible for cleaving *MAT* and instigating mating-type switching, *HO*, and insensitive to *Dam* methylases and some restriction enzymes (Nasmyth 1982; Singh and Klar 1992; Gottschling 1992; Loo and Rine 1994). Further investigation found evidence of Sir-mediated compaction of chromatin within the silenced domain (Weiss and Simpson 1998; Ravindra *et al.* 1999; Ansari and Gartenberg 1999). More recent, *in vitro* analysis of the system supports this view by quantifying chromatin fiber compaction in the presence and absence of different components of silent chromatin (Swygert *et al.* 2018). In their study, Swygert *et al* found that addition of Sir3 alone stabilizes nucleosomes and occludes DNA linkers from the chromatin array. Furthermore, when the complete Sir2,3,4 complex is added, chromatin is compacted to a nm measurement on par with 30nm fibers (Swygert *et al.* 2018), the secondary structure that serves as the gold standard for chromatin compaction (reviewed in Tremethick 2007; Wu *et al.* 2007). These results combined reinforce a previously proposed model wherein a Sir3-dimer bridges and stabilizes adjacent nucleosomes, while interactions between Sir3 and the Sir2-4 complex drive fiber compaction (Oppikofer *et al.* 2013). Taken together, the finding that silent chromatin is compact and displays reduced sensitivity to certain enzymatic reactions led to the assumption of a Sir-dependent secondary structure at silent loci that acts to sterically occlude activator protein interactions with the underlying promoters, resulting in the inability of RNA Pol II to promote transcription from these loci.

A series of studies on the mechanism of silencing with regard to the occlusion of Pol II machinery resulted in inconclusive and/or contradictory findings. At the time that I began my studies on the mechanism of silencing, two additional models of Sir silencing had been proposed and supported. In Chen and Widom's 2004 paper "Mechanism of transcriptional silencing in yeast", researchers concluded that pre-initiation complex machinery, RNA Pol II, and elongation machinery were occluded from transgenes inserted in silent chromatin. They found, however, that activators of exogenous transgenes inserted in silenced loci were able to access their sequence-specific binding sites in the presence of Sir proteins (Chen and Widom 2005). In addition to the low-resolution techniques used at the time, the minimal study of endogenous silencing at *HML* and *HMR* conducted in this study was obfuscated by two design oversights. These

experiments failed to take into account a secondary, silencing-independent regulation of *HML* occurs by way of the a1/*α2* corepressor formed in cells that expresses both *MATa* and *MATα* at the same time (Siliciano and Tatchell 1986; Herskowitz 1989; Goutte and Johnson 1993). The a1/α2 corepressor targets include the bi-directional promoter in *MATα* and *HMLα.* Prior studies failed to take this repression into account when designing their experiments. Furthermore, sequence identity between *MATα* and *HMLα*, or *MATa* and *HMRa* made it impossible to distinguish protein interactions between each set of the two loci.

A few years later, another study came out with contradictory findings supporting a model where silent chromatin was accessible to Pol II but halted transcription at the transition from initiation to elongation (Gao and Gross 2008). *In vitro* studies on the matter found supporting evidence for both models. Incubation of a Gal4-VP16 template with the Sir complex produced only a modest reduction in transcriptional activation, indicating accessibility of the reporter to RNA Pol II (Johnson *et al.* 2009). The same researchers later proposed that Sir proteins act as a block for transcription elongation (Johnson *et al.* 2013). A few years before I began my doctoral research, another student in the Rine lab took a novel approach to answering the same question. Dave Steakley utilized the insertion of a completely heterologous, T7 prokaryotic promoter at *HMR* to measure the extent of Sir-based silencing (Steakley and Rine 2015). Sir proteins indeed acted as a substantial barrier to transcription, resulting in a 200-fold reduction in gene expression in *SIR4* vs *sir4Δ* cells. However, replacement of the native *HMR* promoter with a Gal4 promoter led to loss of silencing of the locus when induced. All studies prior to my investigation of the mechanism of silencing at *HML* failed to assay the recruitment of the native activator of the locus, Rap1, in silent chromatin. Chapter 2 of this dissertation focuses on the context-dependent function of Rap1 in silencing and activation, and attributes a heretofore unappreciated role for promoter-bound Rap1 in enhancing the silent state.

1.6 Rap1 – a paradox in gene expression regulation

Central to all of the topics discussed above in yeast is Repressor/activator protein (Rap1). This essential, 827 amino acid long non-catalytic protein was first identified as a silencer binding element (denoted in it's former alias silencer binding factor E (SBF-E)) and was quickly discovered to bind the upstream activating sequences (UAS) of *MATα* and ribosomal protein genes (Shore and Nasmyth 1987). The protein comprises an N-terminal BRCT domain, a large, dispensable intrinsically disordered region, a DNA-binding domain, two Myb-type α-helical bundles, and a disordered C-terminal interaction domain (Feldmann and Galletto 2014). Rap1 has many known interaction partners, and it is proposed that these context-specific interactions may dictate the function of Rap1 (Shore and Nasmyth 1987; Cockell *et al.* 1995; Liu and Lustig 1996; Garbett *et al.* 2007; Layer *et al.* 2010; Shi *et al.* 2013). As discussed previously, Rap1 plays critical roles in the establishment of silencing mediated through C-terminal interactions with Sir3 and Sir4. It carries out this role both at the silencers and the telomeres, where it binds telomerase-generated $C_{1\text{-}3}A$ repeats. In mammalian cells, Rap1 conserves its role as a

telomere-binding protein and serves an important function in the DNA damage response (Martinez *et al.* 2010; Irie *et al.* 2019; Bonetti *et al.* 2020; Khattar and Tergaonkar 2020). Recent studies have also shown mammalian Rap1 may function in a diverse set of nontelomeric functions, including regulation of pluripotency through Tip60 (Zhang *et al.* 2019; Barry *et al.* 2022).

The protein-DNA interactions between yeast Rap1 and its various binding sequences display a few peculiarities. First, it has a notable variety of binding sequences genome wide, which are variations on the consensus 13-mer ACACCCRYACAYY (Lieb *et al.* 2001; Piña *et al.* 2003). In an attempt to understand the site-specific role of Rap1 as a recruiter of silencing proteins rather than transcription machinery, a former member of the Rine lab investigated whether the non-consensus, low-affinity Rap1 binding sequence found at *HMR-E* dictated Rap1 function (Teytelman *et al.* 2012). Contrary to initial predictions, swapping the *HMR-E* binding site variant for a consensus binding motif had no effect on the establishment or maintenance of silencing (Teytelman *et al.* 2012). Of additional interest is the finding that Rap1-DNA interactions are particularly long-lived both *in vitro* and *in vivo* studies (Vignais *et al.* 1987; Lieb *et al.* 2001; Lickwar *et al.* 2012; Mivelaz *et al.* 2020). During my time in grad school, multiple studies in our lab were focused on identifying the carrier of epigenetic memory, specifically focusing on nucleosomes. Gavin Schlissel developed a clever assay to track a single (or a few) histones through DNA replication and cell division and found that nucleosomes could in fact remember their position (Schlissel and Rine 2019). Daniel Saxton tested the hypothesis that nucleosomes are the carriers of epigenetic memory by altering the number of nucleosomes in the silenced domain, reasoning that lessening the number of nucleosomes, and thus having fewer opportunities for transmitting the silent state to a daughter cell, would increase the chance that the state were not remembered. This hypothesis was thus largely discounted. Combined, these experiments led me to the notion that there must be some other mode of transmitting epigenetic memory. This idea was the original impetus for investigating Rap1 dwell-time as a differentiator of its function; if Rap1 were maintaining epigenetic memory of silencing, then would expect to see extremely long dwell times when Rap1 was bound to silencers.

Finally, Rap1 was identified early as a “pioneer factor”, a term used to describe a class of proteins that are unique in their ability to access their binding sites in the presence of nucleosomes, thus establishing domains of open chromatin and facilitating binding and recruitment of other transcription factors (Yu and Morse 1999; Mayran and Drouin 2018; Zaret 2020). Only a few proteins in yeast are given the title of pioneer factor: Rap1, Abf1, Reb1, and Cbf1 (Yu and Morse 1999; Yan *et al.* 2018; Donovan *et al.* 2019; Mivelaz *et al.* 2020; Zaret 2020). Curiously, all these proteins are characterized by dual functionality. Rap1, Abf1, and Reb1 have roles in Sir-mediated silencing (Shore *et al.* 1987; Shore and Nasmyth 1987a; Kurtz and Shore 1991; Sussel and Shore 1991; Moretti and Shore 2001; Ellahi and Rine 2016), while Cbf1 is a centromere binding factor that recruits differential cofactors to determine function (Bram and Kornberg 1987; Baker *et al.* 1989; Mellor *et al.* 1990; Moreau *et al.* 2003; Kent *et al.* 2004). Pioneer factors are typically utilized in priming the genome for largescale chromatin-landscape reorganizations associated with

development (reviewed in Zaret 2020; Larson *et al.* 2021). Although yeast do not develop and differentiate in the same way as multicellular eukaryotes, the work represented in Chapter 2 investigates the context-dependent role of Rap1 and speculates about the function of Rap1 in mediating adaptability to environmental stresses through gene expression regulation.

How Rap1 mediates two apparently opposing functions has remained a mystery. Although the putative interaction domains of Rap1 and Sir proteins have been identified, to date it has not been possible to identify clear separation-of-function mutations interfering with activation but not silencing due to Rap1 being essential for viability (Moretti *et al.* 1994; Cockell *et al.* 1995, 1998; Wotton and Shore 1997; Moretti and Shore 2001; Luo *et al.* 2002; Garbett *et al.* 2007; Feeser and Wolberger 2008; Layer *et al.* 2010; Johnson and Weil 2017). Many post-translational modifications to Rap1 have been identified using Mass Spectrometry but have not been characterized further for function (Albuquerque *et al.* 2008; Swaney *et al.* 2013; Lanz *et al.* 2021; Bhagwat *et al.*). There are many examples of so-called master regulators having opposing cellular functions based on post-translational modification. These include the Glucocorticoid receptor, one of the best documented cases of context dependent switch in function for a transcription factor, and the differential phosphorylation of Clr4^{SUV39H} which correlates with a switch in methylation state of H3K9, and thus epigenetic expression state, in *S. pombe* (Jackson and Lopes 1996; Love *et al.* 2017; Weikum *et al.* 2017; Bailey *et al.* 2021; Kuzdere *et al.* 2022). While I was never able to pinpoint an exact residue or set of residues responsible for differential function, I have always favored this hypothesis as a potential explanation for how a single protein bound to the same locus is able to behave so differently. I have outlined a few of the ways I investigated the possibility of post-translational modification mediating Rap1 function in the appendices of this dissertation.

1.7 Contextualizing dual-function transcription factors in gene expression regulation

I began by talking about cell-fate determination and fidelity, and ended by dissecting the intricacies of a single, dual-function transcription factor. I hope that I have laid out this introduction in a way that leads the reader through my thought processes. Driven by curiosity regarding the mechanisms by which epigenetic state is so robustly maintained across cell divisions, I focused my research on a paradoxical protein whose dysfunction would be devastating to the cell. This work highlights the many modes of epigenetic regulatory mechanisms integrated by cells to give rise to a vast spectrum of context-specific and finely tuned gene expression patterns.

Beyond the role of Rap1 in *S. cerevisiae*, these findings have implications, broadly, in eukaryotic regulation of cell-type fidelity across cell divisions. Dual-function transcription factors can be recruited to promoters and, in a context-dependent manner, serve as co-activators or co-repressors to finely tune gene expression, in part through the effects of local concentration of interaction partners. These transcription factors can be involved in pathogenesis (*PR-1, PR-10a* in *Arabidopsis* (Boyle and Després 2010)) or housekeeping function (*Sp3* (Valin and Gill 2007)), but most commonly appear in cell

specification through differential gene expression: Pit1, C/EBPβ, Oct1, Glucocorticoid receptor, and YY1 to name a few (Scully *et al.* 2000; Latchman 2001; Mo *et al.* 2004; Ma 2005; Rosenfeld *et al.* 2006; Boyle and Després 2010). The widespread binding of these proteins to chromatin and their implications in developmental gene expression programming emphasizes the importance of their functional precession. Dysregulation of dual-function transcription factors has broader significance in diseases such as cancer. In conclusion, these findings provide new insights into the mechanisms of gene expression and highlight the importance of considering the context in which transcription factors function.

Chapter 2:

Context dependent function of the transcriptional regulator Rap1 in gene silencing and activation in *Saccharomyces cerevisiae*[1]

2.1 Abstract

In *Saccharomyces cerevisiae,* heterochromatin is formed through interactions between site-specific DNA-binding factors, including the transcriptional activator Rap1, and Sir proteins. Despite a vast understanding of the establishment and maintenance of Sir-silenced chromatin, the mechanism of gene silencing by Sir proteins has remained a mystery. Utilizing high resolution chromatin immunoprecipitation, we found that Rap1, the native activator of the bi-directional *HML*α promoter, bound its recognition sequence in silenced chromatin and, surprisingly, its binding was enhanced by the presence of Sir proteins. In contrast to prior results, various components of transcription machinery were not able to access *HML*α in the silenced state. These findings disproved the long-standing model of indiscriminate steric occlusion by Sir proteins and led to investigation of the transcriptional activator Rap1 in Sir-silenced chromatin. Using a highly sensitive assay that monitors loss-of-silencing events, we identified a novel role for promoter-bound Rap1 in the maintenance of silent chromatin through interactions with the Sir complex. We also found that promoter-bound Rap1 activated *HML*α when in an expressed state, and aided in the transition from transcription initiation to elongation. Highlighting the importance of epigenetic context in transcription factor function, these results point toward a model in which the duality of Rap1 function was mediated by local chromatin environment rather than binding-site availability.

2.2 Significance Statement

The coarse partitioning of the genome into regions of active euchromatin and repressed heterochromatin is an important, and conserved, level gene expression regulation in eukaryotes. Repressor Activator Protein (Rap1) is a transcription factor that promotes the activation of genes when recruited to promoters, and aids in the establishment of heterochromatin through interactions with silencer elements. Here, we investigate the role of Rap1 when bound to a promoter in silent chromatin and dissect the context-specific epigenetic cues that regulate the dual properties of this transcription factor. Together, our data highlight the importance of protein-protein interactions and local chromatin state on transcription factor function.

2.3 Introduction

Cellular identity can be defined by the array of expressed and repressed genes in a cell. Thus, two cells with identical genomes can exhibit vastly different phenotypes. Due

[1] A version of this work is published as: Context dependent function of the transcriptional regulator Rap1 in gene silencing and activation in *Saccharomyces cerevisiae.* Bondra, E.R., Rine, J. *(2023).* https://www.biorxiv.org/content/10.1101/2023.05.08.539937v1

to the wide variety of expression patterns needed for normal development and function, eukaryotic gene expression is controlled by many different processes ranging from gene-specific combinatorial effects of transcription factors to domain-wide compaction or accessibility of chromatin. Further, modifications to chromatin promote differential regulation via both the recruitment and restriction of transcriptional activators and repressors (1). The coarse partitioning of the genome into regions of actively expressed euchromatin and repressed heterochromatin is a characteristic of eukaryotic genomes and a major point of gene expression regulation (2). The stability of cell type is controlled, in large part, by the faithful propagation of cell-type-specific patterns of gene expression over cellular divisions. Breakdown of finely tuned expression programs can lead to aberrant gene expression, disease, or cell death.

In *Saccharomyces cerevisiae*, heterochromatin is controlled by the Silent Information Regulator (Sir) proteins which assemble at the cryptic mating-type loci, *HML* and *HMR,* and the telomeres (3–5). Study of the recruitment and spread of these proteins has been fundamental in understanding the establishment and maintenance of heterochromatin (6). The canonical view of the establishment of silencing posits that Sir proteins are recruited to nucleation sites termed silencers (7–10). The *E* and *I* silencers, negative *cis*-regulatory sequences, flank both *HML* and *HMR* and are the sites from which Sir proteins spread across these loci in a sequence-independent manner. Recent evidence from our laboratory indicates that, in addition to these silencers, the promoter of *HML (HML-p)* acts as an early nucleation site of silencing (11). Common to all three of these early-recruitment loci (*HML-E, HML-I,* and *HML-p)* is the presence of a binding site for Repressor activator protein 1 (Rap1) (8, 10, 12, 13).

Rap1 is best characterized in its role as an essential transcription factor that activates hundreds of genes across the genome including the majority of ribosomal protein genes (14–18). Much of Rap1 research has focused on the activator function of the protein. *In vitro* studies of Rap1 classify it as a “pioneer factor”, a term used to described a class of proteins that are unique in their ability to bind to DNA in the presence of nucleosomes, establish domains of open chromatin, and facilitate binding and recruitment of other transcription factors (18–22). In addition to the Sir proteins, Rap1 functions in establishing and maintaining silent chromatin at *HML, HMR,* and telomeres by binding to silencers and recruiting Sir proteins, in combination with two other silencer-binding proteins, the Origin Recognition Complex (ORC) and the transcription factor ARS-binding factor 1 (Abf1) (23–29). How Rap1 mediates two apparently opposing functions has remained a mystery.

Despite decades of research utilizing Sir silenced chromatin as a model for heterochromatic gene repression, the fundamental question regarding the mechanism of Sir-based silencing has remained inadequately answered. In the most broad-scale model, Sir proteins form a macromolecular complex that blocks, wholesale, protein-DNA interactions in silent chromatin, including transcription factors accessing their cognate binding sites. This model is supported by evidence of expression state-dependent cleavage and modification of enzyme recognition sites in silent or active chromatin (30, 31). A more nuanced version of this mechanism supports specific pre-initiation complex interference by Sir proteins. Here, DNA-binding activators access their binding sites in

Sir-silenced chromatin, but subsequent assembly of a functional pre-initiation complex is somehow hindered (32, 33). Yet other work suggests a downstream-inhibition model whereby silencing acts by prohibiting formation of mature transcripts rather than transcriptional initiation, and is based on results indicating no difference in recruitment of TATA-Binding Protein (TBP) nor RNA Pol II to silent chromatin, but instead a marked absence of elongation factors and mRNA capping machinery (34, 35). Thus, the extent to which transcription machinery is occluded, and the specificity of such blockage, has remained inconclusive.

Sequence identity between the mating-type locus *MAT* and the auxiliary *HML* allows a unique opportunity to study the role of Rap1 in both silent and expressed contexts, and how local chromatin state affects function. The promoters of *MATα* and *HMLα* are identical in sequence and, thus, each contains a Rap1 binding site. Rap1 binding at *MAT* is responsible for activation of *α1* and *α2* (36, 37). The presence of this same promoter binding site at *HML*, which is constitutively silenced, offers an opportunity to test predictions of the various models of silencing. While it is generally understood that Rap1 binding at the silencers *HML-E* and *HML-I* recruits Sir proteins to mediate silencing, the role for Rap1 at the promoter is posited to be an activator (8, 36, 37). To date, it is unclear to what extent Rap1 binds its recognition site in a heterochromatinized context, and whether it contributes to either silencing or activation of the *HML* locus.

Prior studies have been unable to query the endogenous activator at the *HML* due to the difficulty of distinguishing binding at this locus to binding at *MAT*. To better understand the dichotomy of Rap1 function, we utilized endogenous tagging of the protein in combination with high-resolution ChIP-seq and RNA measurements to characterize the contributions of Rap1 to silencing and expression at *HML*. We investigated the *in vivo* residence times of Rap1 to further characterize the interaction between Rap1 and chromatin.

2.4 Results

2.4.1 Rap1 bound to the promoter of *HML* in a silenced state but failed to recruit transcription machinery

Previous studies addressing the mechanism of silencing have yielded contradictory and sometimes paradoxical results, due in part to the low-resolution techniques used at the time (Chen and Widom 2005; Sekinger and Gross 2001; Gao and Gross 2008; Loo and Rine 1994; Steakley and Rine 2015). In studies attempting to characterize the limiting steps of Pol II recruitment to a silenced locus, regions of sequence identity between *MAT* and *HML* and *HMR* have interfered with the unambiguous assignment of recruitment of different factors to the loci (**figure 2.1A**). Moreover, a secondary, silencing-independent regulation of *HML* occurs by way of the a1/α2 corepressor formed in cells that expresses both *MATa* and either *MATα* or *HMLα* at the same time (Siliciano and Tatchell 1986; Herskowitz 1989; Goodnight and Rine 2020). The a1/α2 corepressor targets include the bi-directional promoter in *MATα* and *HMLα.* To ensure unambiguous interpretation of our results regarding recruitment to *HML*, we designed and performed experiments in strains lacking *MATα* and wherein the

α2 coding sequence at *HML* was replaced by the coding sequence for the *Cre* recombinase (*hmlα2Δ::Cre*), thus avoiding these confounding factors. Similarly, to characterize enrichment at *MATα*, we performed experiments in strains lacking both *HML and HMR (hmlΔ hmrΔ).*

We tagged endogenous Rap1 with 3xV5 at the N-terminus in order to retain both its essential activating and repression functions, permitting accurate representation of Rap1 enrichment at *HML* and *MAT* (**figure S2.1.A,B**). Utilizing Chromatin Immuno-precipitation followed by next-generation sequencing (ChIP-seq) we determined that Rap1 was in fact bound to the promoter of *HML* in silenced chromatin (**figure 2.1.B**). Compared to the extent of enrichment at *MATp*, Rap1 was unexpectedly enriched at the silenced locus relative to the unsilenced (**figure 2.1.B**).

Strong enrichment of Rap1 at the *HML* promoter under wild-type conditions was incompatible with the generalized steric-hinderance model and led us to reconsider the remaining hypotheses; either that silencing occurs at some point after the recruitment of trans-activators but before that of RNA Pol II, or silencing blocks elongation, analogous to paused RNA polymerase II in other eukaryotes (Chen and Widom 2005; Sekinger and Gross 2001; Gao and Gross 2008; Loo and Rine 1994; Steakley and Rine 2015). To distinguish between these mechanisms, we endogenously tagged a set of proteins intimately involved in RNA Pol II-dependent transcription: TATA binding protein-Associated Factor 1 (Taf1), RNA Polymerase B 3 (Rpb3), and Elongation Factor 1 (Elf1). As with our tagged Rap1, epitope tags did not affect fitness of cells with the tagged versions as the only form of this protein in the cell (**figure S2.1.A,B**).

TFIID is one of the first factors recruited to transcription initiation sites (Reinberg *et al.* 1998; Levine and Tjian 2003; Hantsche and Cramer 2017). A subunit of TFIID, Taf1, has proposed interactions with Rap1 making it a compelling protein of interest for assessing recruitment of transcription machinery to silent chromatin (Moretti and Shore 2001; Garbett *et al.* 2007). In contrast to previous reports, TFIID showed no enrichment at *HML* in silenced chromatin, but bound to the promoter of the expressed *MAT* locus (**figure 2.1.C**). Given this result, it was therefore unsurprising that neither a major subunit of RNA Pol II, Rpb3, nor the elongation factor Elf1 exhibited any binding to silenced chromatin (**figure 2.1.D, figure S2.1.C**). As an internal positive control, we mapped enrichment of each protein at *MAT* in *hmrΔ hmlΔ* cells, where the recruitment of each followed expected patterns; the initiation factor Taf1 was localized over the promoter, while the RNA Pol II subunit Rpb3 was enriched over the gene bodies (**figure 2.1.C,D**). Furthermore, all three proteins were substantially enriched at *RPS4A,* a ribosomal protein gene that is also a known Rap1 target (**figure 2.1, figure S2.1.C**). These data revealed that Sir-silenced chromatin was not entirely refractory to protein binding, but specifically to RNA pol II transcription machinery. In sum, we found robust recruitment of the endogenous activator to native Sir-silenced *HML* and narrowed the step at which silencing occurs to a point between recruitment of the activator, Rap1, and the formation of the pre-initiation complex.

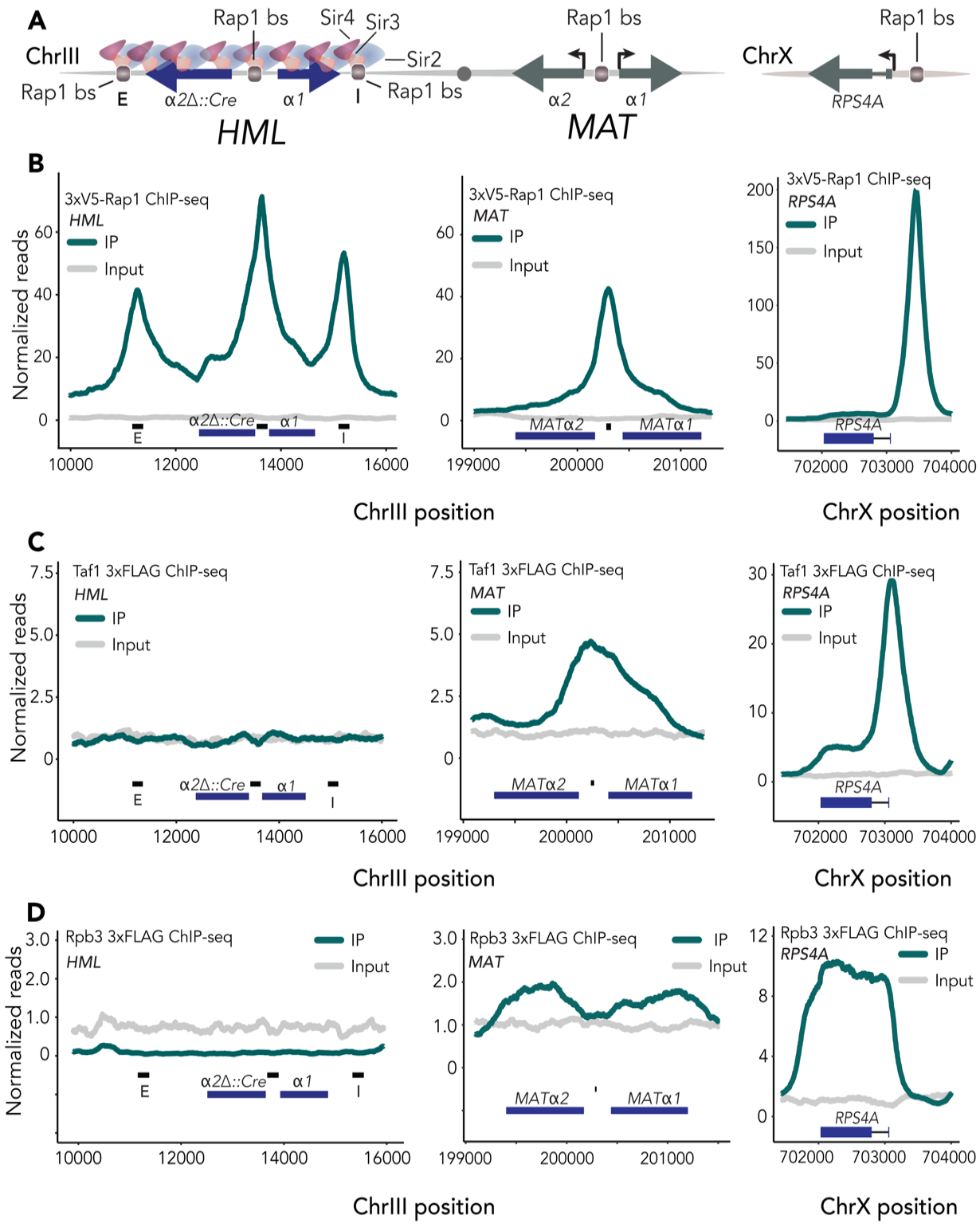

Figure 2.1. Rap1 bound the promoter of *HML* in a silenced state but failed to recruit the pre-initiation complex.

Figure 2.1 (continued from previous page): For all ChIP-seq experiments, read counts were normalized to the non-heterochromatic genome-wide median. IP and input values are plotted on the same scale. IP samples are shown in dark green, input values are in grey. Data shown are the average of two ChIP-seq experiments unless otherwise noted.

(A) Schematic of *HMLα* and *MATα* on chromosome III. Sir proteins keep *HML* transcriptionally silenced. Rap1 binding sites at *HML-E*, *HML-I,* and the promoter of both *HML* and *MAT* are noted.

(B) Left, averaged normalized reads for ChIP-seq in two 3xV5-Rap1 samples at *HML* in *SIR* cells. Black bars represent 200 bp surrounding Rap1 binding sites at *HML-E, HML-p* and *HML-I,* respectively. Middle, same as left but showing *MAT.* Right, same as (left,middle) but at *RPS4A.*

(C) Same as (B) but for Taf1-3xFLAG-KanMX.

(D) Same as (B,C) but for Rpb3-3xFLAG-KanMX.

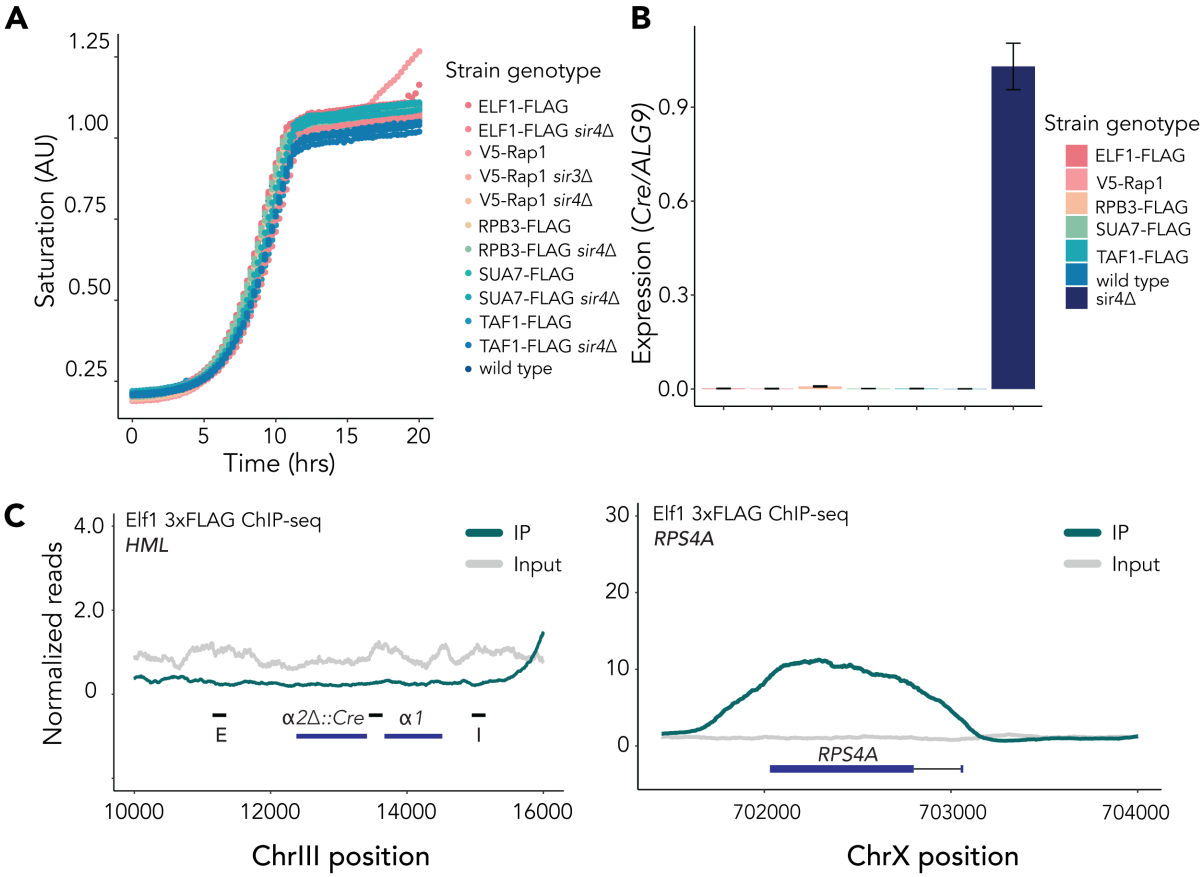

Figure S2.1. Introduction of epitope tags did not affect viability or silencing.

A. Growth curves for representative strains for each of the genotypes listed over 20 hours.

B. RT-qPCR quantification of *Cre* expression at *hmlα2Δ::*Cre in representative strains for each of the genotypes listed, normalized to the control locus *ALG9.*

C. Averaged normalized reads for ChIP-seq of two Taf1-3xFLAG samples at *HML* (left) and *RPS4A* (right) in *SIR* cells. Black bars represent 200 bp surrounding Rap1 binding sites at *HML-E, HML-p* and *HML-I,* respectively. IP samples are shown in dark green, input values are in grey. Coverage for only one sample is plotted for input. IP and input are plotted on the same scale.

2.4.2 Rap1 contributed to the maintenance of silent chromatin at the native *HML* promoter

Given that Rap1 was enriched at the *HML* promoter in silenced chromatin, but TFIID was not, we investigated the possibility that promoter-bound Rap1 somehow contributed to silencing the locus. We generated a strain with a two base-pair mutation in the Rap1 binding site at the promoter which is known to strongly decrease expression of *α1* and *α2* (Siliciano and Tatchell 1986; Giesman *et al.* 1991). Upon mutating GG to TC, we saw significant reduction of Rap1 at its consensus binding sequence within the *HML* promoter (**figure 2.2.A, figure S2.2.C,D**). However, introduction of this binding site mutation did not affect enrichment of Rap1 at other loci genome-wide **(figure S2.2.A**).

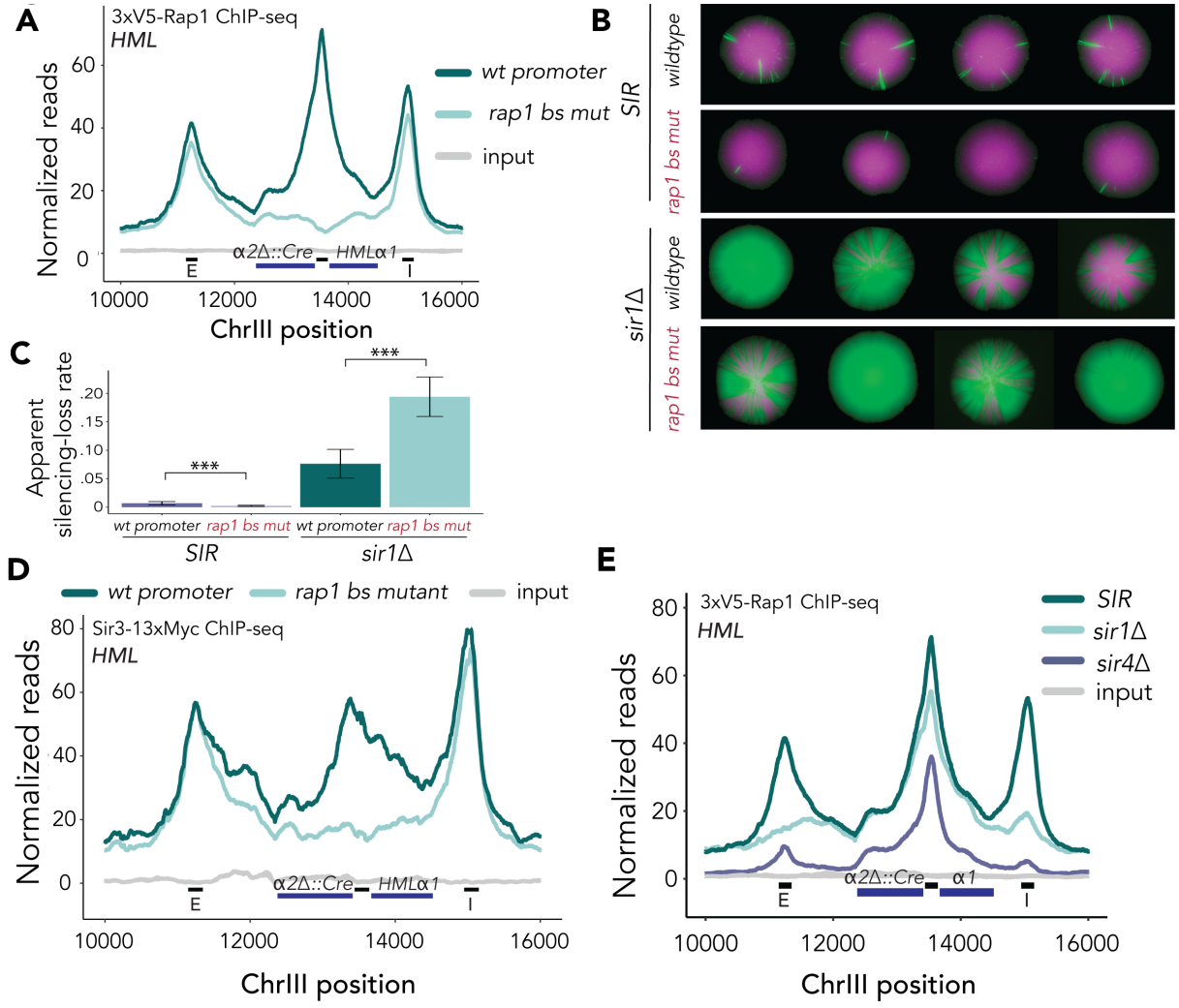

Figure 2.2. Rap1 contributes to the maintenance of silent chromatin at the native *HML* promoter

Unless otherwise stated, ChIP-seq data represented averaged reads of two biological replicates over the locus, normalized as in figure 2.1. Black bars along x-axis represent 200 bp surrounding Rap1 binding sites at *HML-E, HML-p,* and *HML-I,* respectively. IP and input values are plotted on the same scale.

Figure 2.2 *(continued from previous page)*

(A) Normalized reads mapped to *HML* in two 3xV5-Rap1 ChIP-seq experiments for wild-type and mutant Rap1 binding motif at the promoter.
(B) Representative CRASH colonies for *SIR* and sir1Δ cells with wild-type and mutant Rap1 binding site at *HML-p*.
(C) Apparent silencing-loss rate for genotypes described in (B) ± SD. The following number of events was recorded for each sample: *SIR* wt promoter (n = 271933); *SIR* rap1 bs mutant (n = 773105); *sir1Δ* wt promoter (n = 151846); *sir1Δ* rap1 bs mutant (n = 90211). p-values (p<2.2e-16) for both comparisons were calculated using a two-sided t-test.
(D) Normalized ChIP-seq reads for Sir3-13xMyc mapped to *HML* for wild-type and mutant Rap1 binding motif at the promoter.
(E) Normalized ChIP-seq reads for 3xV5-Rap1 mapped to *HML* in *sir1Δ, sir4Δ* and *SIR* cells.

To evaluate the impact of the Rap1 binding site mutation (rap1 bs mutant) on silencing of *HML*, we introduced the two base-pair mutation into a previously developed strain that allows sensitive monitoring of loss-of-silencing events (Dodson and Rine 2015). This assay, Cre-Reported Altered States of Heterochromatin (CRASH), allows for highly sensitive measurements of loss of silencing events by expression of *HMLα2Δ::Cre* and a subsequent recombination event that results in a unidirectional switch from red fluorescence to green fluorescence (**figure 2.2.B** *top panel*, **figure S2.2.B**) (Dodson and Rine 2015). Silencing is a robust process which fails approximately once in every 1000 cell divisions (Thurtle and Rine 2014; Dodson and Rine 2015). To increase the level of expression to a measurable amount and broaden the dynamic range, we deleted the *SIR1* gene (*sir1Δ)* in a strain with the rap1 bs mutation and the CRASH background. *sir1Δ* cells exist in a bimodal state of expression at *HML* (Pillus and Rine 1989). Recent evidence from our lab has shown that even silenced *sir1Δ* cells exhibit reduced binding of all other Sir proteins across the locus (Saxton and Rine 2022). These cells therefore represent a weakened heterochromatic domain. Interestingly, mutation of the Rap1 binding site at the *HML*-promoter in *sir1Δ* cells did not show reduced sectoring (**figure 2.2.B**, bottom panel). We utilized flow cytometry to quantify the sensitive changes to the silenced domain observed with the CRASH assay (Janke et al. 2018). The loss rates from flow cytometry experiments mirrored the results seen in colonies of Sir^+ cell with and without the rap1 bs mutant promoter (**figure 2.2.B,C**). Surprisingly, in *sir1Δ* cells the apparent silencing-loss rate was higher in rap1 bs mutant cells than in those with the wild-type promoter (**figure 2.2.C**). This indicated that promoter-bound Rap1 contributed to silencing *per se* at *HML*. Notably, this result likely underestimated the contribution of Rap1 to silencing, because the rap1bs mutation would also be expected to reduce expression of the *Cre* gene from the *HMLα2* promoter.

Given that Rap1 binding to the promoter at *HML* intrinsically enhanced silencing, we hypothesized that Rap1 may contribute to silencing through enhancing the stability of silent chromatin. To assess this, we performed ChIP-seq of a Myc-tagged allele of Sir3 as a proxy for enrichment of the Sir complex across the locus. Congruous with our finding that apparent silencing-loss rate was higher in the weakened Sir state of *sir1Δ* cells, Sir3 occupancy was reduced in rap1 bs mutant cells (**figure 2.2.D**). This reduction was particularly striking over the promoter, showing an approximate 3-fold reduction in Sir3 occupancy at this locus. In contrast, Sir3 enrichment at *HML-E* and *HML-I* was unaffected.

Although Sir3 enrichment was reduced by deletion of the Rap1 binding site, measurements in Sir-competent cells by both CRASH (**figure 2.2.B**) and RT-qPCR (**figure 2.3.A**) revealed that cells were able to maintain silencing. This further supported a model in which interactions between Sir proteins and Rap1 cooperate to form and maintain silenced chromatin.

Cooperativity between Sir proteins and Rap1 would predict that, similarly to the diminished enrichment of Sir3 in rap1 bs mutant cells, enrichment of Rap1 at the promoter may be decreased by the absence of Sir proteins. To test this, we performed Rap1 ChIP-seq in *sir4Δ* cells, in which the Sir complex is absent from the *HM* loci (**figure 2.2.E**). Rap1 enrichment at the *HML* promoter in silenced cells (*SIR)* was found to be significantly greater than that in unsilenced *(sir4Δ)* cells (**figure 2.2.E, figure S2.2.D,H**; Student's t-test p = 0.024). We also found a substantial decrease in Rap1 occupancy at the silencers *HML-E* and *HML-I* despite sequence-specific recruitment of Rap1 to these loci preceding Sir protein recruitment in canonical models for the establishment of silencing **(figure 2.2.E, figure S2.2.D**). Rap1 enrichment at *HMR-E,* which has a Rap1 binding site important for silencing, was reduced by a similar amount in the absence of Sir proteins (**figure S2.2G**). As an independent test of whether diminished occupancy of Rap1 at *HML* in *sir4Δ* cells was due to a disruption of the interaction between Sir4 and the C-terminal domain of Rap1, we performed ChIP-seq in *sir3Δ* cells as well and found the results to be nearly identical (**figure S2.2.E,F**). The reduction in Rap1 occupancy in the absence of Sir3 was evident at the *HML-E* and *HML-I* silencers (**figure S2.2.E,F**). Again, as an internal positive control, Rap1 enrichment at *MATα* was found to be similar to that at unsilenced *HML* and less than the enrichment at HML in silenced chromatin (**figure 2.1.B, figure 2.2.E, figure S2.2.H**). As expected, Rap1 binding at *MATa* did not vary based on the availability of the Sir complex (**figure S2.2.G**).

To expand upon the finding that Rap1 enrichment varied with local availability of Sir proteins, we performed ChIP-seq of Rap1 in *sir1Δ* cells (**figure 2.2.E**), acknowledging that the ratio of cells with silenced or expressed *HML* loci differ between cultures. In this setting, *sir1Δ* cells represent a context in which Sir-silenced chromatin is weakened. Rap1 was enriched to an intermediate level at *HML-p* in these cells (**figure 2.2.E**). Furthermore, we found a relative decrease in Rap1 at the silencers at the silencers where Sir1 is known to play a critical role in silencing establishment and has a direct effect (**figure 2.2.E**) (Shore and Nasmyth 1987b; Buchman *et al.* 1988a; Laurenson and Rine 1992; Loo and Rine 1994; Hoppe *et al.* 2002). Collectively, these data inferred that cooperative interactions existed between Sir proteins and Rap1 (**figure 2.1.B, figure 2.2.E**). Taken together these findings established a novel and specific contribution of promoter-bound Rap1 to silencing, where it was previously thought to have potential only for activation.

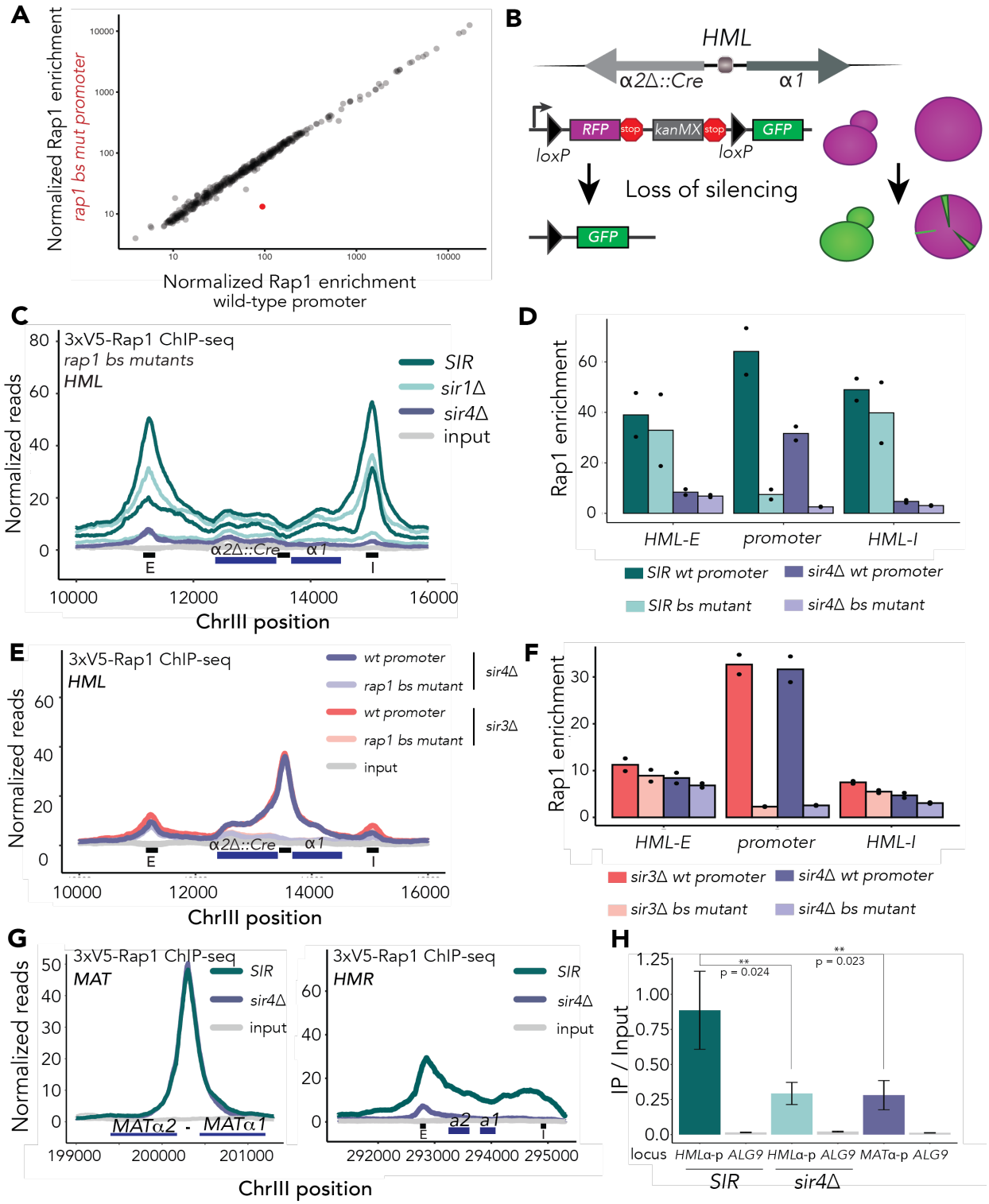

Figure S2.2 Supporting information for Rap1's role in strengthening silencing.

A. Normalized Rap1 ChIP signal for top 500 peaks as defined by MACS in cells with or without the rap1 bs mutation at *HMLp*. Plotted values represent the average of two biological replicates. The peak corresponding to *HMLp* is shaded in red and is the most significantly different between the two.

Figure S2.2 *(continued from previous page)*

B. CRASH assay experimental design. In this strain, *HMLα2* is replaced with Cre recombinase (*hmlα2Δ::*Cre). A cassette in which an *RFP* and a selectable marker are flanked by loxP sites and driven by the strong *TDH3* promoter resides at the unrelated *URA3* locus. Downstream of loxP-RFP-kanMX-loxP is GFP with no promoter. Upon loss of silencing at *HML*, *Cre* expression induces an irreversible switch from RFP-kanMX expression to GFP expression (**figure S2.2.B**). In a colony, GFP-positive sectors represent a loss-of-silencing event that was enough to allow expression of even one Cre transcript in the cell at the vertex of the sector, with the subsequent progeny represented in the growth outwards.
C. Normalized reads mapped to *HML* in two 3xV5-Rap1 in *sir1Δ* (light green), *sir4Δ* (purple) and *SIR* (dark green) ChIP-seq experiments. All strains harbor the two base-pair change in the Rap1 binding motif at the promoter (rap1 bs mut). Light grey represents input samples. Black bars along x-axis represent 200 bp surrounding Rap1 binding sites at *HML-E, HML-p,* and *HML-I,* respectively. IP and input values are plotted on the same scale.
D. Quantification of Rap1 enrichment from figure 2A and 2E over each of the three black bars representing *HML-E, HML-I,* and *HML-P.* Black dots represent individual replicates with the mean shown as colored bars.
E. Normalized reads mapped to *HML* in 3xV5-Rap1 ChIP-seq experiments. *sir4Δ* wild-type *HMLp* and rap1 bs mutant *HMLp* cells are in dark and light purple, respectively. *sir3Δ* wild-type *HMLp* and rap1 bs mutant *HMLp* cells are in dark and light pink, respectively. Light grey represents input samples. Each plot is the average of two biological replicates. Light grey represents input samples. Black bars along x-axis represent 200 bp surrounding Rap1 binding sites at *HML-E, HML-p,* and *HML-I,* respectively. IP and input values are plotted on the same scale.
F. Quantification of Rap1 enrichment from (E) over each of the three black bars representing *HML-E, HML-I,* and *HML-P.* Black dots represent individual replicates with the mean shown as colored bars.
G. (Left) Normalized reads mapped to *MAT* in two 3xV5-Rap1 ChIP-seq experiments, averaged. (Right) Normalized reads mapped to *HMR* in two 3xV5-Rap1 ChIP-seq experiments, averaged. Dark green lines represent *SIR* cells. Dark purple lines represent *sir4Δ* cells. Grey lines represent input samples. The Rap1 binding site at the bidirectional promoter is represented by a black line on the x-axis (left). Black bars along x-axis represent 200 bp surrounding *HMR-E, HMR-p,* and *HMR-I,* respectively IP and input values are plotted on the same scale.
H. ChIP-qPCR of 3xV5-Rap1 IP / Input enrichment at the *HML*α-promoter in *SIR* and *sir4Δ,* and at the *MAT*α promoter, and each at a negative control locus *ALG9.* N = 3; Unpaired t-test p = 0.024 between *HML*α-promoter in *SIR* and *sir4Δ;* p = 0.023 between *HML*α-promoter and *MAT*α promoter.

2.4.3 Promoter-bound Rap1 activated transcription of unsilenced *α2* and aided the transition from initiation to elongation at unsilenced *HML*.

Rap1 is required for normal transcription of *α2* and *α1* at *MAT* (Giesman *et al.* 1991). Therefore, by abrogating Rap1 enrichment at the cognate *HML* promoter site we presumably disrupted expression of the locus to some degree. To assess the extent to which Rap1 at the *HML* promoter had the potential to also serve as a transcriptional activator at this site, we performed reverse-transcription quantitative polymerase chain reaction (RT-qPCR) to measure mRNA expression from the *HMLα* locus in Sir+ and Sir- cells. Expression of *HMLα* was nearly undetectable in *SIR+* cells. However, in *sir4*Δ cells, which have no Sir protein recruitment to the locus, expression of *α2* from *HML* was

comparable to its expression from *MAT* (**figure 2.3.A**). In contrast, we saw an approximate 5-fold reduction in *HMLα2* expression in rap1 bs mutant cells as compared to wild-type *HML-p,* which was comparable to the reduction caused by the same binding site mutation at *MAT* (**figure 2.3.A**). This result was consistent with our finding that rap1 bs mutant cells have lower rates of sectoring than their wild-type promoter counterparts in the CRASH assay (**figure 2.2.B**, second panel). Since the CRASH assay relies on the transcription of *HMLα2Δ::Cre* for excision of the RFP cassette, the reduction in sectoring tracked with reduced transcription. These data confirmed previous work on the role of Rap1 at *MAT* (Siliciano and Tatchell 1986; Giesman *et al.* 1991), and extended those conclusions by establishing that Rap1 contributes significantly and equivalently to expression of the alpha genes at both the unsilenced *HML* and native *MAT* loci (**figure 2.3.A**).

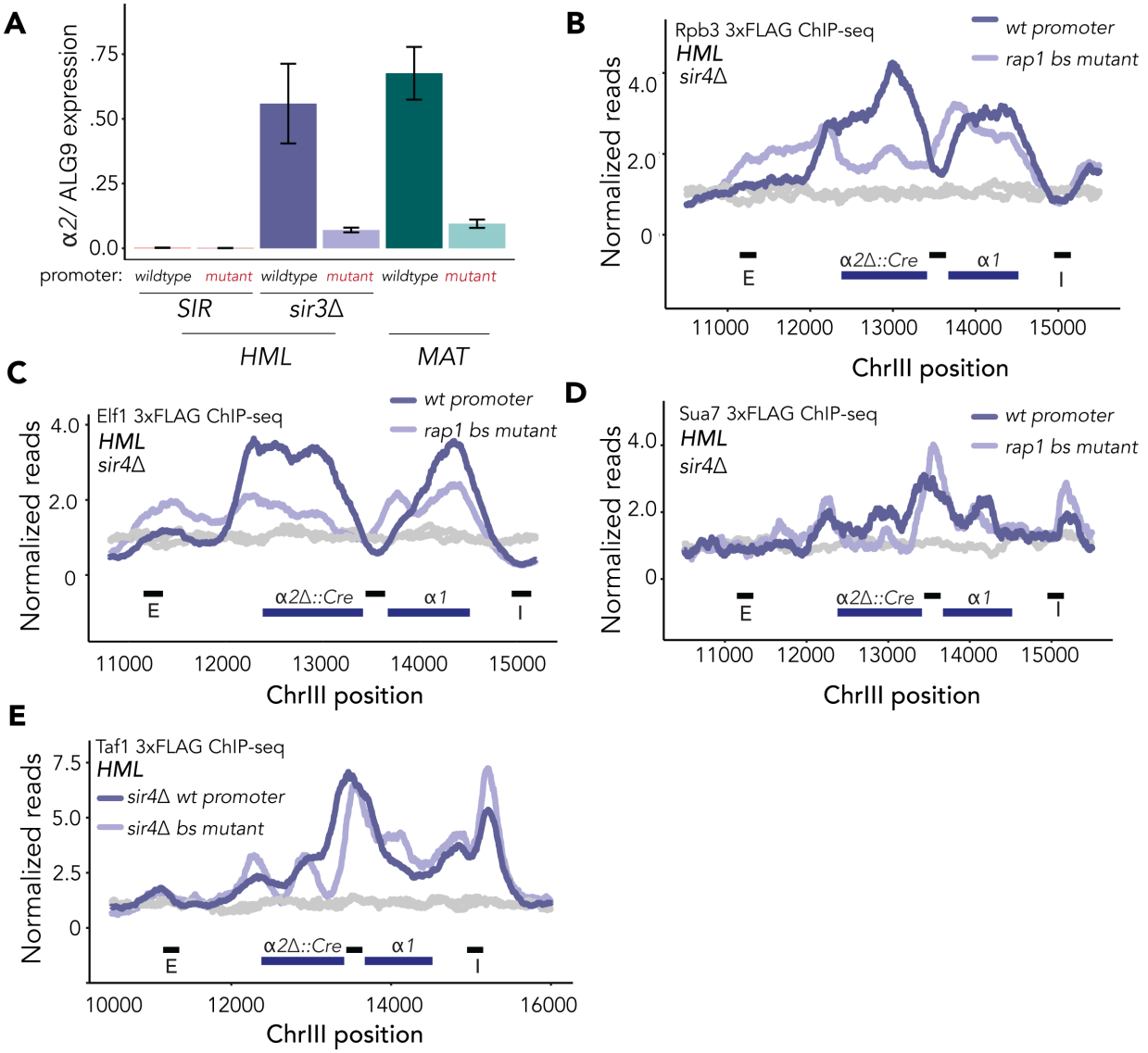

Figure 2.3. Promoter-bound Rap1 activated transcription of unsilenced *α2* and aided the transition from initiation to elongation at unsilenced *HML*.

Figure 2.3 *(continued from previous page)*

For all ChIP-seq experiments, read counts were normalized to the non-heterochromatic genome-wide median. IP and input values are plotted on the same scale. Data shown are the average of two ChIP-seq experiments, unless otherwise noted.

(A) RT-qPCR quantification of *α2* expression at *HML* and *MAT* normalized to control locus *ALG9*. Each plot consists of an average of 2 biological replicates with 3 technical replicates for each. Error bars represent ± SD.

(B) Normalized reads for ChIP-seq of Rpb3-3xFLAG at *HML* in *sir4Δ* cells.

(C) Same as (B) but for Elf1-3xFLAG-KanMX.

(D) Same as (B,C) but for Sua7-3xFLAG-KanMX. This dataset is from only one sample.

(E) Same as (B,C) but for Taf1-3xFLAG-KanMX.

To understand which step of transcription Rap1 contributed to the most, we performed ChIP-seq of tagged proteins in *sir4Δ* cells with and without the rap1 bs mutation at the promoter. As predicted by the decrease in gene expression (**figure 2.3.A**), enrichment of major Pol II subunit Rpb3 and elongation factor Elf1 over the gene bodies of *HMLα2* and *α1* was decreased (**figure 2.3.B,C**). We noted, however, a non-canonical binding pattern of these proteins over the bi-directional promoter. Rather than exhibiting the same decreased occupancy as the coding sequence, Elf1 and Rpb3 were enriched at the promoter in rap1 bs mutant cells relative to their wild-type counterparts (**figure 2.3.B,C**). This pattern is indicative of a failure in promoter escape, or the transition to productive elongation (Fujiwara *et al.* 2019). Furthermore, we found enrichment of TFIIB subunit Suppressor of AUG 7 (Sua7) over the promoter in rap1 bs mutant cells relative to wild type cells (**figure 2.3.D**). TFIIB typically dissociates from the promoter at the initiation stage and does not travel with RNA Pol II as it transcribes (Deng and Roberts 2007). Together these findings demonstrated a role for Rap1 in promoter escape of actively transcribed genes.

2.4.4. *In vivo* Rap1 residence time did not correlate with differences in function at *HML* and *MAT*

ChIP-seq offers a static view of protein-DNA interactions across the genome. In light of recent focus on protein dynamics as a critical lens through which to study transcription, we hypothesized that the dynamics of Rap1–DNA interactions may vary between heterochromatin and euchromatin, due to the distinct compositions of the two structures. To test this hypothesis, we utilized the rapid nuclear depletion strategy afforded by the anchor-away technique to remove unbound Rap1 from the nucleus (**figure S2.3.A**) (Haruki *et al.* 2008). To induce Rap1 depletion, we generated a strain harboring the necessary protein tag components to take advantage of the large flux of ribosomal proteins across the nuclear membrane during their assembly and thus deplete the target from the nucleus (**figure S2.3.A**) (Haruki *et al.* 2008). Due to the nature of the anchor-away experiment, wherein Rap1 was depleted over time, it was important to include a spike-in control for downstream analysis of the ChIP-seq data. We used cells from the closely related species *Saccharomyces paradoxus* which allowed unique mapping of sequences from each species (Vale-Silva *et al.* 2019; Ono and Greig 2020).

Normalizing to number of reads in each sample assigned to *S. paradoxus,* we fit ChIP-seq enrichment data to a non-linear regression model as described by the DIVORSEQ method (de Jonge *et al.* 2020). This allowed us to calculate the apparent k_{off} for each peak, and thus a proxy for the *in vivo* residence time **(figure S2.3.A**). We characterized the fits and apparent residence times for 377 Rap1-bound loci across the genome, in replicate, at which Rap1 binding decayed over time (**figure S2.3.B-G**).

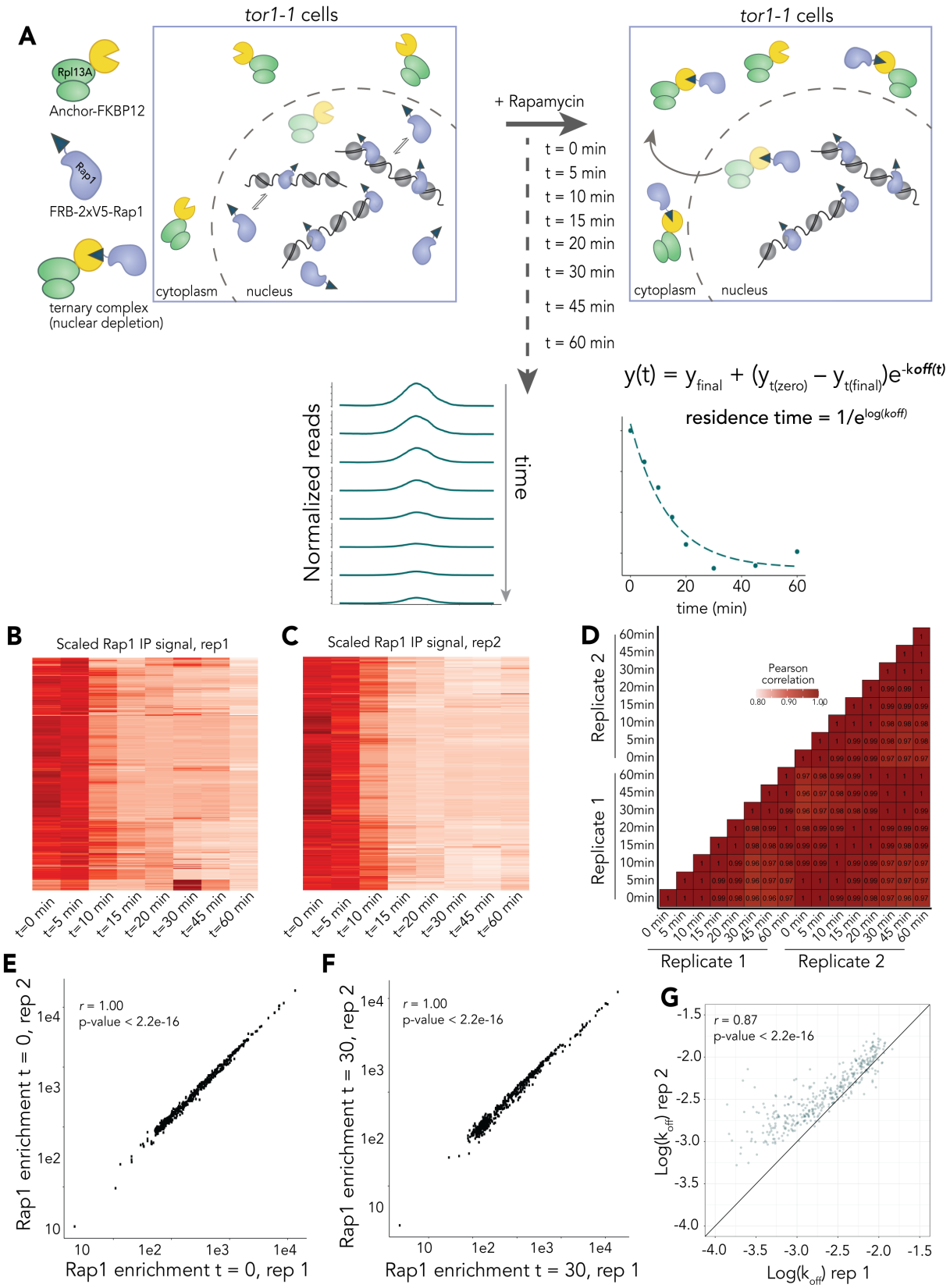

Figure S2.3. Design and validation of Rap1 anchor away experiment in biological duplicates.

Figure S2.3. *(continued from previous page)*

A. Experimental setup for Anchor Away. A strain harboring a 2xV5-FRB (FK506 binding protein–rapamycin binding domain) tag at amino-acid 134 in the N-terminus of the protein and the requisite RPL13a-FKBP12 fusion protein, to which rapamycin binds and establishes an interaction surface for the FRB domain, was constructed. Normalized peaks were fit to a non-linear regression model and the k-off rate was extracted.
B. Clustered heatmaps of normalized peak coverage over the Anchor Away time-course for biological replicate 1.
C. Same as (B) but for biological replicate 2.
D. Pearson correlation coefficients, scaled by color, for each pairwise comparison of each time point in two biological replicates.
E. Correlation between Rap1 enrichment at time = 0 (DMSO) in replicate 1 on x-axis, and Rap1 enrichment at time = 0 in replicate 2 on y-axis. Pearson correlation $r = 1.00$, p-value < 2.2e-16.
F. Same as (E) but for timepoint t = 30 minutes after addition of rapamycin. Pearson correlation $r = 1.00$, p-value < 2.2e-16.
G. Correlation between the calculated $\log(k_{off})$ values for all 377 analyzed peaks for biological replicate 1 on x-axis and replicate 2 on y-axis. Pearson correlation $r = 0.87$.

As previously discussed, the sequence identity between genes at *HML* and *MAT* has obscured analysis of both loci from a single cell. We therefore introduced a series of synonymous single nucleotide polymorphisms to *HML* to allow unambiguous assignment of high-throughput sequencing reads to either *MAT* or *HML* (**figure 2.4.A**), similar to Goodnight and Rine 2020. The residence time of Rap1 at the promoter in silent (*HML)* and active *(MAT)* chromatin was similar, although initial Rap1 enrichment was decreased at *MAT* as seen previously (**figure 2.4.B**). The dwell-time of Rap1 bound to silencers was also similar (**figure 2.4.C,D**). These results indicated that the dual functions of Rap1 could not be attributed to differences in dynamics, but rather resulted from local chromatin contexts and possibly other protein-protein interactions.

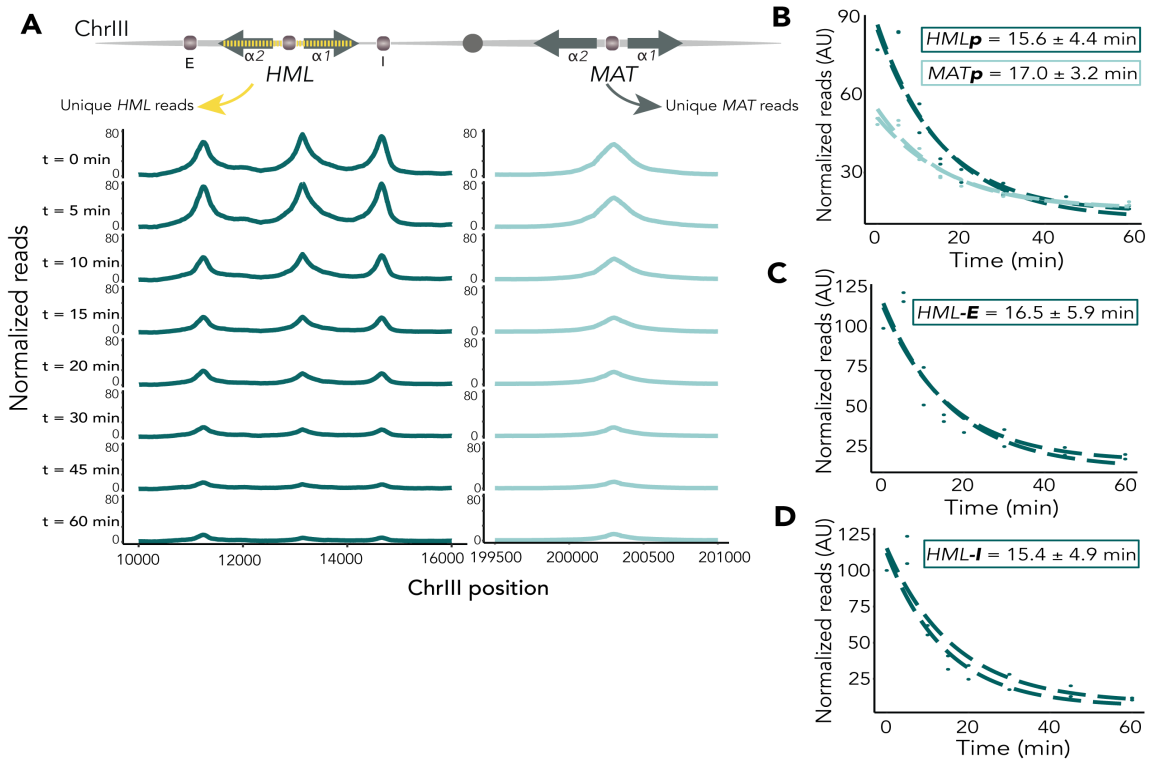

Figure 2.4: *In vivo* Rap1 residence time did not reflect differences in chromatin state
Decay of Rap1 occupancy at *HML* and *MAT* by anchor away

(A) Top, schematic of introduction of SNPs to enable unique mapping of *HML* and *MAT* in a strain that contains both. Below, Rap1 enrichment by two, averaged ChIP-seq experiments at *HML* (left) and *MAT* (right) over time-course, plotted on the same y-axes.

(B) Fitted non-linear regressions for residence times of *HML-p* and *MAT-p.* Each replicate is shown separately. ± SE of average residence time

(C) Fitted non-linear regressions for residence times of *HML-E* as in (B).

(D) Fitted non-linear regressions for residence times of *HML-I* as in (B), (C).

2.4.5 Genome-wide analysis of *in vivo* Rap1 apparent residence times

As chromatin state did not appear to contribute to differences in Rap1 apparent off-rate, we tested whether other context-specific cues contributed to this metric. We defined 1118 regions of Rap1 occupancy genome-wide (**figure S2.4.A**). Using cutoffs similar to those previously described (de Jonge *et al.* 2020), we refined this set and ultimately measured Rap1 off-rate at 377 Rap1 binding sites genome-wide (**figure 2.5.A, figure S2.4**). To assess the contribution of Rap1 apparent dwell-time to function in transcriptional regulation, we selected Rap1 enrichment peaks that were within 500 bp upstream of open reading frame and assigned peaks to these respective genes. This dataset was then subdivided into quartiles based on residence time: shortest (n = 95), short (n = 95), long (n = 93), longest (n = 94). Of note, 42 of the 96 subtelomeric peaks (defined as located within 15 kb from the ends of telomeres) displayed poor fits due to a lack of decay over time (**figure S2.4.C**). These peaks were almost exclusively the Rap1-bound loci at the most telomere-proximal positions, or within 500 bp of the ends of

chromosomes. Conversely, subtelomeric peaks that ranged from 500 bp – 15 kb from the ends of telomeres exhibited shorter dwell-times relative to telomeric regions, though, ultimately, dwell-time did not correlate with distance from chromosome end (**figure S2.4.E,F**). These findings underscored a difference in dynamics between Rap1 bound at the very ends of chromosomes, which presumably functions as a structural element in telomere end-protection, and Rap1 bound at subtelomeric loci, which may be involved in heterochromatin-mediated silencing.

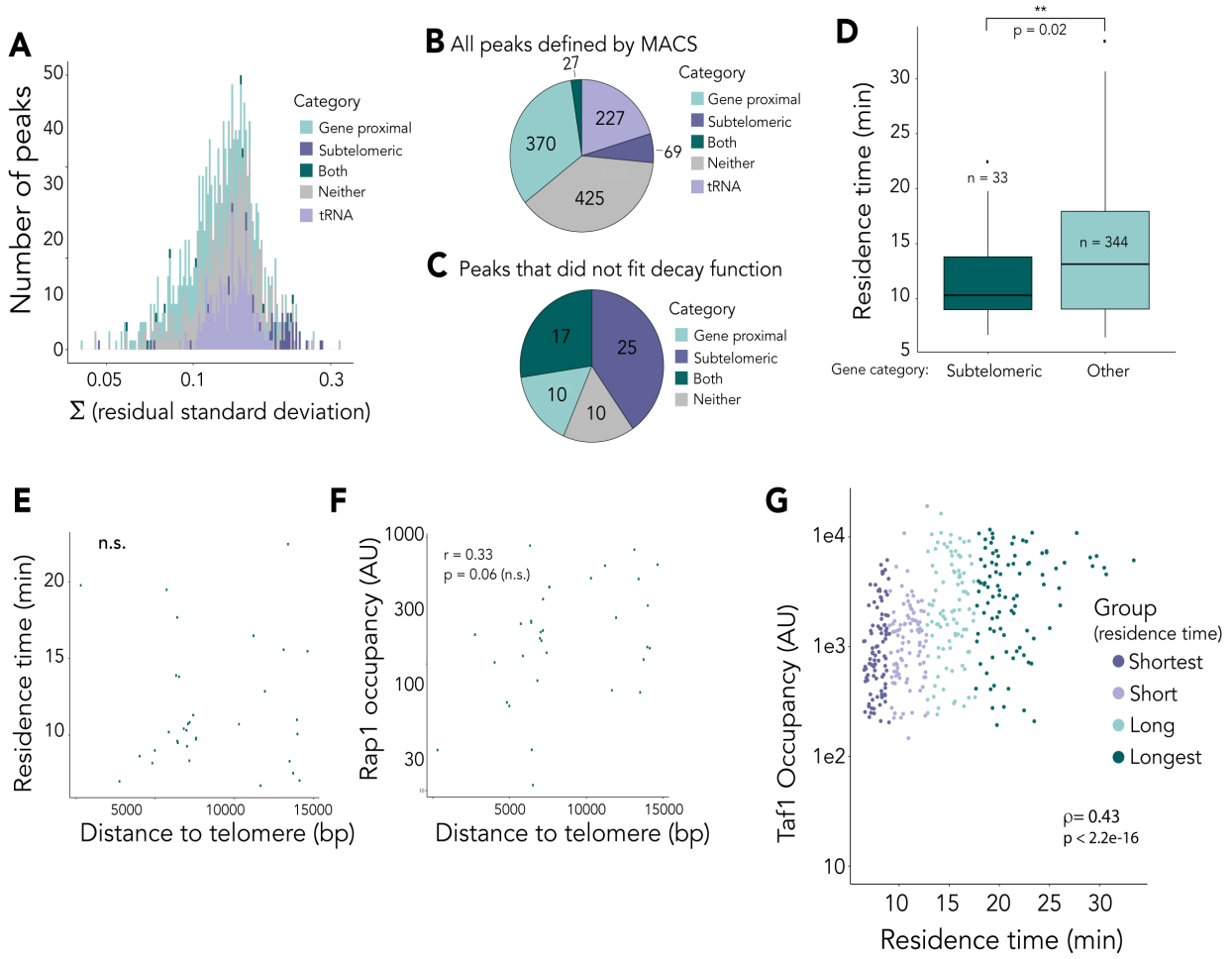

Figure S2.4. Peak filtering and analysis of subtelomeric Rap1 apparent residence times. All data represent the average of two biological replicates.

A. A histogram quantifying the standard-deviation of the residuals for each peak that had a calculated p-value of the $\log(k_{off}) < 0.05$ (n=1056). Peak classifications are denoted by colors in legend.
B. A pie chart representing the breakdown of peak classifications of all peaks defined by MACS (see *Methods*) by number (total = 1118).
C. A pie chart representing the breakdown of peaks, by classification, from (C) that did not fit the decay function (p-value of the $\log(k_{off}) > 0.05$) (total = 62).
D. Box plot quantifying the average residence time for peaks near genes classified as subtelomeric (left, dark green), or all other peaks (right, light green). One-way ANOVA test showing significance p = 0.02.

Figure S2.4 *(continued from previous page)*

E. Correlation relating distance to telomere in basepairs on the x-axis and average calculated residence time on y axis for peaks categorized as subtelomeric. No significant correlation.
F. Correlation relating distance to telomere in basepairs on the x-axis and Rap1 occupancy (enrichment at t=0) on the y-axis for peaks categorized as subtelomeric. Pearson correlation $r = 0.33$, p-value = 0.06 (not significant).
G. Correlation between Rap1 apparent residence time (x-axis) and Taf1 enrichment at corresponding Rap1 peaks. Spearman correlation coefficient $\rho = 0.43$, p-value < 2.2e-16.

As ChIP-seq peak heights reflect a static view of occupancy of chromatin binding proteins, we tested the correlation between Rap1 occupancy (enrichment at time=0) and apparent dwell-time (**figure 2.5.B**). There was a significant positive correlation between these two factors (Pearson correlation coefficient $r = 0.45$, p-value < 2.2e-16), but much of the variation remained unaccounted for. Rap1 targets vary greatly in expression. Indeed, ribosomal protein genes whose transcripts make up nearly 60% of total mRNAs in the yeast cell (Woolford and Baserga 2013) were enriched for longer apparent dwell-times as reported previously (**figure 2.5.C**) (Lickwar *et al.* 2012). Presumably, stable Rap1 binding would allow for efficient recruitment of pre-initiation complex machinery via TFIID–Rap1 interactions (Garbett *et al.* 2007). Utilizing our previously generated dataset of Taf1 ChIP-seq as a proxy for TFIID occupancy, we compared dwell-time to Taf1 enrichment. Overall, there was a positive correlation between apparent residence time and Taf1 ChIP signal (**figure S2.4.G**, Spearman correlation coefficient $\rho = 0.43$, p-value < 2.2e-16), and a significant difference in Taf1 occupancy between the shorter and longer Rap1 dwell times (**figure 2.5.D**, ANOVA, p < 2.2e-16). To investigate further the role of Rap1 binding dynamics in transcription regulation, we generated summary distribution plots (meta-gene analyses) of nascent transcripts associated with the Rap1-bound loci genome-wide. Utilizing published datasets (Pelechano *et al.* 2013; Couvillion *et al.* 2022), we plotted nascent, elongating Pol II occupancy reported by Native Elongating Transcript sequencing (NET-seq) for each transcript proximal to a Rap1 peak. This meta-gene analysis showed that longer apparent Rap1 dwell-time correlated with greater NET-seq signal and thus an inferred higher transcriptional output (**figure 2.5.E**). These data reinforced the proposed model in which longer apparent dwell-time corresponded to higher transcriptional activity, perhaps working through stable recruitment of the pre-initiation complex. Thus, we associated apparent Rap1 residence time with gene expression.

Many studies identify Rap1 as an important modulator of nucleosome-free regions through interactions with the chromatin remodeling complex RSC (Knight *et al.* 2014; Kubik *et al.* 2015, 2017; Challal *et al.* 2018). *In vitro* experiments find Rap1 dwell-times to be dependent on the chromatin environment. Specifically, introduction of nucleosomes to naked DNA is anti-correlated with stable Rap1 binding (Mivelaz *et al.* 2020). We therefore hypothesized that, similarly to other transcription factors, apparent Rap1 dwell-time would be inversely correlated with nucleosome occupancy, and that Rap1 binding stability was related to its role in determining nucleosome-free regions. Using a published dataset that utilized a chemical cleavage method to precisely map single nucleosomes with high accuracy genome-wide in yeast (Chereji *et al.* 2018), we created a meta-gene analysis mapping histone H3 positioned 500 bp upstream and downstream of each Rap1 peak

(**figure 2.5.F**). The averaged nucleosome occupancy for each quartile group of residence times revealed that longer dwell time corresponded to a broader nucleosome-free region, with a notably weakened -1 positioned nucleosome (**figure 2.5.F**). We then compared how nucleosome occupancy corresponded to Rap1 occupancy (IP enrichment at time = 0). When positioning data were grouped by initial enrichment instead of dwell-time, we found a consistent anti-correlation between histone occupancy centered over the Rap1 peak and relative Rap1 occupancy (**figure 2.5.G**). As total enrichment is a function of both on-rate and off-rate, we surmised that the differences we observed in correlations between nucleosome occupancy and Rap1 enrichment versus apparent dwell-time may have reflected differences in on-rate. In sum, these data supported and extended the hypothesis that Rap1 binding and nucleosome occupancy were inversely correlated *in vivo*, and connected this attribute to transcriptional output.

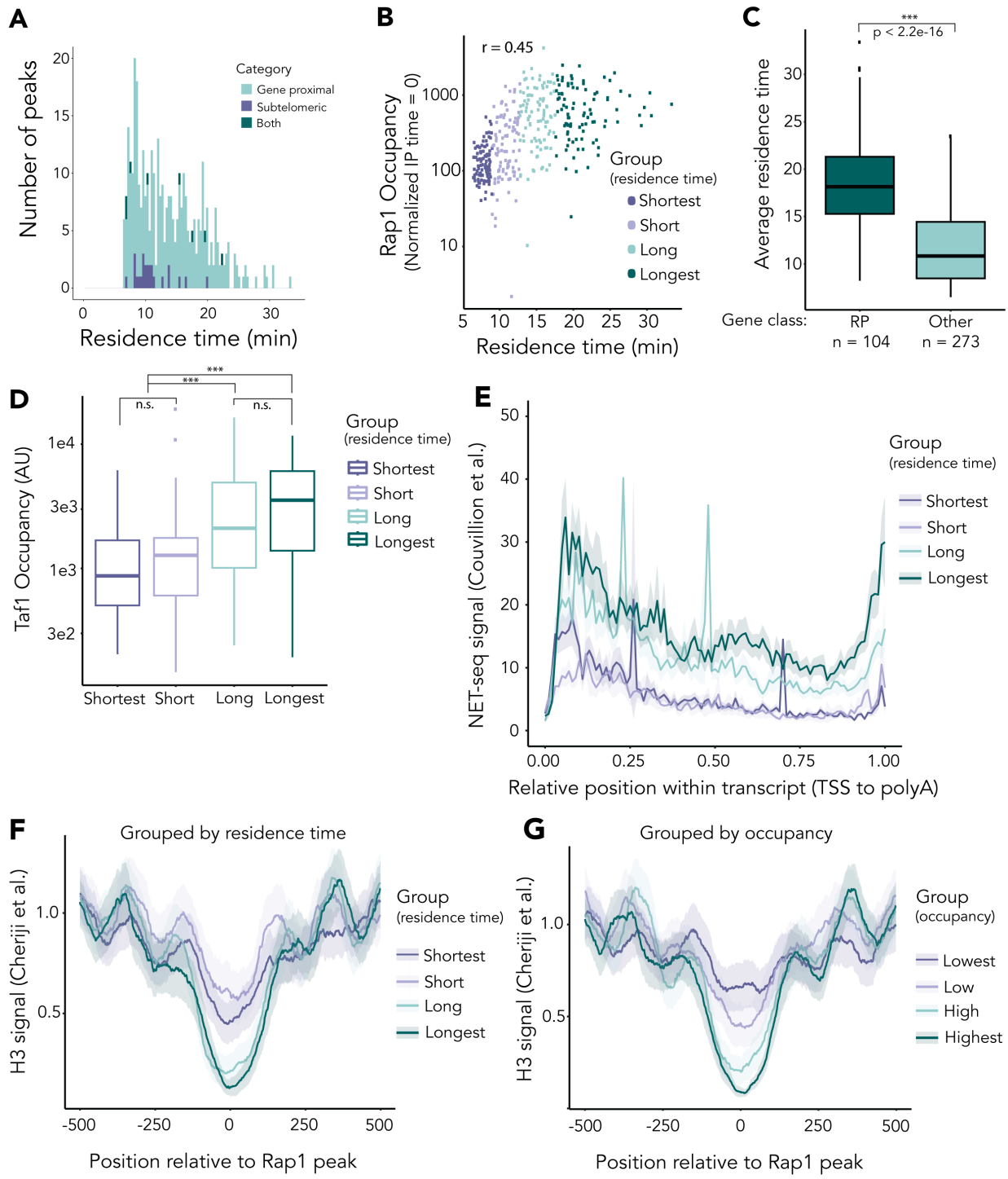

Figure 2.5. Genome-wide analysis of *in vivo* Rap1 apparent residence times supports and extends previous models that Rap1 dwell-time is correlated with transcriptional output

All figures comprise data obtained from the average of two biological replicates. Peak set (n=377) was divided into quartiles based on residence time for analysis unless otherwise noted. For gene-level analyses, Rap1 peaks were assigned to ORFs for which a Rap1 peak summit was within 300bp upstream of ORF start.

Figure 2.5 *(continued from previous page)*

(A) Average apparent Rap1 residence time in minutes of the 377 binding sites evaluated genome-wide categorized as gene-proximal, subtelomeric, or both.
(B) Correlation between average Rap1 occupancy before depletion (enrichment at t=0) and the average apparent residence times for all 377 Rap1-bound peaks (Pearson correlation r = 0.45, p-value < 2.2e-16).
(C) Difference in apparent residence times between sites that are classified as regulating Ribosomal Protein genes (n = 104, dark green) and all other sites (n = 273, light green). The p-value was calculated using a Mann-Whitney U test (p < 2.2e-16).
(D) Quantification, by mean apparent residence time quartile, of normalized Taf1 occupancy levels at the Rap1 binding sites. These levels are defined as the amount of Taf1 enrichment (in reads) covering the Rap1-bound loci. Significance was calculated using a one-way ANOVA followed by Tukey's HSD test (p < 2.2e-16).
(E) Mean profiles display NET-seq coverage (Couvillion *et al.* 2022) with 95% confidence intervals (displayed as transparent filling) within neighboring transcript(s). Coverage was scaled according to transcript length.
(F) Summary distribution plots of average H3 enrichment (Chereji *et al.* 2018) centered on Rap1 peaks and spanning 500bp+/-. Coverage was grouped by apparent-residence time quartiles. The confidence intervals are indicated as in figure 5E, with a transparent fill denoting 95% confidence intervals.
(G) Same as F, but peaks grouped by ranked Rap1 occupancy at t=0.

2.5 Discussion

This study explored the enigmatic ability of Rap1 protein to function in both gene activation and repression. Earlier work discounted the possibility that the function of Rap1 was determined by subtle differences in its recognition sequence (Teytelman *et al.* 2012). Other work suggested that Sir-silenced chromatin could inhibit binding of at least some proteins to their recognition sites (Loo and Rine 1994; Sekinger and Gross 2001; Chen and Widom 2005; Gao and Gross 2008). In contrast, our findings established that silenced chromatin did not block Rap1's recognition of its binding site in silent chromatin. Instead, our data revealed a more nuanced and unexpected way in which Rap1 and Sir proteins mutually reinforced each other in the assembly of silenced chromatin.

Rap1, bound to its recognition sequence within the bi-directional promoter between *HML α1* and *HMLα2* served opposing functions depending on the state of the surrounding chromatin. The promoter-adjacent binding site at *HML* was robustly enriched for Rap1 binding in the presence of Sir proteins. In contrast, transcription initiation factors were undetectable at the promoter harboring the Rap1 binding site. Strikingly, Rap1 at the bi-directional promoter internal to *HML* resulted in increased enrichment of Sir proteins at *HML*, and vice versa. Moreover, *HML*-promoter-bound Rap1 contributed to the stability of silent chromatin when weakened (**figure 2.2**). In addition, we determined a role for Rap1 in promoting the transition from initiation to elongation, which may be dependent on its role in nucleosome positioning.

Our results agreed with earlier work that Sir-silenced chromatin can inhibit some proteins from binding their recognition sequences (Loo and Rine 1994; Chen and Widom 2005; Gao and Gross 2008; Steakley and Rine 2015). Despite ample Rap1 enrichment

at a Sir-silenced *HML,* we found no evidence of the pre-initiation complex bound at the *HML* promoter in silent chromatin, nor any indication that silencing acts by blocking Pol II elongation (**figure 2.1**). Our study used tagged forms of Taf1, Sua7, Rpb3, and Elf1, each expressed from their native promoter with no untagged alleles present, as proxies for TFIID, TFIIB, RNA Pol II, and elongation machinery, respectively. Previous reports find TATA-binding protein (TBP) and TFIIH to be present in the context of Sir-silenced chromatin (Gao and Gross 2008). These studies relied on the low-resolution techniques available at the time, while our experiments utilized heavily controlled, modern setups that allowed clear interpretation of results. Further apparent discrepancies between our results and prior studies on the mechanism of silencing may lie in the choice of factors queried for enrichment at the silent locus. Although we did not evaluate TFIIH subunits, TFIIH recruitment to a locus follows, and is dependent on, TFIID binding (Saunders *et al.* 2003), and we did not find evidence of TFIID enrichment in the presence of Sir proteins (**figure 2.1**). Relatedly, we chose Taf1 as the proxy for the pre-initiation complex based on studies revealing nearly all genes in the yeast genome are TFIID-dependent and that Taf1 is necessary for recruitment of TBP and assembly of the pre-initiation complex (PIC) (Li *et al.* 2002; Shen *et al.* 2003; Warfield *et al.* 2017). In summary, our results demonstrate that Sir-silencing occurred through a pre-initiation complex interference mechanism, whereby the presence of Sir proteins competitively inhibited the ability of Rap1 to recruit the transcription machinery.

While apparent off-rates for Rap1 did not differ between silenced and unsilenced chromatin, we found greater enrichment of Rap1 in the presence of Sir proteins both at the promoter and silencers of *HML* (**figure 2.1, figure 2.2, figure 2.4**). This study focused on the dual functions of Rap1 at three binding sites in heterochromatic *HMLα* versus one site in euchromatic *MAT*α*,* taking advantage of the sequence identity between the two loci in *S. cereivisiae.* The experimental setup of our studies did not allow for direct comparison to dwell-times at *HMR*. However, we found further evidence of a positive feedback mechanism between binding of Sir proteins and Rap1 at the *HMR-E* silencer, where Rap1 enrichment was diminished in the absence of Sir proteins (**figure S2.2.G**). Taken together, we inferred that the enhanced ChIP-based enrichment of Rap1 in the presence of Sir proteins was consistent with an increase in the frequency of Rap1 binding events in this context. However, inferences regarding off-rate through the anchor-away method are limited by the method affecting primarily the loss of free Rap1, and any changes in on-rate are speculative. Nevertheless, our dwell-time data were consistent with those described by a related but different technique that reports on local competition between Rap1 molecules (Lickwar *et al.* 2012). Our data supported a hypothesis that interactions between Sir proteins and Rap1 resulted in greater recruitment of both to silenced chromatin than would be achieved by the affinity of Rap1 for its binding site alone.

The *sir1Δ* genotype has long been used as a case study in epigenetics, as *sir1Δ* cells exist in a mixed, bi-stable population of silenced and unsilenced *HM*-loci despite having the same genotype (Pillus and Rine 1989; Saxton and Rine 2019). Our samples of *sir1Δ* cells were prepared from unsorted cultures. The *sir1Δ-rap1* bs mutant strain revealed two distinct patterns of Rap1 enrichment across *HML* (**figure S2.2C**). Notably,

one sample almost exactly matched the enrichment pattern seen in a *sir4Δ-rap1* bs mutant. From this we inferred a higher rate of cell-switching to a more *sir4Δ*-like state when Rap1 was absent from the *HML* promoter. Furthermore, we found the apparent silencing-loss rate in *sir1Δ-rap1* bs mutant cells to be greater than in a *sir1Δ* alone (**figure 2.2.B,C**). In the *sir1Δ* mutant the density of Sir proteins at the silent locus is less than in wild type, creating a paucity of Rap1-Sir interactions and, more broadly, a decrease in stability of the silent locus (Saxton and Rine 2022). Combined, these data reflected the importance in Rap1-Sir protein interactions particularly over the promoter in the weakened *sir1Δ* silent domain. The weakened interactions could allow for more opportunities for transcription machinery to interact with Rap1 and shift the balance in favor of transient derepression. We propose that Rap1 acts as a toggle in the competition between transcription and silencing of *HML*.

Although the putative interaction domains of Rap1 and Sir proteins have been identified (Moretti *et al.* 1994; Cockell *et al.* 1995, 1998; Moretti and Shore 2001), to date it has not been possible to identify clear separation-of-function mutations interfering with activation but not silencing due to Rap1 being essential for viability. By indirect means, the activation domain of Rap1 has been shown to interact with various TFIID components (Garbett *et al.* 2007; Papai *et al.* 2010). Despite the activation domain and C-terminal interaction domain appearing to be non-overlapping by those analyses, one explanation for the occlusion of the pre-initiation complex from Sir-silenced chromatin would be if binding of Sir proteins to Rap1 rendered the activation domain inaccessible to TFIID. Our data were compatible with the idea that interactions between Rap1 and Sir proteins are mutually exclusive to interactions between Rap1 and TFIID subunits. In this model the balance of silencing versus activation would tip slowly toward fully silenced as the local concentration of Sir proteins increased.

In agreement with previous findings of other transcription factors, our data showed that nucleosome positioning was correlated with Rap1 dwell-time (de Jonge *et al.* 2020). In our anchor-away dataset, Rap1-bound loci with the longest apparent residence time were characterized by a well-defined nucleosome-free region centered on the Rap1 binding site, and a broader nucleosome-depleted region with an unstable -1 positioned nucleosome (**figure 2.5.F**). Conversely, loci with shorter dwell-times corresponded with a narrowing of the nucleosome-free region centered on the Rap1 peak, and an associated relative enrichment in the presence of histones over these peaks (**figure 2.5.F**). These data suggested that Rap1 binding in the presence of a nucleosome was less stable, as is reported *in vitro* (Mivelaz *et al.* 2020). We identified a further anti-correlation between nucleosome occupancy and Rap1 occupancy (enrichment at t=0, **figure 2.5.G**). By taking both the static occupancy measurement and the apparent dwell-time function into account, we inferred a variable on-rate that supports this hypothesis. These data indicated that nucleosome positioning relative to Rap1 peak summit played an important role in determining both the level to which Rap1 was enriched at those sites, and the apparent residence times once bound. However, it would be equally valid to infer that strong Rap1 binding depleted nucleosomes to a greater extent than weak Rap1 binding.

Based upon the positive correlation between Rap1 residence time and enrichment of Taf1, we hypothesized that the variability in expression strength at different Rap1-

bound loci may be due in part to variability in Rap1 dwell-time (**figure 2.5.D, figure S2.4.G**). Furthermore, nascent transcript abundance correlated with Rap1 dwell-time (**figure 2.5.E**). Thus, we have confirmed and extended previous models suggesting the role of Rap1 in transcriptional activation was dependent, in part, on Rap1 binding dynamics (Kubik *et al.* 2015, 2017; Challal *et al.* 2018; Wu *et al.* 2018). In summary, apparent residence time may be attributed to competition with nucleosomes, with the creation of a stable nucleosome depleted region allowing for higher rates of transcription.

Rap1 binding results in MNase-refractory positions that mimic those created by a nucleosome. Additionally, Rap1 occupancy is an important determinant of the size and patterning of the nucleosome depleted regions to which it binds, while removal of Rap1 may result in remodeling of the nearby chromatin (Badis *et al.* 2008; Hartley and Madhani 2009; Ganapathi *et al.* 2011; Knight *et al.* 2014; Kubik *et al.* 2015; Challal *et al.* 2018). There is also evidence that Sir protein avidity for nucleosomes creates a robust pattern of nucleosome occupancy at *HML* and *HMR* (Wang *et al.* 2015). Alteration to the nucleosome depleted region in the bi-directional promoter in the absence of Rap1 could generate a block to productive transcription. We observed a narrowed Taf1 peak in rap1 bs mutant cells, which may indicate reduced access of TBP to the TATA-box (**figure 2.3.E**). Rap1 binding is necessary for downstream recruitment of the chromatin remodeler complex RSC to maintain a nucleosome depleted region (Kubik *et al.* 2017). Without Rap1 binding, and recruitment of chromatin remodelers, these sites may be less accessible to subunits of TFIID and other pre-initiation complex machinery. Furthermore, in the context of unsilenced *HML,* Elf1 and Rpb3 appeared to pile up over the bi-directional promoter in the absence of Rap1, which indicated a blockade in the progression of transcription (**figure 2.3**). Our finding that the switch from RNA Polymerase II initiation to elongation was hindered in the absence of Rap1 could reflect a change in the promoter architecture upon removal of Rap1.

Rap1 has been described as a pioneer factor with the ability to access cognate binding sites in the presence of a nucleosome array *in vitro* (Luo *et al.* 2014; Mivelaz *et al.* 2020). Rap1 bound to its promoter site in Sir-silenced chromatin extends this view *in vivo* (**figure 2.1**). In a broader context, pioneer factors are typically utilized by the cell during periods of drastic genomic restructuring, such as during fertilization in metazoans. Their pervasive binding to regions of the genome allows for poising of the genome for activation of cell-fate-specific gene expression (Larson *et al.* 2021; Zaret 2020). In their haploid life cycles, yeast continuously undergo chromatin landscape restructuring in the form of DNA replication during replicative aging. Furthermore, it is important for the single-celled organism to readily adapt to environmental stresses. Rap1 is necessary for the Gcn4-mediated regulation of ribosomal protein genes which occurs upon amino acid starvation (Devlin *et al.* 1991). Perhaps the downstream effect of Rap1-mediated nucleosome-free regions is to more readily enable the genome to activate certain genes under stress conditions by promoting the transition from transcription initiation to elongation.

In summary, we found that Rap1 has a complex and context-dependent role in the regulation of gene expression, with the ability to both stabilize the Sir-silencing complex at a silenced promoter and promote transcriptional elongation at the same locus in the

absence of Sir proteins. In this way, Rap1 can be compared to Glucocorticoid receptor, a transcription factor well studied for its context-specific roles in vertebrate gene regulation (reviewed in 88, 89), and Ume6, a meiotic regulator that can act as a repressor or activator depending on its cofactors (Jackson and Lopes 1996). Like the glucocorticoid receptor, one possible explanation of how Rap1 may be able to bind DNA in heterochromatin but not recruit transcription machinery may be the presence of post-translational modifications to the Rap1 protein. In a thematically similar concept, recent data reveals differential phosphorylation of $Clr4^{SUV39H}$ correlates with a switch in methylation state of H3K9 in *S. pombe* (Bailey *et al.* 2021; Kuzdere *et al.* 2022).

This work highlights the many modes of epigenetic regulatory mechanisms integrated by cells to give rise to a vast spectrum of context-specific and finely tuned gene expression patterns. Beyond the role of Rap1 in *S. cerevisiae,* these findings have implications, broadly, in eukaryotic regulation of cell-type fidelity across cell divisions. Dual-function transcription factors can be recruited to promoters and, in a context-dependent manner, serve as co-activators or co-repressors to finely tune gene expression, in part through the effects of local concentration of interaction partners. In conclusion, these findings provide new insights into the mechanisms of gene expression and highlight the importance of considering the context in which transcription factors function.

2.6 Materials and Methods

Yeast strains

Strains used in this study are listed in **Table 2.1**. All strains were derived from the *S. cerevisiae* W303 background (except strain JRy15212 which was derived from *S. paradoxus YPS138* – a gift from the Brar/Ünal labs) using standard genetic techniques and CRISPR-Cas9 technology (Burke *et al.* 2000; Gietz and Schiestl 2007; Brothers and Rine 2019). Deletions were generated using one-step replacement with marker cassettes (Goldstein and McCusker 1999; Gueldener *et al.* 2002). Details of strain construction for epitope-tagged proteins and mutants can be found in *2.7 -Supplementary Methods.* Relevant oligonucleotides used for strain construction can be found in **Table 2.2**. Tagged strains were confirmed by PCR and Sanger sequencing, as well as Immuno-blot analysis, and were validated for viability and silencing as described in *2.7 - Supplementary Methods*.

CRASH colony imaging

Colonies were plated onto 1.5% agar plates containing yeast nitrogen base without amino acids, 2% dextrose, and supplemented with complete supplement mixture (CSM)-Trp to minimize background fluorescence. Colonies were incubated for 5–7 days at 30 °C, then imaged as described in (Fouet and Rine 2023).

Flow cytometry and calculations of apparent loss-of-silencing rate in CRASH strains

This experiment was carried out as described in (Janke et al 2018 and Fouet and Rine 2023). To summarize: strains were streaked for single colonies on YPD, with multiple single colonies used as technical replicates for each sample. Strains were then back-diluted in growth medium containing G418 to select for cells that had not yet lost silencing. Cells were diluted and grown in liquid CSM until mid-log phase and harvested by centrifugation, then resuspended in PBS at approximately 0.5 OD. Samples were processed as described in Fouet and Rine 2023. The apparent silencing-loss rate was calculated as previously described (Janke *et al.* 2018; Fouet and Rine 2023). See 2.7 - *Supplementary Methods* for details.

RNA extraction and RT-qPCR

RNA extraction and RT-qPCR was carried out as in (Goodnight and Rine 2020). See *2.7 - Supplementary Methods* for details. Each reaction was performed in triplicate, with the matched non-reverse-transcribed sample run simultaneously. cDNA abundance was calculated using a standard curve and normalized to the reference gene *ALG9.* Oligonucleotides used for qPCR are listed in **Table 2.2.**

Chromatin Immunoprecipitation, ChIP-qPCR, and Library preparation

For ChIP-seq experiments (**figures 2.1, 2.2, 2.3**), cells were grown in YPD overnight in 5mL cultures then back-diluted to a concentration of OD600 ~ 0.1 in 50mL YPD the following day. Cells were grown to mid-log phase (OD600 ~ 0.6-1.0) and ~5×10^8 cells were crosslinked in a final concentration of 2% formaldehyde at room temperature for 15 min. The formaldehyde was quenched using a final concentration of 1.5M of Tris for 5 min.

For Anchor Away ChIP-seq experiments (**figures 2.4, 2.5**), cells were grown overnight in YPD, then back-diluted to OD600 ~ 0.1 in 50mL YPD the following day, then grown for two-three doublings and collected at OD600 ~ 0.8. Rapamycin (LC Laboratories, Cat No. R-5000) was added to a final concentration of 7.5 μM. Additions of rapamycin were staggered such that all time points were ready at the same OD (~0.8). Samples were fixed and quenched as above. ~5×10^8 cells were collected for each sample. 5% S. *paradoxus* cells by OD were spiked into each *S. cerevisiae* sample and processed according to the chromatin immunoprecipitation protocol.

Cell lysis and chromatin immunoprecipitation was performed as described in Goodnight and Rine 2020. Details can be found in *2.7 - Supplementary Methods*. For all samples, ~850 µL soluble chromatin were collected for immunoprecipitation, and 50 µL was reserved for Input. For all ChIP samples, 50 μL DynaBeads Protein G magnetic beads (ThermoFisher Scientific catalog number 10003D) per sample were equilibrated by washing 5x in FA Lysis buffer + 0.1% SDS + 0.05% Tween, then resuspended in in 50 μL per sample of FA Lysis buffer + 0.1% SDS + 0.05%. IP for 3xV5-Rap1 was performed using 5µL mouse monoclonal V5 (ThermoFisher Scientific catalog no R96025). For all 3xFLAG-tagged proteins (Taf1, Sua7, Elf1, Rpb3), IP was performed using 5µL mouse monoclonal anti-FLAG® M2 antibody (Millipore Sigma, product no F1804. Beads and

antibodies were incubated for >3 hours in an end-over-end rotator at 4°C and then rinsed once with 500uL FA Lysis buffer + 0.1% SDS + 0.05% Tween. All immunoprecipitations were performed in an end-over-end rotator at 4°C overnight in the presence of 0.5 mg/mL BSA (NEB B9000S). Following the overnight incubation, the following washes were performed as in Goodnight and Rine 2020 (*see 2.7 - Supplementary Methods*). Samples were eluted by adding 100 μL TE + 1% SDS to the beads. Input samples were brought to a total volume of 100 μL with TE + 1% SDS. The beads and elution buffer were incubated at 65°C overnight to reverse crosslinking. In the morning, 5 uL 10mg/mL RNase A was added to each sample and incubated for 1 hr at 37°C. 10 μL of 800 U/mL Proteinase K (ThermoFisher Scientific, EO0491) was then added to each ample and incubated for 1 additional hour at 65°C. DNA was purified using a QIAquick PCR purification kit (Qiagen 28104).

For ChIP-qPCR, ChIP samples were diluted 10-fold and Input samples were diluted 100-fold in nuclease-free water. Reactions were set up in triplicate and run using the same reagents and parameters as for RT-qPCR above. Abundance was calculated using a standard curve for each primer set, and the ratio of IP/Input was plotted. Oligonucleotides used for this experiment can be found in **Table 2.2**.

Libraries were prepared for high-throughput sequencing according to manufacturer's recommendations using the Ultra II DNA Library Prep kit (NEB E7645L). Samples were multiplexed and paired-end sequencing was performed using either a MiniSeq or NovaSeq 6000 (Illumina; San Diego, CA).

Alignment and mapping

Sequencing reads were aligned using Bowtie2 (Langmead and Salzberg 2012), using options = "--local --soft-clipped-unmapped-tlen --no-unal --no-mixed --no-discordant" to a reference genome. For standard ChIP-seq experiments (**figures 2.1, 2.2, 2.3**) the genome file was derived from SacCer3 and modified to include, where appropriate, the mutant *HML-p* rap1 binding site mutation, *hmlα2::Cre, matΔ,* and *hmrΔ,* or *hmlΔ hmrΔ* in the case of *MATσ* strains. Analysis was performed using custom Python scripts derived from Goodnight and Rine 2020. Fragments ranging from 0-500bp were mapped, Reads were normalized to the non-heterochromatic genome-wide median (i.e., to the genome-wide median excluding rDNA, subtelomeric regions, and all of chromosome III), and converted to bedgraphs for display. For coverage calculations in **figure S2.2A,** peak summits were defined by MACS3 callpeak, using a cutoff of $q < 0.01$. Peaks were defined as 150bp on either side of the summit. Peaks were ranked by fold-enrichment and we counted read coverage over the 500 most enriched regions using featureCounts (Liao *et al.* 2014). Scatterplots were generated using ggplot2 (Wickham 2009).

For Anchor-Away experiments, a custom, concatenated hybrid genome was generated using modified SacCer3 (unique *HML* sequence, *hmrΔ*) and the *S. paradoxus* genome CBS432 (genbank). Reads were aligned as above using Bowtie2. Number of mapped read segments were calculated using SAMtools idxstats (Li *et al.* 2009), from which number of reads assigned to the *S. paradoxus* genome were recovered. Total number of *S. paradoxus* reads for each sample was collected, excluding the rDNA due to

its vast variability in copy number. *S. paradoxus* read count served as the normalization factor for each sample.
All displays of ChIP-seq normalized coverage over a defined region were displayed using a custom Rscript and ggplot2.

Peak-calling and filtering for Anchor-Away experiments

We followed the framework for peak calling and filtering laid out in (de Jonge et al. 2020). To summarize: MACS peak filtering was performed to identify regions of distinct peaks across the *S. cerevisiae* genome in control samples (DMSO-IP, time 0) using a no-tag control sample as the input over which the program defined peaks. Summits were defined using the callpeak function and options "-f BAMPE -g 1.2e7 -q 0.01 --keep-dup=auto -B --call-summits". Therefore, only peaks that met a q value < 0.01 cutoff were maintained, identifying 1118 Rap1-bound regions genome-wide. Peaks were defined as 150bp on either side of the summit as defined by MACS, resulting in 302bp-wide peaks. We counted read coverage over each region in duplicate Rap1-depletion sample, and these values were normalized to the *S. paradoxus* read counts per sample as described above.

Peaks at each locus were fit using the exponential decay model described in de Jonge et al, filtering for peaks with p-value $\log(k_{off}) < 0.05$. The fits were done in R with the nls function using the formula: "nls(ChIP ~SSasymp(time, yf, y0, log_koff)". Further explanation of peak filtering can be found in *2.7 - Supplementary Methods*. The 377 peaks used in the analyses for **figures 2.5, S2.3, and S2.4** represent peaks that fit the non-linear regression model and were within 300bp upstream of an ORF and/or located in the subtelomeric region (defined as 15kb from the ends of chromosomes).

Other datasets

H3 occupancy genome-wide for analysis of the relationship between Rap1 apparent dwell-time or Rap1 enrichment to nucleosome position was downloaded from GEO Accession GSE97290 (Chereji *et al.* 2018).

To visualize summary distribution plots of elongating RNA polymerase II signal as they related to Rap1 binding sites and dwell-time, we first defined full transcripts spanning from transcription start sites (TSSs) to poly-A tracts by identifying the most abundant, stable transcript isoforms in a dataset generated by TIF-seq (Transcript IsoForm sequencing; GEO Accession GSE39128) (Pelechano *et al.* 2013). We then averaged the corresponding Native Elongating Transcript sequencing signal (NET-seq) from four biological replicates in GEO Accession GSE159603 (Couvillion *et al.* 2022).

2.7 Supplementary Methods

Yeast strain construction

C-terminal tags (Rpb3-3xFLAG:KanMX, SUA7-3xFLAG-KanMX, ELF1-3xFLAG:KanMX, TAF1-3xFLAG:KanMX) were generated by amplifying the 3XFLAG::KanMX sequence from pJR2601 (p3FLAG-KanMX; (Gelbart *et al.* 2001)) with primers that included 40 bp of sequence identity with either side of the amplicon, followed by a transformation. The 3xV5-Rap1 N-terminally tagged allele was generated by

amplifying the 3xV5 sequence from pJR3191 pFA61-3xV5-NatMX6 with sequence identity to the N-terminal insertion site on either side, then integrated using CRISPR-Cas9 technology as described (Brothers and Rine 2019). Rap1 was tagged N-terminally to avoid genetic manipulations of the Rap1 C-terminus, since doing would likely have interrupted interactions with Sir proteins or Rap1 interacting factors and thus obscured our interpretations in the context of silent chromatin. The rap1 binding site mutation was generated by using CRISPR-Cas9-mediated targeting of the *HML-p* sequence coupled with an oligonucleotide extension that incorporated the 2 bp mutation and obliterated the PAM sequence. The mutant allele of *HML* that included synonymous SNPs was used to distinguish sequencing between *MAT*α and *HMLα* in short sequencing reads, utilized in the Anchor Away experiments, was generated by cloning together synthetic DNA gene blocks (Integrated DNA Technologies) and a previously published allele of *HML* (Goodnight and Rine 2020), and integrated using CRISPR-Cas9 technology. Relevant geneBlocks can be found in **Table 2.3.** We recapitulated the Rap1 Anchor Away strain first published in (Kubik *et al.* 2015) by amplifying the 2xV5-FRB sequence from a plasmid and integrating it, at a sequence corresponding to amino acid 134 in the *RAP1* CDS, into the Anchor Away parent strain (gifted from Craig Peterson, originally from (Haruki *et al.* 2008)) by CRISPR-Cas9. The *S. paradoxus* strain was generated similarly, but transformed into YSP138 (a gift from the Brar/Ünal labs). All strains used in this study can be found in **Table 2.1**.

Validation of epitope-tagged strains

To address the possibility that endogenous tagging of the proteins studied impacted viability or silencing, growth-curves for representative strains were conducted over a 24 hour window. We found no difference in growth rates between wild type yeast and any of our endogenously-tagged strains (**figure S2.1A**). Furthermore, introduction of epitope tags to representative strains resulted in no silencing defects as measured by RT-qPCR of *HML*α*2Δ::Cre* (**figure S2.1B**).

Calculations of apparent loss-of-silencing rate in CRASH strains

Flow cytometry was done on a BD LSR Fortessa using the BD FACSDiva software (BD Biosciences) and FITC and PE-TexasRed filters. Events were analyzed and processed using FlowJo Software (BD Life Sciences) and the flowAI R package (Monaco *et al.* 2016) as described in Fouet and Rine 2023. Samples were grouped by population; GFP+ RFP+, GFP+ RFP-, GFP- RFP+ and GFP- RFP-. The apparent silencing-loss rate was calculated by quantifying the number of cells that were transitioning from RFP to GFP expression (those expressing both RFP and *GFP*), divided by the sum of all cells still expressing RFP (RFP+ GFP+ and RFP+ GFP-) (Janke *et al.* 2018; Brothers and Rine 2019; Fouet and Rine 2023).

RNA extraction and RT-qPCR

Briefly, at least ~$2x10^7$ cells were grown and collected by centrifugation for each sample. RNA was purified using the RNeasy Mini Kit (Qiagen 74104; Hilden, Germany) according to manufacturer's instructions, including on-column DNase digestion (Cat No.

79254). RNA was quantified by NanoDrop, and 2mg of RNA was reverse transcribed using SuperScript III reverse transcriptase (Thermo Fisher Scientific catalog number 18080044) and an 'anchored' oligo-dT primer. A matched non-reverse-transcribed sample was generated simultaneously. The DyNAmo HS SYBR Green qPCR kit (Thermo Fisher Scientific F410L), including a Uracil-DNA Glycosylase (Thermo Fisher Scientific EN0362) treatment, was used for qPCR and samples were run using an Agilent Mx3000P thermocycler.

***S. paradoxus* spike-in**

A Rap1-V5 tagged strain of *S. paradoxus* was grown in parallel and fixed at the same saturation. As the *S. paradoxus* cells did not contain all other components of the Anchor-Away methodology, notably the *tor1-1* mutation, they were not exposed to rapamycin. After fixation, cells were washed twice in ice-cold TBS.

Cell lysis and chromatin isolation

Cells were washed twice in ice-cold TBS and twice in ice-cold FA lysis buffer (50 mM HEPES, pH 7.5; 150 mM NaCl, 1 mM EDTA, 1% Triton, 0.1% sodium deoxycholate) + 0.1% SDS + protease inhibitors (cOmplete EDTA-free protease inhibitor cocktail, Sigma-Aldrich 11873580001). Cell pellets were then either flash frozen or lysed. For lysis, cell pellets were resuspended in 800uL FA lysis buffer + 0.1% SDS and ~500 μL 0.5 mm zirconia/Silica beads (BioSpec Products; Bartlesville, OK) were added. Cells were lysed using a FastPrep-24 5G (MP Biomedicals; Irvine, CA) with 6.0 m/s beating for 20 s followed by 2 min on ice, repeated four times total. Lysate was transferred to a new microcentrifuge tube, and beads were rinsed with 300uL FA lysis buffer + 0.1% SDS and the remaining lysate was transferred to the same microcentrifuge tube. The cell lysate was transferred to 15 mL Bioruptor Pico tubes along with ~200µL of the corresponding sonication beads (Diagenode C010200031) and sonicated using a Bioruptor Pico (Diagenode B01060010) for 10 cycles of 30 s ON followed by 30 s OFF. After sonication, samples were spun at 4°C for 30 min at 17 k RCF to pellet cellular debris, and ~900 µL of the chromatin-containing supernatant was saved.

ChIP sample washes following overnight immunoprecipitation

Each sample was washed in the following manner, with ~5 minutes washing by incubating on an end-over-end mixer between each step: 2x washes with FA Lysis + 0.1% SDS + 0.05% Tween; 2x washes with Wash Buffer #1 (FA Lysis buffer + 0.25 M NaCl + 0.1% SDS + 0.05% Tween); 2x washes with Wash Buffer #2 (10 mM Tris, pH 8; 0.25 M LiCl; 0.5% NP-40; 0.5% sodium deoxycholate; 1 mM EDTA + 0.1% SDS + 0.05% Tween); and 1x wash with TE + 0.05% Tween.

Peak filtering for anchor away experiment

We evaluated goodness of fit by calculating the standard-deviation of the residuals for each peak (**figure S2.4.A**). Those peaks that did not fit the non-linear regression model were excluded from further analysis (**figure S2.4.B,C**). We found 227 Rap1 peaks that were centered over tRNA genes or Ty elements (**figure S2.4.A**). These loci all

displayed relatively short apparent residence times and fit the non-linear regression model well (**figure S2.4.A,B**). Despite this, we excluded them from further analysis as there is no known connection between Rap1 and Pol III transcribed genes, and it is known that highly transcribed loci are often artifacts of hyper-ChIPability (Park 2009; Teytelman *et al.* 2013). The 377 peaks used in the analyses for figures 5, S3, and S4 represent peaks that fit the non-linear regression model and were within 300bp upstream of an ORF and/or located in the subtelomeric region (defined as 15kb from the ends of chromosomes).

Data availability: All ChIP-seq datasets (raw and processed) are available at NCBI Gene Expression Omnibus (GEO): Series GSE227763.

2.8 Acknowledgments

We are grateful to past members of the Rine laboratory for helpful discussions in the planning of this work. We give special thanks to Davis Goodnight for his valuable experimental guidance and keen editing, and to Marc Fouet for his generosity with all things microscopy. We thank Paige Diamond for her invaluable assistance with data analysis and discussion. We also thank Elçin Ünal and Danielle Hamm for providing critical feedback on this manuscript. This work relied on the Vincent J Coates Genomics Sequencing Laboratory at UC Berkeley. This work was funded by grants from the National Institutes of Health to JR (R35GM139488). EB received support from a National Science Foundation Graduate Research Fellowship (Grant No. 1752814) and NIH Training Grant (T32GM007232).

Table 2.1: Yeast strains used in Chapter 2: All strains listed were generated for this study and derived from the W303 background except JRy15212. Unless otherwise noted, all strains are *ADE2; can1-100; leu2-3,112; ura3-1; lys2-; TRP1.*

Strain Number	Mating type	Relevant genotype
JRy15063	a	*hmlα2Δ::CRE, hmlαp*Rap1bs-mutation, ura3Δ::pGPD:loxP:yEmRFP;tCYC1:hygMX:loxP:yEGFP:tADH1; 3xV5_Rap1-N-terminal, SIR3-13xMyc-KanMX*
JRy15067	a	*hmlα2Δ::CRE, hmlαp*Rap1bs-mutation, ura3Δ::pGPD:loxP:yEmRFP;tCYC1:hygMX:loxP:yEGFP:tADH1; 3xV5_Rap1-N-terminal, SIR3-13xMyc-KanMX*
JRy15077	a	*hmlα2Δ::CRE, ura3Δ::pGPD:loxP:yEmRFP;tCYC1:hygMX:loxP:yEGFP:tADH1; 3xV5_Rap1-N-terminal, SIR3-13xMYC-KanMX*
JRy15078	a	*hmlα2Δ::CRE, ura3Δ::pGPD:loxP:yEmRFP;tCYC1:hygMX:loxP:yEGFP:tADH1; 3xV5_Rap1-N-terminal, SIR3-13xMYC-KanMX*
JRy15142	α	hmlΔ::NatMXhmrΔ::HygMX, 3xV5-Rap1; MATα-Rap1*bs
JRy15143	α	hmlΔ::NatMXhmrΔ::HygMX, 3xV5-Rap1; MATα-Rap1*bs
JRy15144	α	hmlΔ::NatMXhmrΔ::HygMX, 3xV5-Rap1
JRy15145	α	hmlΔ::NatMXhmrΔ::HygMX, 3xV5-Rap1
JRy15247	Δ	*matΔ::klLEU2 hmlα2Δ::CRE, ura3Δ::pGPD:loxP:yEmRFP;tCYC1:hygMX:loxP:yEGFP:tADH1; 3xV5_Rap1-N-terminal*
JRy15248	Δ	*matΔ::klLEU2 hmlα2Δ::CRE, ura3Δ::pGPD:loxP:yEmRFP;tCYC1:hygMX:loxP:yEGFP:tADH1; 3xV5_Rap1-N-terminal*
JRy15258	Δ	*matΔ::klLEU2 hmlα2Δ::CRE, ura3Δ::pGPD:loxP:yEmRFP;tCYC1:hygMX:loxP:yEGFP:tADH1; 3xV5_Rap1-N-terminal; hmrΔ::NatMX*
JRy15259	Δ	*matΔ::klLEU2 hmlα2Δ::CRE, ura3Δ::pGPD:loxP:yEmRFP;tCYC1:hygMX:loxP:yEGFP:tADH1; 3xV5_Rap1-N-terminal; hmrΔ::NatMX*
JRy15324	Δ	*hmlα2Δ::CRE, hmlαp*Rap1bs-mutation, ura3-1; 3xV5_Rap1-N-terminal ; hmrΔ::HygMX; matΔ::k.l.LEU2; sir1Δ::KanMX*
JRy15325	Δ	*hmlα2Δ::CRE, hmlαp*Rap1bs-mutation, ura3-1; 3xV5_Rap1-N-terminal ; hmrΔ::HygMX; matΔ::k.l.LEU2; sir1Δ::KanMX*
JRy15327	Δ	*matΔ::klLEU2 hmlα2Δ::CRE, ura3Δ::pGPD:loxP:yEmRFP;tCYC1:hygMX:loxP:yEGFP:tADH1; 3xV5_Rap1-N-terminal; hmrΔ::NatMX; sir1Δ::KanMX*
JRy15328	Δ	*matΔ::klLEU2 hmlα2Δ::CRE, ura3Δ::pGPD:loxP:yEmRFP;tCYC1:hygMX:loxP:yEGFP:tADH1; 3xV5_Rap1-N-terminal; hmrΔ::NatMX; sir1Δ::KanMX*
JRy15334	Δ	*hmlα2Δ::CRE, hmlαp*Rap1bs-mutation, ura3-1; 3xV5_Rap1-N-terminal ; matΔ::k.l.LEU2*

(continued on following page)

Table 2.1 *(continued from previous page)*

JRy15335	Δ	*hmlα2Δ::CRE, hmlαp*Rap1bs-mutation, ura3-1; 3xV5_Rap1-N-terminal ; matΔ::k.l.LEU2*
JRy15337	Δ	*hmlα2Δ::CRE, ura3Δ::pGPD:loxP:yEmRFP;tCYC1:hygMX:loxP:yEGFP:tADH1; 3xV5_Rap1-N-terminal; sir3Δ::klURA3; matΔ::k.l.LEU2*
JRy15338	Δ	*hmlα2Δ::CRE, ura3Δ::pGPD:loxP:yEmRFP;tCYC1:hygMX:loxP:yEGFP:tADH1; 3xV5_Rap1-N-terminal; sir3Δ::klURA3; matΔ::k.l.LEU2*
JRy15340	Δ	*hmlα2Δ::CRE, ura3Δ::pGPD:loxP:yEmRFP;tCYC1:hygMX:loxP:yEGFP:tADH1; 3xV5_Rap1-N-terminal; sir4Δ::k.l.URA3; matΔ::k.l.LEU2*
JRy15341	Δ	*hmlα2Δ::CRE, ura3Δ::pGPD:loxP:yEmRFP;tCYC1:hygMX:loxP:yEGFP:tADH1; 3xV5_Rap1-N-terminal; sir4Δ::k.l.URA3; matΔ::k.l.LEU2*
JRy15343	Δ	*hmlα2Δ::CRE, hmlαp*Rap1bs-mutation, ura3Δ::pGPD:loxP:yEmRFP;tCYC1:hygMX:loxP:yEGFP:tADH1; 3xV5_Rap1-N-terminal ; sir4Δ::k.l.URA3; matΔ::k.l.LEU2*
JRy15344	Δ	*hmlα2Δ::CRE, hmlαp*Rap1bs-mutation, ura3Δ::pGPD:loxP:yEmRFP;tCYC1:hygMX:loxP:yEGFP:tADH1; 3xV5_Rap1-N-terminal ; sir4Δ::k.l.URA3; matΔ::k.l.LEU2*
JRy15346	Δ	*hmlα2Δ::CRE, hmlαp*Rap1bs-mutation, ura3Δ::pGPD:loxP:yEmRFP;tCYC1:hygMX:loxP:yEGFP:tADH1; 3xV5_Rap1-N-terminal ; sir3Δ::klURA3; matΔ::k.l.LEU2*
JRy15347	Δ	*hmlα2Δ::CRE, hmlαp*Rap1bs-mutation, ura3Δ::pGPD:loxP:yEmRFP;tCYC1:hygMX:loxP:yEGFP:tADH1; 3xV5_Rap1-N-terminal ; sir3Δ::klURA3; matΔ::k.l.LEU2*
JRy15212	α	S. paradoxus Z1.1 ho::HygMX ura3::KanMXBarcode TRP LEU HIS Rap1-2xV5
JRy15237	α	can1-100his3-11,15, leu2-3,112, -1, ura3, fpr1::NAT, RPL13A-2xFKBP12:: Rap1(134)-FRB_2xV5 bar1Δ::k.l.URA3 hmlαΔ::UniqueHMLwithSNPs TOR1(S1972I); hmrΔ::HygMX
JRy15238	α	can1-100his3-11,15, leu2-3,112, -1, ura3, fpr1::NAT, RPL13A-2xFKBP12:: Rap1(134)-FRB_2xV5 bar1Δ::k.l.URA3 hmlαΔ::UniqueHMLwithSNPs TOR1(S1972I); hmrΔ::HygMX
JRy15261	α	can1-100his3-11,15, leu2-3,112, -1, ura3, TOR1(S1972I), fpr1::NAT, RPL13A-2xFKBP12:: Rap1(134)-FRB_2xV5 bar1Δ::k.l.URA3 hmlαΔ::UniqueHMLwithSNPs sir4Δ::HIS3; hmrΔ::HygMX
JRy15262	α	can1-100his3-11,15, leu2-3,112, -1, ura3, TOR1(S1972I), fpr1::NAT, RPL13A-2xFKBP12:: Rap1(134)-FRB_2xV5 bar1Δ::k.l.URA3 hmlαΔ::UniqueHMLwithSNPs sir4Δ::HIS3; hmrΔ::HygMX
JRy15280	α	hmlΔ::NatMXhmrΔ::HygMX, 3xV5-Rap1; MATα-Rap1*bs mutant; RPB3-3xFLAG-KanMX
JRy15281	α	hmlΔ::NatMXhmrΔ::HygMX, 3xV5-Rap1; MATα-Rap1*bs mutant; RPB3-3xFLAG-KanMX
JRy15282	α	hmlΔ::NatMXhmrΔ::HygMX, 3xV5-Rap1; RPB3-3xFLAG-KanMX
JRy15283	α	hmlΔ::NatMXhmrΔ::HygMX, 3xV5-Rap1; RPB3-3xFLAG-KanMX

(continued on following page)

Table 2.1 *(continued from previous page)*

JRy15352	Δ	*hmlα2Δ::CRE, hmlαp*Rap1bs-mutation, ura3Δ::pGPD:loxP:yEmRFP;tCYC1:hygMX:loxP:yEGFP:tADH1; 3xV5_Rap1-N-terminal ; RPB3-3xFLAG-KanMX; hmrΔ::HygMX; matΔ::k.l.LEU2*
JRy15353	Δ	*hmlα2Δ::CRE, hmlαp*Rap1bs-mutation, ura3Δ::pGPD:loxP:yEmRFP;tCYC1:hygMX:loxP:yEGFP:tADH1; 3xV5_Rap1-N-terminal ; RPB3-3xFLAG-KanMX; hmrΔ::HygMX; matΔ::k.l.LEU2*
JRy15355	Δ	*hmlα2Δ::CRE, ura3Δ::pGPD:loxP:yEmRFP;tCYC1:hygMX:loxP:yEGFP:tADH1; 3xV5_Rap1-N-terminal; sir4Δ::k.l.URA3; RPB3-3xFLAG-KanMX; hmrΔ::HygMX; matΔ::k.l.LEU2*
JRy15356	Δ	*hmlα2Δ::CRE, ura3Δ::pGPD:loxP:yEmRFP;tCYC1:hygMX:loxP:yEGFP:tADH1; 3xV5_Rap1-N-terminal; sir4Δ::k.l.URA3; RPB3-3xFLAG-KanMX; hmrΔ::HygMX; matΔ::k.l.LEU2*
JRy15358	Δ	*hmlα2Δ::CRE, hmlαp*Rap1bs-mutation, ura3Δ::pGPD:loxP:yEmRFP;tCYC1:hygMX:loxP:yEGFP:tADH1; 3xV5_Rap1-N-terminal ; sir4Δ::k.l.URA3; RPB3-RxFLAG-KanMX; hmrΔ::HygMX; matΔ::k.l.LEU2*
JRy15359	Δ	*hmlα2Δ::CRE, hmlαp*Rap1bs-mutation, ura3Δ::pGPD:loxP:yEmRFP;tCYC1:hygMX:loxP:yEGFP:tADH1; 3xV5_Rap1-N-terminal ; sir4Δ::k.l.URA3; RPB3-RxFLAG-KanMX; hmrΔ::HygMX; matΔ::k.l.LEU2*
JRy15366	Δ	*matΔ::klLEU2 hmlα2Δ::CRE, ura3Δ::pGPD:loxP:yEmRFP;tCYC1:hygMX:loxP:yEGFP:tADH1; 3xV5_Rap1-N-terminal; hmrΔ::NatMX; ELF1-3xFLAGKanMX*
JRy15367	Δ	*matΔ::klLEU2 hmlα2Δ::CRE, ura3Δ::pGPD:loxP:yEmRFP;tCYC1:hygMX:loxP:yEGFP:tADH1; 3xV5_Rap1-N-terminal; hmrΔ::NatMX; ELF1-3xFLAGKanMX*
JRy15369	Δ	*matΔ::klLEU2 hmlα2Δ::CRE, ura3Δ::pGPD:loxP:yEmRFP;tCYC1:hygMX:loxP:yEGFP:tADH1; 3xV5_Rap1-N-terminal; hmrΔ::NatMX; SUA7-3xFLAGKanMX*
JRy15370	Δ	*matΔ::klLEU2 hmlα2Δ::CRE, ura3Δ::pGPD:loxP:yEmRFP;tCYC1:hygMX:loxP:yEGFP:tADH1; 3xV5_Rap1-N-terminal; hmrΔ::NatMX; SUA7-3xFLAGKanMX*
JRy15372	Δ	*hmlα2Δ::CRE, hmlαp*Rap1bs-mutation, ura3-1; 3xV5_Rap1-N-terminal ; hmrΔ::HygMX; matΔ::k.l.LEU2; ELF1-3xFLAGKanMX*
JRy15373	Δ	*hmlα2Δ::CRE, hmlαp*Rap1bs-mutation, ura3-1; 3xV5_Rap1-N-terminal ; hmrΔ::HygMX; matΔ::k.l.LEU2; ELF1-3xFLAGKanMX*
JRy15374	Δ	*hmlα2Δ::CRE, hmlαp*Rap1bs-mutation, ura3-1; 3xV5_Rap1-N-terminal ; hmrΔ::HygMX; matΔ::k.l.LEU2; SUA7-3xFLAGKanMX*
JRy15375	Δ	*hmlα2Δ::CRE, hmlαp*Rap1bs-mutation, ura3-1; 3xV5_Rap1-N-terminal ; hmrΔ::HygMX; matΔ::k.l.LEU2; SUA7-3xFLAGKanMX*
JRy15377	Δ	*hmlα2Δ::CRE, hmlαp*Rap1bs-mutation, ura3Δ::pGPD:loxP:yEmRFP;tCYC1:hygMX:loxP:yEGFP:tADH1; 3xV5_Rap1-N-terminal ; sir4Δ::k.l.URA3; hmrΔ::HygMX; matΔ::k.l.LEU2; ELF1-3xFLAGKanmX*

(continued on following page)

Table 2.1 *(continued from previous page)*

JRy15378	Δ	*hmlα2Δ::CRE, hmlαp*Rap1bs-mutation, ura3Δ::pGPD:loxP:yEmRFP;tCYC1:hygMX:loxP:yEGFP:tADH1; 3xV5_Rap1-N-terminal ; sir4Δ::k.l.URA3; hmrΔ::HygMX; matΔ::k.l.LEU2; ELF1-3xFLAGKanmX*
JRy15380	Δ	*hmlα2Δ::CRE, hmlαp*Rap1bs-mutation, ura3Δ::pGPD:loxP:yEmRFP;tCYC1:hygMX:loxP:yEGFP:tADH1; 3xV5_Rap1-N-terminal ; sir4Δ::k.l.URA3; hmrΔ::HygMX; matΔ::k.l.LEU2; SUA7-3xFLAGKanmX*
JRy15403	Δ	*hmlα2Δ::CRE, ura3Δ::pGPD:loxP:yEmRFP;tCYC1:hygMX:loxP:yEGFP:tADH1; 3xV5_Rap1-N-terminal; sir4Δ::k.l.URA3; hmrΔ::HygMX; matΔ::k.l.LEU2; ELF1-3xFLAG-Kanmx*
JRy15404	Δ	*hmlα2Δ::CRE, ura3Δ::pGPD:loxP:yEmRFP;tCYC1:hygMX:loxP:yEGFP:tADH1; 3xV5_Rap1-N-terminal; sir4Δ::k.l.URA3; hmrΔ::HygMX; matΔ::k.l.LEU2; ELF1-3xFLAG-Kanmx*
JRy15406	Δ	*hmlα2Δ::CRE, ura3Δ::pGPD:loxP:yEmRFP;tCYC1:hygMX:loxP:yEGFP:tADH1; 3xV5_Rap1-N-terminal; sir4Δ::k.l.URA3; hmrΔ::HygMX; matΔ::k.l.LEU2; SUA7-3xFLAG-Kanmx*
JRy15431	Δ	*matΔ::klLEU2 hmlα2Δ::CRE, ura3Δ::pGPD:loxP:yEmRFP;tCYC1:hygMX:loxP:yEGFP:tADH1; 3xV5_Rap1-N-terminal; hmrΔ::NatMX; RPB3-3xFLAG-KanMX*
JRy15432	Δ	*matΔ::klLEU2 hmlα2Δ::CRE, ura3Δ::pGPD:loxP:yEmRFP;tCYC1:hygMX:loxP:yEGFP:tADH1; 3xV5_Rap1-N-terminal; hmrΔ::NatMX; RPB3-3xFLAG-KanMX*
JRy15435	α	hmlΔ::NatMXhmrΔ::HygMX, 3xV5-Rap1; MATα-Rap1*bs, TAF1-3xFLAG-KanMX
JRy15436	α	hmlΔ::NatMXhmrΔ::HygMX, 3xV5-Rap1, TAF1-3xFLAG-KanMX
JRy15437	α	hmlΔ::NatMXhmrΔ::HygMX, 3xV5-Rap1, TAF1-3xFLAG-KanMX
JRy15438	Δ	*matΔ::klLEU2 hmlα2Δ::CRE, ura3Δ::pGPD:loxP:yEmRFP;tCYC1:hygMX:loxP:yEGFP:tADH1; 3xV5_Rap1-N-terminal; hmrΔ::NatMX; TAF1-3xFLAGKanMX*
JRy15439	Δ	*matΔ::klLEU2 hmlα2Δ::CRE, ura3Δ::pGPD:loxP:yEmRFP;tCYC1:hygMX:loxP:yEGFP:tADH1; 3xV5_Rap1-N-terminal; hmrΔ::NatMX; TAF1-3xFLAGKanMX*
JRy15440	Δ	*hmlα2Δ::CRE hmlαp*Rap1bs-mutation, ura3-1; 3xV5_Rap1-N-terminal ; hmrΔ::HygMX; matΔ::k.l.LEU2; TAF1-3xFLAGKanMX*
JRy15441	Δ	*hmlα2Δ::CRE hmlαp*Rap1bs-mutation, ura3-1; 3xV5_Rap1-N-terminal ; hmrΔ::HygMX; matΔ::k.l.LEU2; TAF1-3xFLAGKanMX*
JRy15442	Δ	*hmlα2Δ::CRE, ura3Δ::pGPD:loxP:yEmRFP;tCYC1:hygMX:loxP:yEGFP:tADH1; 3xV5_Rap1-N-terminal; sir4Δ::k.l.URA3; hmrΔ::HygMX; matΔ::k.l.LEU2; TAF1-3xFLAG-Kanmx*
JRy15443	Δ	*hmlα2Δ::CRE,ura3Δ::pGPD:loxP:yEmRFP;tCYC1:hygMX:loxP:yEGFP:tADH1; 3xV5_Rap1-N-terminal; sir4Δ::k.l.URA3; hmrΔ::HygMX; matΔ::k.l.LEU2; TAF1-3xFLAG-Kanmx*

(continued on following page)

Table 2.1 *(continued from previous page)*

JRy15444	Δ	*hmlα2Δ::CRE, hmlαp*Rap1bs-mutation, ura3Δ::pGPD:loxP:yEmRFP;tCYC1:hygMX:loxP:yEGFP:tADH1; 3xV5_Rap1-N-terminal ; sir4Δ::k.l.URA3; hmrΔ::HygMX; matΔ::k.l.LEU2; TAF1-3xFLAGKanmX*
JRy15445	Δ	*hmlα2Δ::CRE, hmlαp*Rap1bs-mutation, ura3Δ::pGPD:loxP:yEmRFP;tCYC1:hygMX:loxP:yEGFP:tADH1; 3xV5_Rap1-N-terminal ; sir4Δ::k.l.URA3; hmrΔ::HygMX; matΔ::k.l.LEU2; TAF1-3xFLAGKanmX*
JRY10790	a	hmlα2Δ::CRE , ura3Δ::pGPD:loxP:yEmRFP;tCYC1:hygMX:loxP:yEGFP:tADH1
JRY12923	Δ	can1-100his3-11,15, leu2-3,112, -1, ura3, matΔ::K.lactisLEU2, TOR1(S1972I), fpr1::NAT, RPL13A-2xFKBP12::
JRy15446	Δ	matΔ::kanMX lys2 his3-11,15 leu2-3,112 can1-100 -1 ura3-1 hmrD::hygMX; hmlαp*Rap1bs-mutation
JRy15447	Δ	matΔ::kanMX lys2 his3-11,15 leu2-3,112 can1-100 -1 ura3-1 hmrD::hygMX;hmlαp*Rap1bs-mutation
JRy15449	Δ	matΔ::kanMX lys2 his3-11,15 leu2-3,112 can1-100 -1 ura3-1 hmrD::hygMX sir3D::K.l.URA3; hmlαp*Rap1bs-mutation
JRy15450	Δ	matΔ::kanMX lys2 his3-11,15 leu2-3,112 can1-100 -1 ura3-1 hmrD::hygMX sir3D::K.l.URA3; hmlαp*Rap1bs-mutation
JRY14511	a	MATa can1-100 his3-11,15 leu2-3,112 lys2 ura3D::GPDpro-loxP-yEmRFP-CYC1term-HygMX-loxP-yEGFP-ADH1term hmlα2Δ::CRE hmlαp*Rap1bs-mutation
JRY14513	a	MATa can1-100 his3-11,15 leu2-3,112 lys2 ura3D::GPDpro-loxP-yEmRFP-CYC1term-HygMX-loxP-yEGFP-ADH1term hmlα2Δ::CRE hmlαp*Rap1bs-mutation sir1Δ::LEU2
JRY14514	a	MATa can1-100 his3-11,15 leu2-3,112 lys2 ura3D::GPDpro-loxP-yEmRFP-CYC1term-HygMX-loxP-yEGFP-ADH1term hmlα2Δ::CRE sir1Δ::LEU2
JRY14515	a	MATa can1-100 his3-11,15 leu2-3,112 lys2 ura3D::GPDpro-loxP-yEmRFP-CYC1term-KanMX-loxP-yEGFP-ADH1term hmlα2Δ::CRE hmlαp*Rap1bs-mutation)
JRY14517	a	MATa can1-100 his3-11,15 leu2-3,112 lys2 ura3D::GPDpro-loxP-yEmRFP-CYC1term-KanMX-loxP-yEGFP-ADH1term hmlα2Δ::CRE hmlαp*Rap1bs-mutation sir1Δ::LEU2
JRY14518	a	MATa can1-100 his3-11,15 leu2-3,112 lys2 hmrΔ::NatMX ura3D::GPDpro-loxP-yEmRFP-CYC1term-HygMX-loxP-yEGFP-ADH1term hmlα2Δ::CRE hmlαp*Rap1bs-mutation sir1Δ::LEU2
JRY14520	a	MATa can1-100 his3-11,15 leu2-3,112 lys2 hmrΔ::NatMX ura3D::GPDpro-loxP-yEmRFP-CYC1term-HygMX-loxP-yEGFP-ADH1term hmlα2Δ::CRE sir1Δ::LEU2
JRY14521	a	MATa can1-100 his3-11,15 leu2-3,112 lys2 hmrΔ::NatMX ura3D::GPDpro-loxP-yEmRFP-CYC1term-KanMX-loxP-yEGFP-ADH1term hmlα2Δ::CRE hmlαp*Rap1bs-mutation

Table 2.2 All oligonucleotides utilized in Chapter 2, with descriptions.

Oligonucleotide Sequence (5´-> 3´)	Description
GACTTTGGTGCAGTTTCAAAATCATC	F-oligo for Rap1 N-term Cas9 guideRNA
AAACGATGATTTTGAAACTGCACCAA	R-oligo for Rap1 N-term Cas9 gRNA
CTACATAAGACACTATTTGCGTACAGATTATCTCAATATGGGTAAACCTATACCTAATCC	Forward primer for amplifying 3xV5 to put into N-term of Rap1
CATATTCTGCTGGTGCAGTTTCAAAATCATCTCGACTAGATGTACTATCCAGTCCTAATA	Reverse primer for amplifying 3xV5 to put into N-term of Rap1
GACTTT GGTTTTGTTTGGGATGCAAT	F gRNA for α2P rap1bs mutation
AAAC ATTGCATCCCAAACAAAACC AA	R gRNA for α2P rap1bs mutation
ATATTTTTAAGTTCCAACATTTTATGTTTCAAAACATTAATGATGTCTGTCTTTTGTTTG	F repair template for alpa2p rap1bs mutation
TGATGTACTTTTCTACATTGGGAAGCAATAAATTGCATCCCAAACAAAAGACAGACATCA	R repair template for alpa2p rap1bs mutation
GACTTT ACATGAAATTCTATCTTAAT	F guide for s paradoxus Rap1-2xV5
AAAC ATTAAGATAGAATTTCATGT AA	R guide for s paradoxus Rap1-2xV5
GTGAGTGGTCCTCCTCTGTCAAACATGAAATTCTATCTTAATGGAGGTGGTGGTGGTTCT	F repair for inserting Rap1-134(FRB-2xV5) into s paradoxus
GATCAATGTCATTCAAAGAATCATGCGCATCAGCGTCGCGTGAGTCCAGTCCTAGCAGTG	R repair for inserting Rap1-134(FRB-2xV5) into s paradoxus
GACTTTATTCTATCTTAATCGCGACG	F primer for sgRNA at aa134 in Rap1 in S cerevisiae
AAACCGTCGCGATTAAGATAGAATA	R primer for sgRNA at aa134 in Rap1 in S cerevisiae
AAGTGGTCCTCCTCTGTCAAATATGAAATTCTATCTTAATGGAGGTGGTGGTGGTTCT	F primer to amplify (FRB-2xV5) to insert into cerevisiae Rap1-134
GATCAATATCATTTAAAGAGTCATGCGCATCAGCGTCGCGTGAGTCCAGTCCTAGCAGTG	R primer to amplify (FRB-2xV5) to insert into cerevisiae Rap1-134
CTTTTCGATGGATGAAGAATTCAAAAATATGGACTGCATTCGGATCCCCGGGTTAATTAA	F primer to add 13xMyc-KanMX to Sir3
GCATATCTATGGCGGAAGTGAAAATGAATGTTGGTGGTCAGAATTCGAGCTCGTTTAAAC	R primer to add 13xMyc-KanMX to Sir3

(continued on following page)

Table 2.2 *(continued from previous page)*

AATGGGTAATACTGGATCAGGAGGGTATGATAATGCTTGGAGG GAACAAAAGCTGGAG	F primer to add 3xFLAG-kanmx to RPB3-cterm
CTTGTTTTTTTTCCTCTATTACGCCCACTTGAGAACTACAGTATA GCGACCAGCATTCAC	R primer to add 3xFLAG-kanmx to RPB3-cterm
TAAAAGAGGCAGAGGCGCCTTGGTAGATAGTGACGATGAA AGGGAACAAAAGCTGGAG	F primer to add 3xFLAG-kanmx to ELF1-cterm
GACCTAAGTAAATATTGTTTTTTCTCAGGACCGGATTA CAGTATAGCGACCAGCATTCAC	R primer to add 3xFLAG-kanmx to ELF1-cterm
TGTAGTGTCTTTGGATAACTTACCGGGCGTTGAAAAGAAA AGGGAACAAAAGCTGGAG	F primer to add 3xFLAG-kanmx to SUA7-cterm
TTCTTGTTCCTATAATTTACTGTTTTATCACTTCATTA CAGTATAGCGACCAGCATTCAC	R primer to add 3xFLAG-kanmx to SUA7-cterm
TCCAATGTATAGCAGTAAAGATAACCCTGCTTCACCAAAG AGGGAACAAAAGCTGGAG	F primer to add 3xFLAG-kanmx to TAF1-cterm
AAGTTTTATTCGATCAATACATCGTTATACTGAATCTA CAGTATAGCGACCAGCATTCAC	R primer to add 3xFLAG-kanmx to TAF1-cterm
GACTTTATTCTATCTTAATCGCGACG	F primer for sgRNA at aa134 in Rap1
AAACCGTCGCGATTAAGATAGAATA	R primer for sgRNA at aa134 in Rap1
AAGTGGTCCTCCTCTGTCAAATATGAAATTCTATCTTAATGGAG GTGGTGGTGGTTCT	F primer to amplify 2xV5-FRB to insert into Rap1-134
GATCAATATCATTTAAAGAGTCATGCGCATCAGCGTCGCGTGA GTCCAGTCCTAGCAGTG	R primer to amplify 2xV5-FRB to insert into Rap1-134
CGTTGCCATGTTGTTGTATG	ALG9 qPCR F
GCCAGCCTAGTATACTAGCC	ALG9 qPCR R
TCCACAAATCACAGATGAGT	α2 CDS qPCR F
GTTGGCCCTAGATAAGAATCC	α2 CDS qPCR R
AAGTTCCAACATTTTATGTTTC	α2-P qPCR F
CATAAAAAGTGAAGGTTAAAAGAAG	α2-P qPCR R

Table 2.3 geneBlocks used in combination with gDG1 (Goodnight and Rine 2020) to generate SNPs in *HML* for experiments and analysis in figures 2.4 and 2.5.

Oligonucleotide Sequence (5´-> 3´)	**Description**
TTGTATTAGACGAGGGACGCAGTGATTTTTGTGTTTGTTTTTAATTAA TTGTGGGATAGGATAGTACCAACTCTTGGAGGAGAGCATTGTGAGT TGTCCAGTCTCTGAAGTTAACTAGTAAGTTTGCGGAGTCAAAGGCG GATGGCTTTTGCCATTTGTGACAGTTGTGCGGCAGCATCTTATTGAA ATAGAGCTGTATTCTGAAGTCCTCTTGTAGAACATCATCCATAGTAA AAAGTAAATCGTCCTGTCCGATTACGAGCTGTAGTAGTGCTGAGAC CCTCTGTATATTTACGTTGCGATGAAGAAGGTAATGGGCGATATATT GATACAATTCCTGAGTTGCATCTTGGATTGAGTTTACGAAGGGTGG CCAGACGGCCAGAAACCTCCAGCCGGAGTTAACAACTAGTAATACG CCATCCATGTTTGCATCAGCGCCGTGCCTATACCAGTCACTGAGTA GAGGTTTTCTTGCTCTTTTTATGTCCAGACTTCTTTTGACGAGGGGG CATACTCTAGAGACACAGGCAGTTGCTTGCAGCAACTGCCGTACGG CCGTTCACATGCTGTCGAGGATTTTTTTTGGGACGATATTGTCATTA TAGGGCAGTGTGTGACTTATGAATTGTTGTAGTAGGACGTCTGTGA TGTTGGAGATTTGTATTTTGTTAACTCTTCTTGACACAATTTGGCCCT GGATAGCGAAGCCTGCGGTTACAAATAGGTCG	geneBlock 1 for unique HML
AATAGAAAAGAGCTTTTTATTTATGTCTAGTATGCTGGATTAAAACTC ATCTGTGATTTGTGGATTTAGAAGGTCTTTAATGGGTATTTTATTCAT TTTTACTTGCTTATCTTCCTTTTTTTCTTGCCCAGTTCTAAGCTGATTT CAATCTCTCCATTATATATATTTTTAAGTTCCAACATTTTAAGTTACAA AACATTAATGATGTCTGGGTTTTGTTTCGGATGCAATTTATTGCTTCC CAATGTAGAATAGTACATCATATGAAACAACTTAAACTCATAACTACT TCTTTTAACCTTCACTTTTTAAGAAATGTATCAACCATATATAATAACT TATTAGACGACATTCACAATATGTTTACATCGAAGCCTGCTTTCAAA ATTAAGAACAAGGCATCCTAATCATACAGAAACACAGCGGTATCAAA AAAGCTGAAAGAAAAACGTCTAGCAGAGCATGTGAGGCCAAGCTGC TTCAATATAATTCGACCACTCAAGAAAGATATCCAGATACCTGTTCC TTCCTCTCGATTTTTAAATAAGATCCAAATTCACAGGATAGCGTCTG GAAGCCAAAATACTCAGTTTCGACAGTTCAATAAAACATCTATAAAA TCTTCAAAGAAATATTTGAACTCATTTATGGCTTTTAGAGCATACTAC TCACAGTTTGGCTCCGGTGTAAAACAGAATGTCTTGTCTTCTCTGCT CGCTGAAGATTGGCACGCGGACAAAATGCAGCACGGAATATGGGA CTACTTCGCGCAACAGTATAATTTTATA	geneBlock 2 for unique HML

Chapter 3:

Investigating the mechanism of subtelomeric silencing in *S. cerevisiae*

3.1 Abstract

For over 40 years, *Saccharomyces cerevisiae* have provided a model for the study of constitutive, chromatin-mediated silencing at the cryptic mating loci *HML* and HMR. Silent Information Regulator (Sir) proteins impart transcriptional silencing through the formation of heterochromatin at the silent mating-type loci *HML* and *HMR*, and at telomeres. Transcription of genes at silenced *HML* and *HMR* is at least 1000-fold lower in *SIR* than *sirΔ* cells (Osborne *et al.* 2011; Dodson and Rine 2015). In contrast, silencing of genes near telomeres, while involving the same machinery, appears to achieve an intermediate level of repression that varies quantitatively from locus to locus (Aparicio *et al.* 1991; Wellinger and Zakian 2012; Ellahi *et al.* 2015). Why such disparities in the degree of silencing at different loci exist and how this tuning is mechanistically achieved remains enigmatic. At telomeres, early experiments informed a model in which a decreasing gradient of repression of genes from telomere-proximal to telomere-distal occurred in response to the spreading of Sir proteins from initiating sites at the $C_{1\text{-}3}A$ repeats formed by telomerase (Gottschling 1992). Recent studies of the binding patterns of Sir proteins have called this model into question, and suggested that Sir proteins bind at discrete loci, rather than extending in a gradient from the telomere (Radman-Livaja *et al.* 2011a; Ellahi *et al.* 2015). These measurements, and all previous reporter-based investigations of silencing at the subtelomeric domains, came from measurements of the average expression of genes in a population of cells, precluding the ability to understand what happens at the level of individual cells; whether the extent of repression measured at a subtelomeric locus results from uniform repression of that locus in all cells, or complete silencing in some cells and full expression of that same gene in others. Subtelomeric domains are enriched in genes of metabolic function, so a degree of stochasticity in expression at the single-cell level might exist to enable environment-specific responses. By developing an acutely-sensitive single- cell-based assay for gene expression at multiple telomeres and uncovering mechanistic features unique to telomeric silencing, this work aimed to uncover the principles governing silencing within subtelomeric domains and its importance in regulating cells in response to their environment.

3.2 Introduction

The stabile patterns of gene expression are mediated, in part, by the physical packaging of the eukaryotic genome into the nucleus. Modifications to chromatin and DNA-bound protein complexes promote differential regulation via recruitment, and restriction, of transcriptional activators and repressors (reveiwed in Rando and Winston 2012). Hence the coarse partitioning of the genome into regions of actively expressed euchromatin and repressed heterochromatin is a fundamentally important process.

Determined to be regional and sequence independent, heterochromatin is epigenetically inherited as cells divide with the ability to reversibly switch between on and off states over multiple generations (reviewed in Gartenberg and Smith 2016). The genomic scales over which regulation occurs vary from promoter-specific activation or repression of individual genes to entire chromosomes by a common regulatory complex, as seen in the mechanism of dosage compensation of sex chromosomes in *D. melanogaster* and *C. elegans* (Meyer and Casson 1986; Conrad *et al.* 2012). Heterochromatin also facilitates regional, promoter-independent repression at well-defined loci (reviewed in Grunstein and Gasser 2013). In *Saccharomyces cerevisiae* domains of heterochromatin are established and maintained by the activity of the four Silent Information Regulator proteins Sir1, Sir2, Sir3, and Sir4 (Hicks *et al.* 1979; Rine *et al.* 1979; Rine and Herskowitz 1987). Sir proteins mediate repression of genes at telomeres, the cryptic mating loci *HML*a and *HMRa*, and the rDNA locus (Rusche *et al.* 2003).

To localize heterochromatin in *Saccharomyces cerevisiae*, the Sir complex must be recruited to sites of nucleation, termed silencers (Abraham *et al.* 1984; Feldman *et al.* 1984; Brand *et al.* 1985; Mahoney and Broach 1989; Laurenson and Rine 1992). At the auxiliary mating cassettes, these nucleation sites are *cis*-acting regulatory elements flanking *HML* and *HMR* comprising of binding sites for the transcription factors Abf1, Rap1, and ORC (Shore *et al.* 1987; Shore and Nasmyth 1987a; Buchman *et al.* 1988a; Kimmerly *et al.* 1988; Bell *et al.* 1993; Foss *et al.* 1993). Silencers are located several hundred base pairs from the bidirectional promoters of *HML*α and *HMRa* and are necessary for silencing gene expression. In contrast to silencing at *HML* and *HMR,* Sir-complex recruitment to telomeres occurs independent of Sir1 (Buchman *et al.* 1988a; Longtine *et al.* 1989; Stavenhagen and Zakian 1998). Instead, Sir3 and Sir4 are recruited to the array of Rap1 found bound among the $C_{1\text{-}3}A$ repeats generated by telomerase (Hecht *et al.* 1995; Lustig *et al.* 1996). Interactions in the carboxyl-terminal domain of Rap1 with Sir3 and Sir4 facilitate heterochromatin formation at telomeres (Lustig *et al.* 1990; Kyrion *et al.* 1993; Cockell *et al.* 1995; Moretti and Shore 2001).

At telomeres, the position-effect variegation (PEV) described by the ability of silencing machinery to impart repression, in an epigenetic and metastable manner, on genes inserted within and adjacent to heterochromatin, is known as telomere position effect (TPE) (Gottschling *et al.* 1990; Stavenhagen and Zakian 1998). Research beginning with Gottschling and colleagues in 1990 informed the field of TPE in yeast. Results from these early experiments led to a prevailing model positing strong repression of genes at or near telomeres, with a decreasing gradient of repression of genes from telomere-proximal to telomere-distal, reflecting variation in the extent of spreading of Sir proteins from telomeres (**figure 3.1**) (Gottschling *et al.* 1990; Aparicio *et al.* 1991; Gottschling 1992; Renauld *et al.* 1993). Further investigation reveals that TPE is varied in strength and occurrence at natural telomeres, calling into question this model (Pryde and Louis 1999; Takahashi *et al.* 2011; Ellahi *et al.* 2015). Furthermore, the common *URA3*-based silencing assay utilized by these experiments may not accurately reflect heterochromatin in all contexts. Instead this assay may reflect an imbalance of ribonucleotide levels, perturbing metabolic processes necessary for growth and thus obfuscating measurement (Rossmann *et al.* 2011; Takahashi *et al.* 2011). Given these

confounding factors, the mechanism by which subtelomeric silencing occurs, and its similarity or difference from constitutive heterochromatin found at loci such as *HML* and *HMR,* remains elusive. This work aimed to study the extent to which Sir binding is responsible for the under-expression, and potential heterochromatic repression, of subtelomeric genes. These experiments were designed and conducted before the work published in Brothers and Rine 2022 (Brothers and Rine 2022), which illuminated the nuances of Sir protein recruitment and spread at subtelomeres. Furthermore, these studies were not completed due to technical reasons and therefore, while thoroughly conceptualized, they are lacking in results.

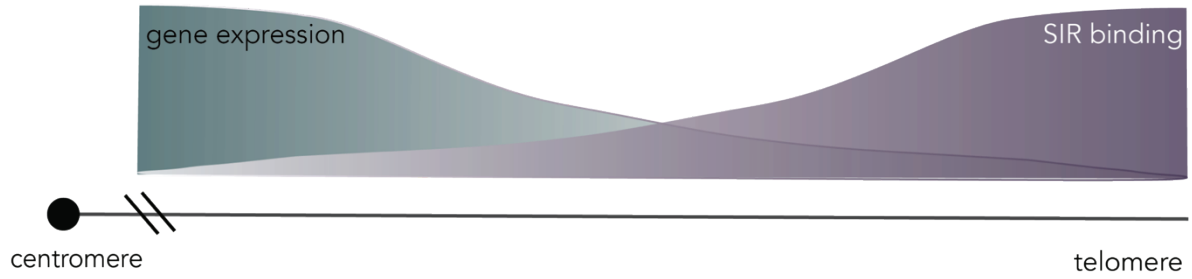

Figure 3.1: The "Gottschling gradient" model of telomere position effect as it relates to Sir protein binding and gene expression.

3.3 Results

3.3.1 A fluorescent reporter system to determine whether silencing is a function of distance from telomere

Reporter genes placed at a few positions on two truncated telomeres (specifically *VII-L* and *V- R*) led to the conclusion that there is a Sir-dependent correlation between distance from telomere and gene expression level (Gottschling *et al.* 1990; Aparicio *et al.* 1991; Gottschling 1992; Renauld *et al.* 1993). More recent data from studies at natural telomeres has revealed this simplistic gradient model to be unrepresentative (Takahashi *et al.* 2011; Thurtle and Rine 2014; Ellahi *et al.* 2015). Rather than being found in a gradient, Sir proteins are located to discrete peaks along subtelomeric domains. Furthermore, only 6% of genes in this region show de-repression of greater than 2-fold in *sirΔ* cells. However, the field still largely operates under the definition of telomere position-effects as originally defined with promoter-independent and domain-specific repression of genes varying with proximity to telomere (**figure 3.1**). Here, I examined whether silencing is truly a function of distance from telomere, based upon the hypothesis that Sir-based silencing increases in a gradient towards the telomere. To test this hypothesis, I generated genetically encoded fluorophores under the control of a Sir-dependent promoter as defined in (Ellahi *et al.* 2015). The gradient model of Sir-dependent telomeric silencing predicts that the expression of a gene 2kb from the telomeric repeats will always be more lowly expressed than the same gene 5kb from the chromosome end, which in turn would be lower than one at 20kb (**figure 3.2**). This model also requires that this gradient of expression be abolished in a *sirΔ* cell **(figure 3.2**). If, instead, no change in the pattern of expression of the reporter genes is observed in *sirΔ* cells, the exciting

possibility of an alternative form of repression must be considered. While reminiscent of the original experiments of Gottschling and colleagues (Aparicio *et al.* 1991; Gottschling 1992; Renauld *et al.* 1993), the experimental design presented here was robust to metabolic effects. Moreover, the strength of this assay lay in the ability to accurately read relative measurements of expression from loci in *cis* along a single chromosome arm within the same cell. Furthermore, combining the fluorescent reporters with flow cytometry would allow for single-cell resolution of expression in thousands of cells in a relatively short period of time.

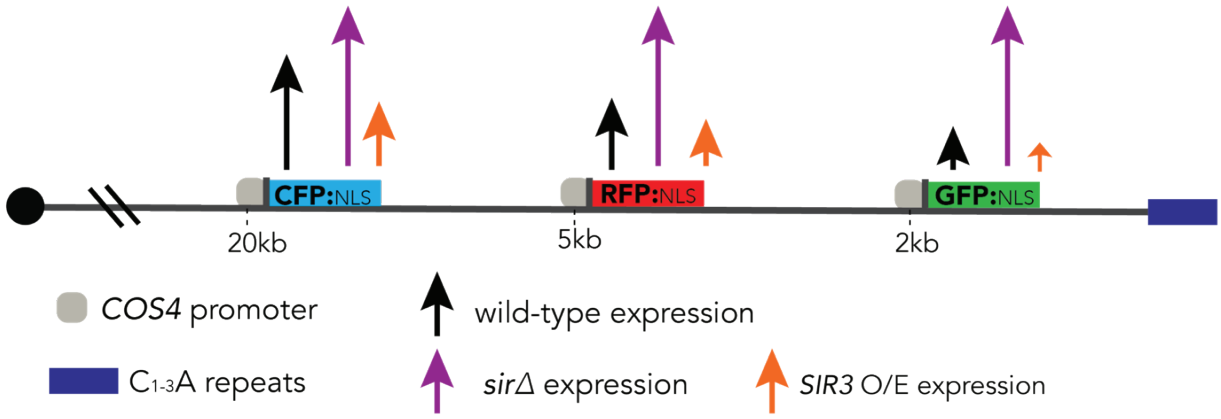

Figure 3.2: A graphical representation of the three-color fluorescent reporter system and how expression patterns would change in the presence of absence of Sir proteins if the gradient model were correct.

Ideally, I aimed to integrate three fluorophores driven by the same promoter at defined positions along one chromosome arm with CRISPR/Cas9-based genome editing (**figure 3.2**). As subtelomeric loci are lowly expressed in relation to most genes in the genome, I added a nuclear localization signal to the fluorescent reporters to increase the brightness and sensitivity of this assay by concentrating the fluorescent signal to the smaller volume of the nucleus (Osborne *et al.* 2011). The fluorescent protein reporters were driven by a common promoter, *COS4*-p, which was defined as a subtelomeric gene that undergoes Sir-based silencing (Ellahi *et al.* 2015). As it is impossible to directly compare fluorescence intensities of different fluorophores, I began by integrating *COS4*p-RFP-PEST.NLS constructs at a locus 2kb or 5kb from the end of telomere *VI-L* (**figure 3.3.A**). I confirmed expression of each reporter with microscopy (figure **3.3.B,C**). I then compared fluorescence intensity of one such reporter when inserted 2kb from the telomeric repeats, versus 5kb (**figure 3.3.D**). I quantified fluorescence intensities using the common imaging software FIJI. My preliminary data revealed a modest, approximately 20% increase in fluorescence, and thus expression, when the reporter was 5kb from the telomere as compared to 2kb (**figure 3.3.D**). While these data lightly supported the idea that expression varied as a function of distance from telomere, the number of events measured, and the accuracy of the measurements, was lacking and thus largely inconclusive. I then quantified the fluorescence intensities of each of these reporters using flow cytometry. I found an approximate 2-fold increase in the average

expression of the RFP reporter when distance from telomere was increased (**figure 3.3.E**).

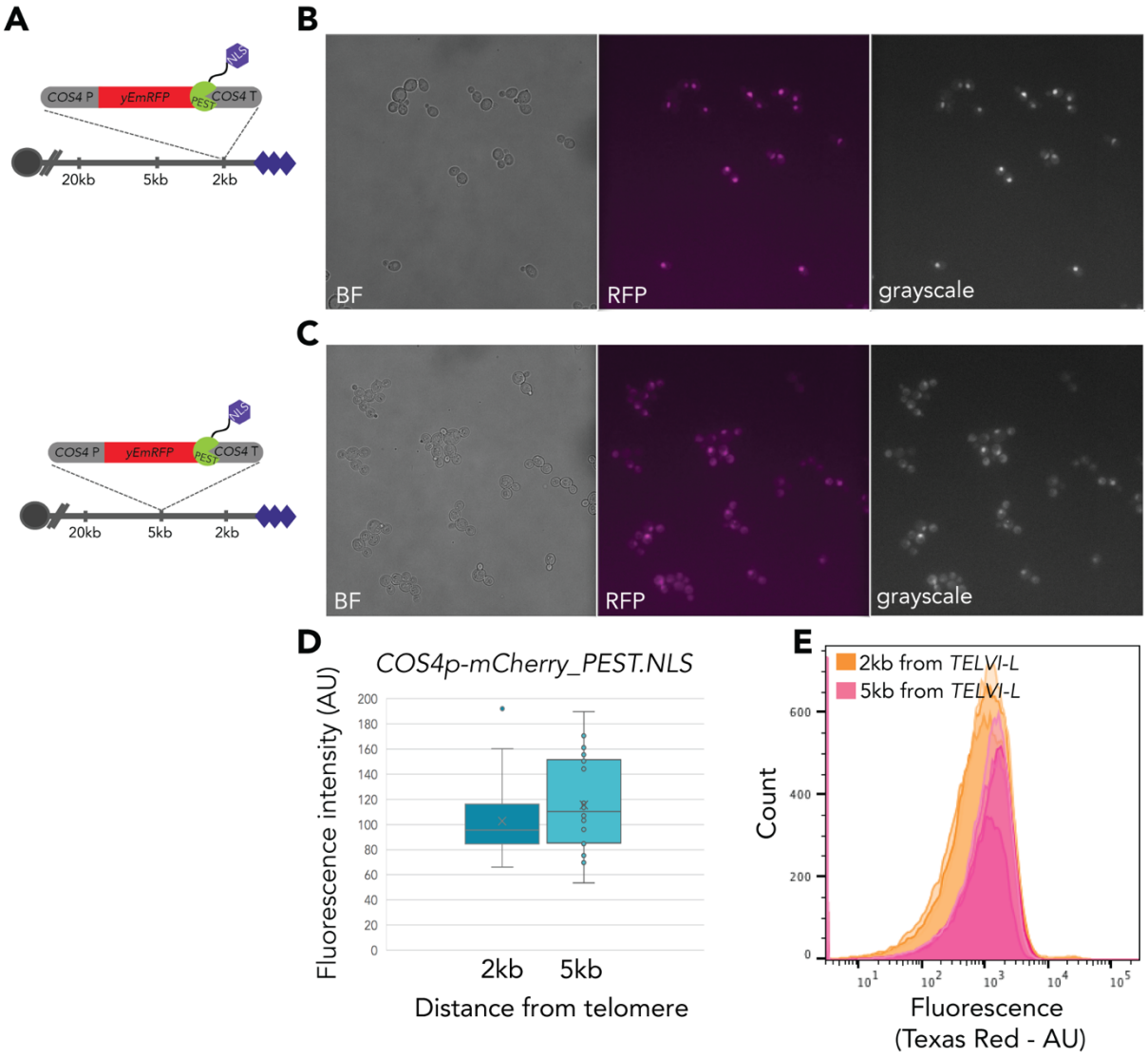

Figure 3.3: Increasing distance from telomere of fluorescent reporter increased average, but not ultimate, fluorescence intensity.

A. Schematic of integrated yeast optimized RFP reporters driven by the *COS4* promoter, with both a PEST and Nuclear Localizatin Signal, and inserted at 2kb or 5kb from the end of telomere *VI-L*.
B. Fluorescence microscopy images of reporter located 2kb from chromosome end. Images are of bright field, RFP, and grayscale.
C. Same as (B) but for reporter 5kb from chromosome end.
D. Quantification of differences in fluorescence between (B) and (C) based on microscopy and imaging software.
E. Quantification of changes in fluorescence between the two reporters in (A) using flow cytometry.

Next, to assess the degree to which expression or silencing of each of these fluorophores was dependent on Sir proteins, I treated cells with the anti-silencing compound nicotinamide (**figure 3.4.A,D**). Nicotinamide (NAM) is a byproduct of the enzymatic deacetylation of histone H4K16 performed by Sir2 (Bitterman *et al.* 2002). When in excess, it is known to inhibit all homologs of Sir2 (HSTs), therefore acting as a proxy for *sir2Δ* cells. I therefore compared fluorescence intensities in cells grown in standard yeast media, YPD, versus those grown in YPD supplemented with NAM. There was no discernible difference in fluorescence intensity between each of the growth conditions by eye, for either an RFP or YFP reporter inserted 2kb from the telomeric repeats on chromosome *VI-L* (**figure 3.4.B,E**). To generate a more robust and quantifiable dataset, I used flow cytometry to measure differences in fluorescence of these reporter constructs in the two growth conditions and found that average, but not ultimate, expression of each reporter increased by approximately 3-fold in the presence of NAM (**figure 3.4.C,F**). These data supported the hypothesis that the extent to which silencing at subtelomeric loci was dependent on Sir proteins was less than at *HML* and *HMR.*

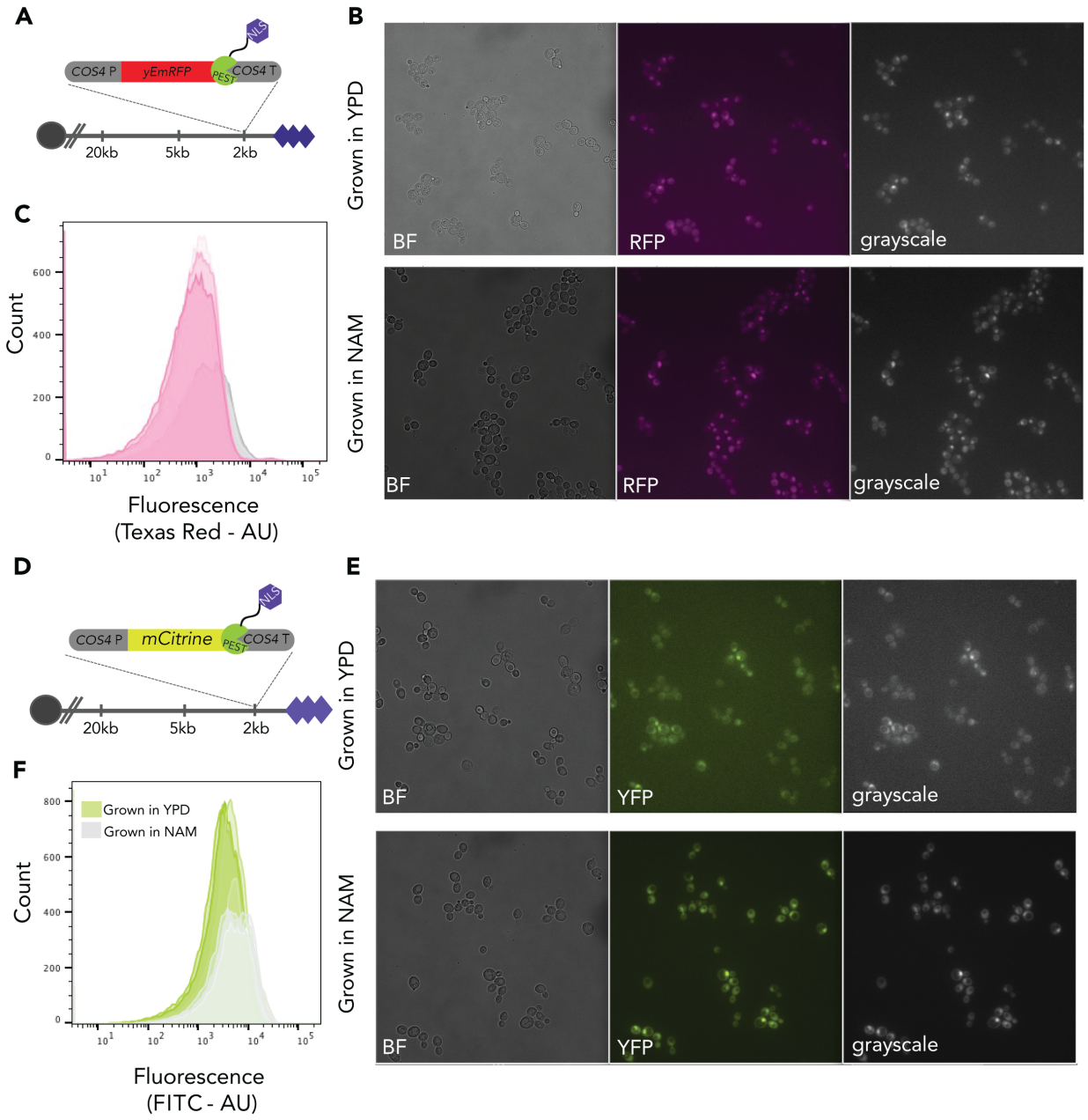

Figure 3.4: Chemical inhibition of silencing led to modest increase in fluorescence intensity of two reporters.

A. Schematic of integrated yeast optimized RFP reporter driven by the *COS4* promoter, with both a PEST and Nuclear Localizatin Signal, and inserted at 2kb or 5kb from the end of telomere *VI-L.*

B. Fluorescence microscopy images of reporter in (A). Images are of bright field, RFP, and grayscale. Top row depicts cells grown in YPD (silenced). Bottom row depicts cells grown in YPD + NAM (unsilenced).

C. Quantification of cells in (B) by flow cytometry.

D-F. Same as (A-C) but with mCitrine reporter.

3.3.2 Investigating spatial co-regulation of genes in subtelomeric domains at single cell resolution

While subtelomeric loci are generally lowly expressed, only a fraction of them are de-repressed in *sirΔ* cells (Ellahi *et al.* 2015). These findings from bulk RNA measurements from populations of cells, precluding the ability to determine whether this intermediate level of repression is the result of high-level expression in a fraction of cells but none in the majority, or an overall lower level of expression. While the experiments described above allowed for targeted and controlled examination of the effect of linear position along a chromosome on silencing, they were limited in the resolution to gain insight into the larger question of spatial co-regulation of endogenous loci in yeast. Furthermore, to evaluate the relative expression of a number of loci on the same chromosome arm, even four-color single-molecule RNA-FISH is limited in the clarity of detection of individual transcripts. To this end, I attempted a technique of sequential RNA-FISH+ (seq-FISH+) (Lubeck *et al.* 2014; Eng *et al.* 2019) to determine whether genes were spatially co-regulated on a cell-to-cell basis, and if that was a function of their proximity to Sir peaks.

Seq-FISH+ is a technique developed by Cai and colleagues (Lubeck *et al.* 2014; Eng *et al.* 2019) wherein primary, RNA sequence-specific probes are hybridized to loci in fixed cells and then secondary probes, coupled to different fluorophores are hybridized to those (**figure 3.5**). These spots are then imaged, creating a pseudocolor per primary probe per locus, stripped, and re-hybridized with a different set of secondary probes. After several rounds of this procedure the readout of each mRNA is a color sequence that defines a unique barcode to that transcript. This technique vastly expands the capacity to measure the exact transcriptional output of many endogenous loci in single cells. By quantifying transcript abundances, I aimed to determine whether a locus was uniformly repressed in all cells, or alternatively, highly transcribed in some cells while silent in others, and whether the surrounding loci behave similarly (**figure 3.6**). Performing this experiment in *SIR* and *sirΔ* cells would yield data quantifying the expression of two classes of genes: those that were subject to telomere position effects where Sir proteins resided, and those that appeared under-expressed by telomere position effect independently of any contribution of Sir proteins. The first class of genes would be the most interesting for determining whether telomeric silencing is similar in mechanism to classically defined heterochromatin.

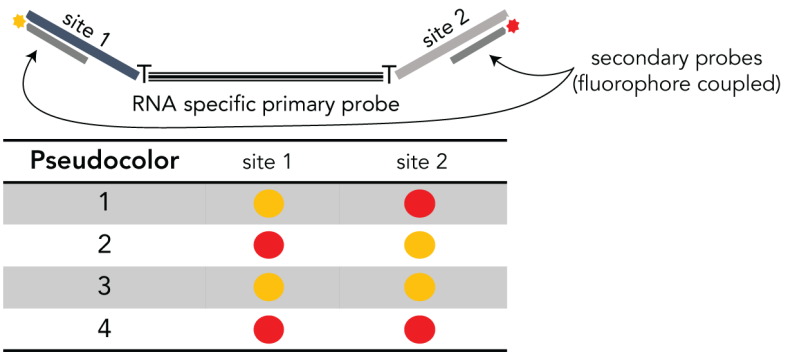

Figure 3.5: Schematic of seq-FISH+ setup.
This method utilizes mRNA-sequence-specific primary probes coupled with fluorescently-conjugated secondary probes to iteratively probe single mRNAs. Pseudocolors represent the combined readout of site1 and site2 secondary probes.

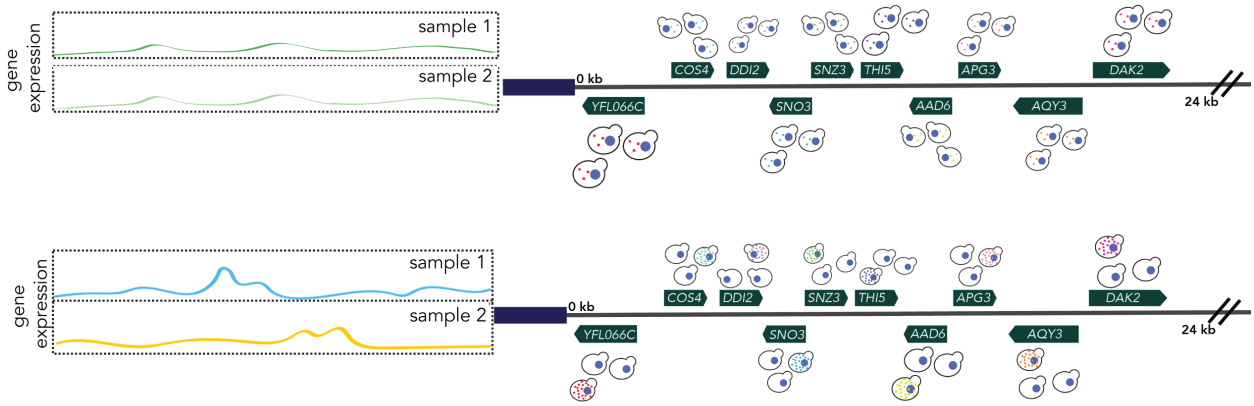

Figure 3.6: Two models for subtelomeric gene expression to explain general under-expression of these loci based on bulk assays.
Top: Under-expression of all loci in a subtelomeric domain may be similarly co-regulated, with all cells exhibiting similar levels of expression of a specific locus.
Bottom: Cells may exhibit stochasticity in their expression patterns, with a locus being silenced in the majority of cells but expressed more highly in a minority of cells.

I began by optimizing the technique for yeast, combining working smRNA-FISH protocols with the concepts of seq-FISH+. I designed the necessary tri-part probes for a set of genes on chromosome *VI-L* for a pilot experiment. Since seq-FISH+ relies on co-localization of fluorophores, I first assessed whether spot localization was consistent across secondary probes and experiments (**figure 3.7**). To do so, we quantified the distribution of spots/cell of two different fluorophores, Cy3 and Cy5, for example loci in multiple experiments. I noted promising co-localization of Cy3 and Cy5 for the *CAF16* locus and the average number of spots for each fluorophore per cell was similar across experiments (**figure 3.7.A,B**). When I used the same protocol with a different locus, *EPL1,* co-localization between fluorophores was again good, but the number of spots per

cell was variable (**figure 3.7.C,D**). Finally, I used the *COS4* locus as the target gene, and found a high level of background that made spot-detection unreliable (**figure 3.7.E-G**). The background levels of fluorescence led to a wide range in number of spots per cell across experiments, obscuring our ability to reliably count transcripts per cell.

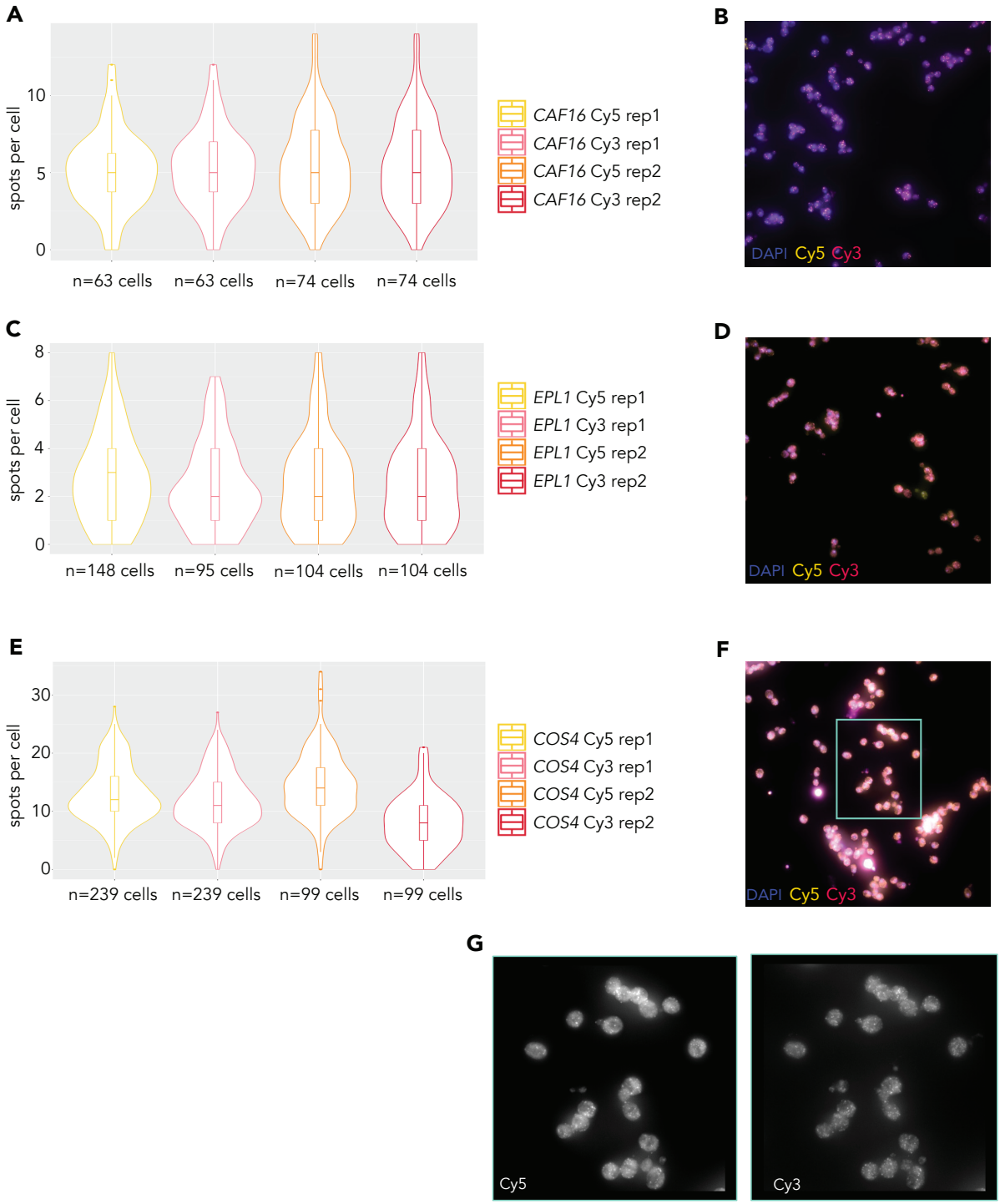

Figure 3.7: Preliminary seq-FISH+ studies revealed variability in specificity of probes which precluded our ability to quantify single mRNAs for a given locus.

Figure 3.7 (*continued from previous page)*

A. Quantification of Cy5 and Cy3 spots (correlating with the secondary probes) for *CAF16* mRNAs in two replicates.
B. Representative image for data quantified in (A).
C. Same as (A) but for *EPL1.*
D. Same as (B) but for *EPL1.*
E. Same as (A)(C) but for *COS4.*
F. Same as (B)(D) but for *COS4.*
G. Zoomed-in inset of teal box displayed in (F), in Cy5 channel (left) and Cy3 channel (right).

These iterations of smRNA-FISH rely on RNA-sequence-specific primary probes that hybridize to target loci. Upon further examination, I realized that subtelomeric genes often exist in gene families comprising multiple paralogs of the same gene (Brown *et al.* 2010). These families arose through genome-wide duplication events and therefore have very high sequence identity to one another (Snoek *et al.* 2014; Dunn *et al.* 2022). The flaw in the experimental design was not realizing the number of loci to which each primary probe might bind. Off-target hybridization events create non-site-specific binding of readout probes, and ultimately the occurrence of background fluorescence spots. Furthermore, the sequence identity between telomere *VI-L* and *XIV-L* made the loci that we were probing particularly problematic.

3.3.3: Distinguishing the effects of telomere length and composition on strength of silencing

Telomeres in *S. cerevisiae* comprise telomerase-generated repeats, which contain an abundance of Rap1 binding sites (Wellinger and Zakian 2012). Rap1 contains a DNA-binding domain, an activation domain, and a large C-terminal interaction domain to which Sir proteins and other partners including Rif1 and Rif2 (Rap interacting factor 1 and 2) bind (Shore and Nasmyth 1987a; Liu *et al.* 1994; Liu and Lustig 1996; Wotton and Shore 1997; Luo *et al.* 2002; Feeser and Wolberger 2008; Shi *et al.* 2013). Rif1 and Rif2 are negative regulators of telomerase; deletion of either causes a lengthening of telomeres with concomitant increases in Rap1 binding sites (Wotton and Shore 1997). Long telomeres are thought to disrupt silencing at *HM* loci by titrating away the limiting level of SIR proteins through interactions with Rap1 (Marshall *et al.* 1987; Bourns *et al.* 1998). To test this hypothesis, I utilized the unmatched sensitivity of the CRASH assay (Dodson and Rine 2015). I confirmed loss of silencing in a *rif1Δ*, consistent with the proposed model (**figure 3.8**). However, *rif2Δ* exhibited no loss of silencing despite also having long telomeres. A *rif1Δrif2*Δ double mutant exhibited phenocopied the *rif1Δ* loss-of-silencing phenotype, meaning *RIF2* is epistatic to *RIF1* in its role related to silencing. These data led me to the hypothesis that Rif1 competed with Sir proteins for binding to Rap1, enhancing the titration of Sir proteins achieved by long telomeres in a *rif1Δ* mutant. In contrast, these observations supported the inference that Rif2 was necessary for SIR-proteins to stably bind Rap1, but not for Rap1 to stimulate telomerase.

If limiting amounts of Sir proteins are responsible for the loss of silencing in cells with long telomeres, overexpression of the Sir complex should rescue the loss-of-silencing phenotype at *HML,* with the rescue strongest in *rif1Δ* and *rif1Δrif2Δ* strains.

Therefore, I generated a 2µ over-expression plasmid containing *SIR2, SIR3,* and *SIR4* each under the regulation of its own promoter and terminator. I found that overexpression of the Sir proteins did in fact partially rescue the loss-of-silencing phenotype associated with *rif1Δ* (**figure 3.8**). In otherwise wild type CRASH cells, sectoring was also reduced implying that overabundance of the Sir proteins stabilizes silencing, in line with other data in the field. Importantly, the level of overexpression of the *SIR* genes was never quantified in these experiments, and therefore these data should not be overinterpreted.

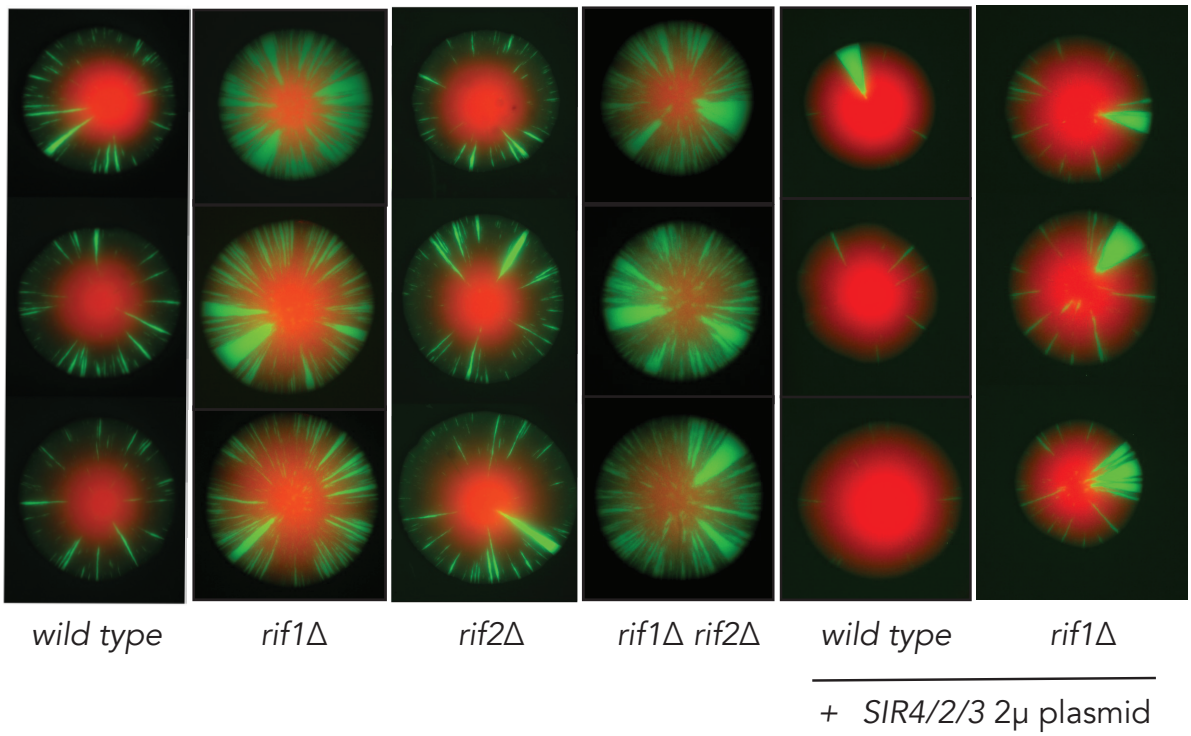

Figure 3.8: Overexpression of Sir2/3/4 rescued *rif1Δ* silencing defect by CRASH. Representative colonies were imaged for each genotype.

3.4: Discussion

The work presented here examined the longstanding *Saccharomyces cerevisiae* position-effect variegation paradigm, which posits that the extent of Sir-based silencing acting on a specific locus is dependent on where within the heterochromatic domain the gene lies, specifically with respect to distance from the telomere. In light of data suggesting a more nuanced effect of Sir proteins on subtelomeric gene silencing, I sought to define the contribution of Sir, and other, proteins to this effect at single-cell resolution. Ultimately, the experiments were largely not executed to a degree that would allow for more than speculation on the answers to these questions due to technical difficulties.

Studies from our laboratory show that within subtelomeric domains, defined as the 20kb most proximal to the telomeric repeats, Sir proteins stably bind at discrete loci rather than extending in a gradient from the telomere (Ellahi *et al.* 2015; Brothers and Rine 2022). Additionally, RNA-seq experiments reveal that the majority of subtelomeric genes

are not influenced by Sir-based silencing, yet all genes in the subtelomeric domains are under-expressed compared to average genome-wide expression levels (Ellahi *et al.* 2015; Kothiwal and Laloraya 2019). These measurements, and all previous reporter-based investigations of silencing at the subtelomeric domains, reflect the average expression of genes in a population of cells, even though a defining feature of PEV in other contexts is cell-to-cell variability in expression.

The three-color fluorescent reporter assay described above stood to prove or disprove the idea of the "Gottschling gradient" of expression. The strengths of the assay lay in its simplicity; it offered a direct test of the effect of distance from telomere on expression in a system that could easily measure thousands of events. Furthermore, I could control for many aspects of the experiment including variation in fluorescence intensities by scrambling the order of fluorophores for each experiment. Additionally, I could assess differences between natural telomeres by easily integrating the reporters at different genomic locations. My preliminary data showed that at one chromosome end, telomere *VI-L*, the effect of moving a reporter from 2kb to 5kb from the telomeric repeats was modest. The reporter increased in expression by only a small amount in cells that had been grown in the presence of NAM and were thus unsilenced. Taken at face value, these results indicated that the gradient model of subtelomeric repression may not be robust. Furthermore, it highlighted a difference between the level of repression imparted by Sir proteins at these subtelomeric loci and at the constitutively silenced *HML* and *HMR.*

The gradient expression model implies that adjacent genes will be similarly regulated, and distal genes less so. If no spatial co-regulation were to be observed, then gradient-based models would be disfavored in favor of a gene-specific method of silencing. It remains to be seen which of these models is supported at single-cell resolution, and what the true contribution of telomere composition is to the variegated expression of some subtelomeric loci and the under-expression of these domains. If loci were not co-regulated by Sir binding, it would have suggested a different underlying regulatory mechanism. While eukaryotes do not typically have operons, there are many examples of biosynthetic gene clusters (Brakhage 2013; Medema *et al.* 2015; Harvey *et al.* 2018) and recent findings have implicated nuclear organization in regulation (Pombo and Dillon 2015). It is possible that some similarly regulated genes are in close proximity to one another and employ a common mechanism of regulation. The proteins encoded in subtelomeric loci are enriched for metabolic function, and thus we hypothesized that a degree of stochasticity in expression at the single-cell level might exist to enable environment-specific responses through a bet-hedging strategy, such as that which leads to low level expression of ß-galactosidase in some *E. coli* cells even in the absence of lactose. Under certain environmental conditions, some phenotypic variation in the population would be beneficial and allow survival with the proper adaptation, even though heterogeneity may not be ideal under controlled conditions. Duplication and diversification of gene families is a way to blindly anticipate and survive environmental changes. The bet hedging strategy predicts that there exists an environment in which all loci that are unregulated in spatial proximity to one another in standard lab conditions are fully silenced or unsilenced in all cells.

In line with this thinking, recent studies from a former Rine lab member show that a polymorphic yeast gene *KTD1* protects against the killer toxin K28 (Andreev *et al.* 2023). They found that different populations of yeast harbor several distinct *KTD1* alleles, some of whose expression is terminated by an early stop codon (Andreev *et al.* 2023). K28 is only robustly expressed in some environmental conditions or locations and the defensive DUP240 gene family appears to be under positive selection and rapid evolution at transmembrane domains (Andreev *et al.* 2023). Additionally, a Bay Area biotech company Hexagon Bio is utilizing the natural variation in fungi to mine these naturally occurring biosynthetic gene clusters and self-resistence elements for secondary metabolites for drug discovery (Harvey *et al.* 2018; Ho *et al.* 2022).

The cumulative data collected from these experiments would have comprehensively characterized the heterochromatin of subtelomeric domains and investigated a mechanism by which it could be regulated. In 2022, work from our laboratory elucidated the extent of Sir protein recruitment and spread to all 32 native telomeres (Brothers and Rine 2022). By using long-read Oxford Nanopore sequencing, which circumvents the sequence identity problem that thwarted our seqFISH+ efforts, researchers track the establishment and spread of subtelomeric silencing at single cell resolution. In sum, the experiments performed in (Brothers and Rine 2022) reveal that only a few native telomeres have a gradient of Sir-complex binding while most recapitulate the discrete binding seen in (Ellahi *et al.* 2015). Furthermore, in contrast to prior research, Sir3 overexpression is not enough to cause significant spread of Sir proteins at most telomeres. While the information gained from these experiments is critical to understanding the composition of subtelomeric domains globally in yeast, it did not address the expression patterns resultant from such Sir binding. Had I the granular information about subtelomeric Sir protein binding at the time the experiments presented in this chapter were conceived, I would have been able to make a more educated choice regarding which subtelomeric domains were good candidates for the single cell expression experiments laid out above.

Broadly, changes in telomere length are implicated in responses to environmental conditions (Romano *et al.* 2013).That external signals modify telomere length in a heritable fashion belies epigenetic control of these domains. Epigenetic variation is increasingly appreciated as underlying heritable traits in plants, including those of agronomic importance. Given the enrichment of subtelomeric genes in rapidly evolving metabolic genes, understanding the mechanism of silencing and gene sequestration at telomeres is pertinent to the development of stress-resistant crops and yield stability. The intersection of climate change with the need for global food security highlight the need to understand heritable variation at all levels. As telomeres are conserved genomic features across all eukaryotes, these findings would be widely applicable.

3.5: Materials and Methods

Yeast strains

Strains used in this study are listed in **Table 3.1**. All strains were derived from the *S. cerevisiae* W303 background using standard genetic techniques and CRISPR-Cas9 technology (Burke *et al.* 2000; Gietz and Schiestl 2007; Brothers and Rine 2019). To insert fluorescent reporters, reporter constructs were first engineered in a pBlueScript(+) backbone in *E. coli.* The endogenous *COS4 CDS* plus promoter and terminator was amplified with oligos denoted in **Table 3.2** and incorporated into pBKS(+) using standard restriction digest cloning. mCitrine was amplified from plamid pÜB917, a gift from the Brar/Ünal labs, and mCherry was amplified from pAD33 with oligos indicated in **Table 3.2**. The plasmid containing *COS4+promoter+terminator* was amplified to exclude the CDS. Then the fluorescent reporters were integrated into the plasmid using Gibson Assembly (NEB, E2611S). To incorporate each reporter construct into the genome, the entire construct was amplified using oligos in **Table 3.2** which had 40bp homology to the region of insertion on both the 5´and 3´ ends of the primers. sgRNA guides were cloned as described in (Brothers and Rine 2019) (oligos found in **Table 3.2**), and constructs were integrated using CRISPR-Cas9 technology into wild type W303 strains (JRY4012 and JRY4013), using selection of both the sgRNA plasmid marker and presence of fluorescence for screening purposes. Deletions were generated using one-step replacement with marker cassettes (Goldstein and McCusker 1999; Gueldener *et al.* 2002).

Flow cytometry measurements of fluorescence readout

For each genotype, three technical replicates of each strain were inoculated in 5mL of YPD (+/- 5mM NAM where applicable) and grown overnight. The following morning, saturated cultures were backdiluted to ~0.1OD in fresh YPD (+/- 5mM NAM where applicable), then grown to mid-log phase (~0.6OD). Cells were harvested by centrifugation, and resuspended 500uL of a solution of 4% paraformaldehyde. Samples were then pelleted again, and washed in 1mL 1X Phosphate Buffered Saline (PBS). Finally, cells were pelleted a third time and resuspended in in 2mL 1X PBS in 14mL polystyrene tubes. Samples were analyzed by flow cytometry immediately. Flow cytometry was performed using a BD LSRFortessa (BD Biosciences) with a FITC filter for mCitrine and a Texas-Red filter for mCherry. At least 10,000 cells were analyzed for each sample. Samples were processed using FlowJo Software (BD Life Sciences). All flow cytometry data were gated identically, omitting aggregates and cellular debris from analysis.

Live-cell Imaging

Strains were grown as described above for flow cytometry. When they reached mid-log phase, a 500 µL aliquot at approximately 0.6-1.0 OD was harvested by centrifugation and resuspended in 2mL YPD (+/- NAM where appropriate). Approximately 4 µL of this resuspension was pipetted onto a 1 cm^2 2% CSM agar pad that had been cut out of a standard CSM plate. When the solution had dried, the pad was inverted onto a 35mm glass-bottom dish and imaged using a Zeiss Z1 inverted fluorescence microscope with a Prime 95B sCMOS camera (Teledyne Photometrics), Plan-Apochromat 63x/1.40 oil immersion objective (Zeiss) filters, MS-2000 XYZ automated stage (Applied Scientific Instrumentation), and Micro-Manager imaging software (Open Imaging). Images were analyzed using FIJI, using BF images to outline cells and (Schindelin *et al.* 2012).

CRASH colony imaging

Imaging was conducted as described in Chapter 2. Briefly, colonies were plated onto 1.5% agar plates containing yeast nitrogen base without amino acids, 2% dextrose, and supplemented with complete supplement mixture (CSM)-Trp to minimize background fluorescence. Colonies were incubated for 5–7 days at 30 °C, then imaged as described in (Fouet and Rine 2023).

smRNA seqFISH+

All aspects of this protocol were done using filter tips. Oligonucleotide sequences for Primary probes (RNA-specific) can be found in **Table 3.3.** Secondary readout probes (fluorescently-coupled) can be found in **Table 3.4.**

Growth and fixation: 5mL YPD cultures of JRY4012 and JRY4013 were inoculated and grown overnight at 30˚C. The following morning, cultures were heavily back-diluted and inoculated in 50mL cultures at OD600 = 0.03, then grown for 4 hours shaking at 30˚C. The entire sample was harvested by centrifugation, then resuspended in 1.84mL YPD. Cells were transferred to new 2mL flip-top tubes, and 160µL 37% formaldehyde was added, inverting to mix. Cells were fixed by rotating end-over-end for 20min at room temperature. Cells were then rotated overnight at 4˚C. The following day, cells were centrifuged at 15000rpm for 1min 30 sec and the superanatant was aspirated.

Digestion of cell wall: Cells were then resuspended and washed in 1.5mL Buffer B (Sorbitol and potassium phosphate, pH7.5) a total of 3 times, then left in ~100µL Buffer B to protect the pellet. For each sample, a mixture of 40µL 200mM ribonucleoside vanadyl complex (RVC) and 425µL Buffer B was mixed together in a 15mL conical tube. Cell pellets were resuspended in 425µL of this mixture, and then 5µL 10mg/mL 100T zymolyase was added to each tube, and vortexed for 2-3 seconds to mix. Cells were spheroplasted by rotating end-over-end in this solution at 30˚C for 30 minutes. Post-digestion cells were centrifuged at 2,000rpm for 3min at 4˚C and the Buffer B / Zymolyase mixture was removed. Cells were resuspended in 1mL Buffer B with gentle pipetting up and down to mix, then centrifuged at 2,000rpm for 3min at 4˚C and resuspended in 70% EtOH and incubated at room temperature for 3.5-4 hours. Formamide was brough to room temperature for at least 30min. 1 part formamide was mixed with 1 part RNase-free 20X SSC buffer and 8 parts Nuclease-free H2O to prepare 10% Formamide Wash Buffer. Cells were centrifuged at 2,000rpm for 3min at 4˚C, then all but 500µL EtOH was removed

and the cells were transferred to 1.5mL low-adhesion tubes, then centrifuged as before and all supernatant was removed. Cells were resuspended in 1mL 10% formamide wash buffer and incubated at room temperature for 20 minutes.

Primary hybridization: 10mL Hybridization buffer 1 (HB1) was made up according to the following formula: 3mL formamide at RT, 1g Dextran Sulfate, 1mL 10mg/mL *E. coli* tRNA, 1mL 20X SSC (RNase-free), 200µL BSA (10mg/mL), 100µL RVC (200nM), and 4.8mL nuclease-free H2O. To each tube containing 250µL HB1 and 25µL RVC, we added 2µL of each primary probe, diluted to 25nM. Tubes were incubated in the dark overnight at 30˚C. The following morning, samples were washed with freshly prepared 10% formamide wash buffer, then spun at 2,000rpm for 3 minutes at RT and resuspended in >800µL formamide wash buffer and incubated in the dark at 30˚C (not rotating) for 30-45min. Samples were collected by centrifugation as before.

Secondary hybridization: 10mL hybridization buffer 2 (HB2) was prepared using the following specifications: 1g Dextran sulfate was dissolved in nuclease-free water and vortexed to mix, then 10mg *E. coli* tRNA were added followed by 1mL 20X SSC (RNase-free), 40µL 50mg/mL BSA, 100µL 200mM RVC and 1mL Formamide (RT). HB2 was aliquoted into 500µL portions and stored at -20ºC. To begin secondary probe hybridization, 100µL HB2 + 10µL RVC were mixed for each sample. 2µL of each 1µM secondary probe stock was added to this mixture in the appropriate combinations. Cells were then resuspended in this mixture and incubated for 30-45min at 30ºC in the dark. Cells were washed 2X with 20% formamide in 2X SSC buffer.

DAPI and anti-fade: a mixture of 3mL 10% FWB and 10µL DAPI were combined. Each sample was resuspended in >800µL DAPI/FWB and incubated at 30˚C in the dark (not rotating) for 30-45 minutes. Meanwhile, anti-bleach reagents (4˚C 10% glucose, 20˚C glucose oxidase and Trolox) were thawed on ice. Samples were collected by centrifugation (2,000 rpm for 3 minutes at RT) then resuspended in 50µL GLOX buffer (for 1mL: 40μL 10% glucose (in nuclease-free H_2O, stored at 4ºC), 10μL 1M Tris, pH 8.0, 100μL RNase-free 20X SSC, 850μL nuclease-free H_2O – all vortexed thoroughly) **without enzymes** and kept at 4˚C until ready to image. Cells were collected by centrifugation (2,000 rpm for 3 minutes at RT) and resuspended in an appropriate volume (100-500µL) GLOX buffer **with** enzymes (0.5μL Catalase, 0.5μL glucose oxidase, 1μL 100mM Trolox, 50µL GLOX buffer). 5µL was pipetted onto an 18mmx18mm coverslip and lowered gently onto a slide. Excess liquid was removed by capillary action with a kimwipe and the slide was set by firmly pressing down and sealing it with clear nail polish. Sample slides were transported to the microscope in a lightproof container.

Imaging: imaging was performed as described in (Goodnight and Rine 2020) on an Axio Observer Z1 inverted microscope (Zeiss) with a 63x oil-immersion objective (Zeiss). Z-stack images were taken with a total height of 8μm and a step size of 0.2μm, then max-projected in FIJI (Schindelin *et al.* 2012). Representative images are presented. For quantification of smRNA spots, cells were manually outlined and automatic spot detection was performed using FISH-quant (Mueller *et al.* 2013) and data was plotted using a custom Rstudio script and ggplot2 (Wickham 2016).

Table 3.1: Strains used in Chapter 3.

Strain	MAT	Relevant genotype (ALL STRAINS ADE2; can1-100; his3-11; leu2-3, 112; trp1; ura3-1; lys2)
JRY15022	a	*mcherry+/-300bpCOS4P+T_PEST.SV40NLS @ 2kb from TEL-VIL*
JRY15023	a	*mcherry+/-200bpCOS4P+T_PEST.SV40NLS @ 2kb from TEL-VIL*
JRY15029	a	*mCitrine+/-300bpCOS4P+T_PEST.SV40NLS @ 2kb from TEL-VIL*
JRY15030	α	*mCitrine+/-300bpCOS4P+T_PEST.SV40NLS @ 2kb from TEL-VIL*
JRY15039	a	*mCherry+/-200bpCOS4P+T_PEST.SV40NLS @ 5kb from TEL-VIL*
JRY04012	a	*can1-100 his3-11 leu2-3,112 lys2 trp1-1 ura3-1 GAL*
JRY04013	α	*can1-100 his3-11 leu2-3,112 lys2 trp1-1 ura3-1 GAL*
JRY15007	α	*ADE2, lys2, TRP1, hmlα2Δ::CRE, ura3Δ::pGPD:loxP:yEmRFP;tCYC1:hygMX:loxP:yEGFP:tADH1; rif2Δ::LEU2*
JRY15044	a	*ADE2, lys2, TRP1, hmlα2Δ::CRE, ura3Δ::pGPD:loxP:yEmRFP;tCYC1:hygMX:loxP:yEGFP:tADH1; rif1Δ::URA3*
JRY15045	a	*ADE2, lys2, TRP1, hmlα2Δ::CRE, ura3Δ::pGPD:loxP:yEmRFP;tCYC1:hygMX:loxP:yEGFP:tADH1; rif1Δ::URA3; rif2Δ::LEU2*

Table 3.2: Oligonucleotides used in strain construction for Chapter 3, as described in the accompanying methods (section 3.5).

Sequence	Description
GATCGCGGCCGCAAAAGTATTATTACGATTATCGAGT	F primer to amplify COS4+promoter+terminator with NotI
GATCGAATTCAAGGTTAATCACATGGCG	R primer to amplify COS4+promoter+terminator with EcoRI
ATTACCGAAAATGTCTAAAGGTGAAGAATTATT	F Gibson primer for mCitrine into COS4cds in pBKS(+)
GTATTTATCTTTATTTGTACAATTCATCAATAC	R Gibson primer for mCitrine itnto COS4cds in pBKS(+)
TTGTACAAATAAAGATAAATACAACTTTTTCAATTTATAT	F Gibson primer for Cos4terminator backbone (inserting mCit)
CTTTAGACATTTTCGGTAATGAGATGGC	R Gibson primer for Cos4promoter backbone (inserting mCit)
ATTACCGAAAATGGTAAGCAAGGGAGAG	F Gibson primer for mScarlet into COS4cds in pBKS(+)
GTATTTATCTTTATTTATATAGTTCATCCATTCCG	R Gibson primer for mScarlet into COS4cds in pBKS(+)

Continued on following page

Table 3.2: *continued from previous page*

CTATATAAAtaaAGATAAATACAACTTTTTCAATTTATAT	F Gibson primer for Cos4terminator backbone (inserting mScar)
CTTGCTTACCATTTTCGGTAATGAGATGGC	R Gibson primer for Cos4promoter backbone (inserting mScar)
GACTTTGACGAACCAGATTTCCAGGG	F sgRNA primer for 2kb Tel6L position
AAACCCCTGGAAATCTGGTTCGTCAA	R sgRNA primer for 2kb Tel6L position
GACTTTATCGTATCGGAGGATGGCTT	F sgRNA primer for 5kb Tel6L position
AAACAAGCCATCCTCCGATACGATAA	R sgRNA primer for 5kb Tel6L position
TTCTTTGTATTCCTCGTCATTTCGCAGCATTCTCTCCACATAT TATTTAAGGATTCCGCT	R Primer to insert 300bpCos4 into 5kb position on Chr6L
AGAAAGTATCGTATCGGAGGATGGCTTGCGAAGCACTAGCT CGCACCTTAAATGTAAA	F Primer to insert 300bpCos4 into 5kb position on Chr6L
AACGTGTAGACCATCAAGTTGATTTTCTTGGGAATAAGATTAT TATTTAAGGATTCCGCT	R Primer to insert 300bpCos4 into 2kb position on Chr6L
AGACGAACCAGATTTCCAGGGCGCACCAATCCCTTCAAAGTT CGCACCTTAAATGTAAA	F Primer to insert 300bpCos4 into 2kb position on Chr6L

Table 3.3: Primary probes used for seqFISH+. Each probe contains a unique, RNA-specific 20-mer (lowercase), readout regions, and a constant section to which a GFP-coupled secondary probe could anneal.

Oligo name	**Sequence**
CAF16-1	GTCGTCCTAGAGGTAGTTCGtACGTGACGGTTGTAACGGAGtcctcaatagcaaattggg aatGAGCATGAATTCTCGCCAAT
CAF16-2	GTCGTCCTAGAGGTAGTTCGtTCGTTAGAGGTATGTCGGACtatttgtacgttaggttacgct ACGTGACGGTTGTAACGGAG
CAF16-3	GTCGTCCTAGAGGTAGTTCGtGAGCATGAATTCTCGCCAATtaacaactgacggatcgga gctTCGTTAGAGGTATGTCGGAC
CAF16-4	GTCGTCCTAGAGGTAGTTCGtACGTGACGGTTGTAACGGAGttcttgtattccatgggatttt GAGCATGAATTCTCGCCAAT
CAF16-5	GTCGTCCTAGAGGTAGTTCGtTCGTTAGAGGTATGTCGGACtcattggcacccacaacta aatACGTGACGGTTGTAACGGAG
CAF16-6	GTCGTCCTAGAGGTAGTTCGtGAGCATGAATTCTCGCCAATtaaagggtggatttaccagc atTCGTTAGAGGTATGTCGGAC
CAF16-7	GTCGTCCTAGAGGTAGTTCGtACGTGACGGTTGTAACGGAGtgcttaccgcttagtaatttct GAGCATGAATTCTCGCCAAT

Continued on following page

Table 3.3: *continued from previous page*

CAF16-8	GTCGTCCTAGAGGTAGTTCGtTCGTTAGAGGTATGTCGGACtggatttttccatcaaggcaa tACGTGACGGTTGTAACGGAG
CAF16-9	GTCGTCCTAGAGGTAGTTCGtGAGCATGAATTCTCGCCAATtatggatcaagaccattgac ctTCGTTAGAGGTATGTCGGAC
CAF16-10	GTCGTCCTAGAGGTAGTTCGtACGTGACGGTTGTAACGGAGtgtccacttgattcatagata tGAGCATGAATTCTCGCCAAT
CAF16-11	GTCGTCCTAGAGGTAGTTCGtTCGTTAGAGGTATGTCGGACtatcttcaacactttcatcatt ACGTGACGGTTGTAACGGAG
CAF16-12	GTCGTCCTAGAGGTAGTTCGtGAGCATGAATTCTCGCCAATttggtcgtttggtagttcgtctT CGTTAGAGGTATGTCGGAC
CAF16-13	GTCGTCCTAGAGGTAGTTCGtACGTGACGGTTGTAACGGAGtaccattccgtacctagata atGAGCATGAATTCTCGCCAAT
CAF16-14	GTCGTCCTAGAGGTAGTTCGtTCGTTAGAGGTATGTCGGACttccctattaatgatactcatt ACGTGACGGTTGTAACGGAG
CAF16-15	GTCGTCCTAGAGGTAGTTCGtGAGCATGAATTCTCGCCAATttaatagttccaagacgccg atTCGTTAGAGGTATGTCGGAC
CAF16-16	GTCGTCCTAGAGGTAGTTCGtACGTGACGGTTGTAACGGAGtcacctctttccctaaaatg atGAGCATGAATTCTCGCCAAT
CAF16-17	GTCGTCCTAGAGGTAGTTCGtTCGTTAGAGGTATGTCGGACtgtccaggattctaaccaat ctACGTGACGGTTGTAACGGAG
CAF16-18	GTCGTCCTAGAGGTAGTTCGtGAGCATGAATTCTCGCCAATtcattctccaacgtacatcga tTCGTTAGAGGTATGTCGGAC
CAF16-19	GTCGTCCTAGAGGTAGTTCGtACGTGACGGTTGTAACGGAGttttgtccatcacttaacctgt GAGCATGAATTCTCGCCAAT
CAF16-20	GTCGTCCTAGAGGTAGTTCGtTCGTTAGAGGTATGTCGGACtccatggctaactgaactctt tACGTGACGGTTGTAACGGAG
CAF16-21	GTCGTCCTAGAGGTAGTTCGtGAGCATGAATTCTCGCCAATtactctccaaggtttcaaga gtTCGTTAGAGGTATGTCGGAC
CAF16-22	GTCGTCCTAGAGGTAGTTCGtACGTGACGGTTGTAACGGAGtagtgacctcatcaagtagt atGAGCATGAATTCTCGCCAAT
CAF16-23	GTCGTCCTAGAGGTAGTTCGtTCGTTAGAGGTATGTCGGACtggcaataacatcgagatc catACGTGACGGTTGTAACGGAG
CAF16-24	GTCGTCCTAGAGGTAGTTCGtGAGCATGAATTCTCGCCAATtaaactccagaagtcttgctc tTCGTTAGAGGTATGTCGGAC
CAF16-25	GTCGTCCTAGAGGTAGTTCGtACGTGACGGTTGTAACGGAGtcatcttctggtttcggtctct GAGCATGAATTCTCGCCAAT
CAF16-26	GTCGTCCTAGAGGTAGTTCGtTCGTTAGAGGTATGTCGGACtatgtgtagcgtagaccact gtACGTGACGGTTGTAACGGAG
CAF16-27	GTCGTCCTAGAGGTAGTTCGtGAGCATGAATTCTCGCCAATttttggccaagccgtcaaaa atTCGTTAGAGGTATGTCGGAC
CAF16-28	GTCGTCCTAGAGGTAGTTCGtACGTGACGGTTGTAACGGAGttatggtatacttggttaggc tGAGCATGAATTCTCGCCAAT
CAF16-29	GTCGTCCTAGAGGTAGTTCGtTCGTTAGAGGTATGTCGGACtccacaatcttacctgatttct ACGTGACGGTTGTAACGGAG
CAF16-30	GTCGTCCTAGAGGTAGTTCGtGAGCATGAATTCTCGCCAATtgaactctacgtctttctgatt TCGTTAGAGGTATGTCGGAC

Continued on following page

Table 3.3: *continued from previous page*

CAF16-31	GTCGTCCTAGAGGTAGTTCGtACGTGACGGTTGTAACGGAGttttagcattgaccacttcag tGAGCATGAATTCTCGCCAAT
CAF16-32	GTCGTCCTAGAGGTAGTTCGtTCGTTAGAGGTATGTCGGACtaaaggccacttgtccatta atACGTGACGGTTGTAACGGAG
CAF16-33	GTCGTCCTAGAGGTAGTTCGtGAGCATGAATTCTCGCCAATtacaaccttattgttgtcatttT CGTTAGAGGTATGTCGGAC
CAF16-34	GTCGTCCTAGAGGTAGTTCGtACGTGACGGTTGTAACGGAGttctagtgctaatggatgca atGAGCATGAATTCTCGCCAAT
CAF16-35	GTCGTCCTAGAGGTAGTTCGtTCGTTAGAGGTATGTCGGACttgattatcacgtttcaaccat ACGTGACGGTTGTAACGGAG
CAF16-36	GTCGTCCTAGAGGTAGTTCGtGAGCATGAATTCTCGCCAATttaccaatctctttgtcaggat TCGTTAGAGGTATGTCGGAC
COS4-1	GTCGTCCTAGAGGTAGTTCGtTGTTGCTCCCGGATTACACGtacatctacacttttctcatttT ACTGGACCTCGCACAATG
COS4-2	GTCGTCCTAGAGGTAGTTCGtTCGTTAGAGGTATGTCGGACttcttttgagattcgagctgtt TGTTGCTCCCGGATTACACG
COS4-3	GTCGTCCTAGAGGTAGTTCGtTACTGGACCTCGCACAATGtaaccaggtaaagctgcttctt TCGTTAGAGGTATGTCGGAC
COS4-4	GTCGTCCTAGAGGTAGTTCGtTGTTGCTCCCGGATTACACGtccagatgcgaaacgctaa ggtTACTGGACCTCGCACAATG
COS4-5	GTCGTCCTAGAGGTAGTTCGtTCGTTAGAGGTATGTCGGACtcgctaagtggtagccataa ttTGTTGCTCCCGGATTACACG
COS4-6	GTCGTCCTAGAGGTAGTTCGtTACTGGACCTCGCACAATGtccaattgttggaaagcttcct TCGTTAGAGGTATGTCGGAC
COS4-7	GTCGTCCTAGAGGTAGTTCGtTGTTGCTCCCGGATTACACGtagtgaaaccataagcggg tatTACTGGACCTCGCACAATG
COS4-8	GTCGTCCTAGAGGTAGTTCGtTCGTTAGAGGTATGTCGGACtgaacaaatactggtcccc aatTGTTGCTCCCGGATTACACG
COS4-9	GTCGTCCTAGAGGTAGTTCGtTACTGGACCTCGCACAATGtgttgtttcgataaggaacgttT CGTTAGAGGTATGTCGGAC
COS4-10	GTCGTCCTAGAGGTAGTTCGtTGTTGCTCCCGGATTACACGttctctttgcaaaactgagtgt TACTGGACCTCGCACAATG
COS4-11	GTCGTCCTAGAGGTAGTTCGtTCGTTAGAGGTATGTCGGACtgaacttggtgtgcttttagtt TGTTGCTCCCGGATTACACG
COS4-12	GTCGTCCTAGAGGTAGTTCGtTACTGGACCTCGCACAATGtcaacttcccaatcatgaggat TCGTTAGAGGTATGTCGGAC
COS4-13	GTCGTCCTAGAGGTAGTTCGtTGTTGCTCCCGGATTACACGtacgaatttagatttgctgcat TACTGGACCTCGCACAATG
COS4-14	GTCGTCCTAGAGGTAGTTCGtTCGTTAGAGGTATGTCGGACttacctaatattccaagccttt TGTTGCTCCCGGATTACACG
COS4-15	GTCGTCCTAGAGGTAGTTCGtTACTGGACCTCGCACAATGtgcccatggcattgaagaaa atTCGTTAGAGGTATGTCGGAC
COS4-16	GTCGTCCTAGAGGTAGTTCGtTGTTGCTCCCGGATTACACGttgttctgaacgcttcttggct TACTGGACCTCGCACAATG
COS4-17	GTCGTCCTAGAGGTAGTTCGtTCGTTAGAGGTATGTCGGACtagagaagggttcgagaa gggtTGTTGCTCCCGGATTACACG

Continued on following page

Table 3.3: *continued from previous page*

COS4-18	GTCGTCCTAGAGGTAGTTCGtTACTGGACCTCGCACAATGtaatgacttaaccttggcagct TCGTTAGAGGTATGTCGGAC
COS4-19	GTCGTCCTAGAGGTAGTTCGtTGTTGCTCCCGGATTACACGtatgtaagggacggaatcct ttTACTGGACCTCGCACAATG
COS4-20	GTCGTCCTAGAGGTAGTTCGtTCGTTAGAGGTATGTCGGACttaaactcccaatgcttcttct TGTTGCTCCCGGATTACACG
COS4-21	GTCGTCCTAGAGGTAGTTCGtTACTGGACCTCGCACAATGtccattgtttttcaacttctctTC GTTAGAGGTATGTCGGAC
COS4-22	GTCGTCCTAGAGGTAGTTCGtTGTTGCTCCCGGATTACACGtgctccatgatttctcagaatt TACTGGACCTCGCACAATG
COS4-23	GTCGTCCTAGAGGTAGTTCGtTCGTTAGAGGTATGTCGGACtgaagtttagcatcttccagg tTGTTGCTCCCGGATTACACG
COS4-24	GTCGTCCTAGAGGTAGTTCGtTACTGGACCTCGCACAATGtgcttaaatcggtaagcttcct TCGTTAGAGGTATGTCGGAC
COS4-25	GTCGTCCTAGAGGTAGTTCGtTGTTGCTCCCGGATTACACGtcgtgacacatatatgcagc atTACTGGACCTCGCACAATG
COS4-26	GTCGTCCTAGAGGTAGTTCGtTCGTTAGAGGTATGTCGGACtggtgcgtaatagaaggca catTGTTGCTCCCGGATTACACG
COS4-27	GTCGTCCTAGAGGTAGTTCGtTACTGGACCTCGCACAATGtaagaatccacccgagatac atTCGTTAGAGGTATGTCGGAC
COS4-28	GTCGTCCTAGAGGTAGTTCGtTGTTGCTCCCGGATTACACGtcccttatattttggaaaccttt TACTGGACCTCGCACAATG
COS4-29	GTCGTCCTAGAGGTAGTTCGtTCGTTAGAGGTATGTCGGACtgtgttccatgctcataatcat TGTTGCTCCCGGATTACACG
COS4-30	GTCGTCCTAGAGGTAGTTCGtTACTGGACCTCGCACAATGtagtcgacaagaactgcatct tTCGTTAGAGGTATGTCGGAC
COS4-31	GTCGTCCTAGAGGTAGTTCGtTGTTGCTCCCGGATTACACGtccactttcttgctcatttattT ACTGGACCTCGCACAATG
COS4-32	GTCGTCCTAGAGGTAGTTCGtTCGTTAGAGGTATGTCGGACtcaatttcgtcccatccattct TGTTGCTCCCGGATTACACG
COS4-33	GTCGTCCTAGAGGTAGTTCGtTACTGGACCTCGCACAATGtagtacctattcattttcctttTC GTTAGAGGTATGTCGGAC
COS4-34	GTCGTCCTAGAGGTAGTTCGtTGTTGCTCCCGGATTACACGttcttcattcttccagacttttT ACTGGACCTCGCACAATG
COS4-35	GTCGTCCTAGAGGTAGTTCGtTCGTTAGAGGTATGTCGGACtacagtcaatcccgtcaaa gatTGTTGCTCCCGGATTACACG
COS4-36	GTCGTCCTAGAGGTAGTTCGtTACTGGACCTCGCACAATGtcggtagaagaagtggctaa atTCGTTAGAGGTATGTCGGAC
COS4-37	GTCGTCCTAGAGGTAGTTCGtTGTTGCTCCCGGATTACACGtgatttcttcgcagatagaac tTACTGGACCTCGCACAATG
COS4-38	GTCGTCCTAGAGGTAGTTCGtTCGTTAGAGGTATGTCGGACtttcaatgatagagcccgca ttTGTTGCTCCCGGATTACACG
COS4-39	GTCGTCCTAGAGGTAGTTCGtTACTGGACCTCGCACAATGtatatatggccatagttccact TCGTTAGAGGTATGTCGGAC
COS4-40	GTCGTCCTAGAGGTAGTTCGtTGTTGCTCCCGGATTACACGtcaggataattgcgcttctttt TACTGGACCTCGCACAATG

Continued on following page

Table 3.3: *continued from previous page*

COS4-41	GTCGTCCTAGAGGTAGTTCGtTCGTTAGAGGTATGTCGGACttacgctaaggactcctcac ttTGTTGCTCCCGGATTACACG
EPL2-1	GTCGTCCTAGAGGTAGTTCGtTGTTGCTCCCGGATTACACGtcgaaccgtcattgatctcta tGAGCATGAATTCTCGCCAAT
EPL2-2	GTCGTCCTAGAGGTAGTTCGtTCGTTAGAGGTATGTCGGACtgaatctagaccgtcatcgt gtTGTTGCTCCCGGATTACACG
EPL2-3	GTCGTCCTAGAGGTAGTTCGtGAGCATGAATTCTCGCCAATttcgactattactgctaccagt TCGTTAGAGGTATGTCGGAC
EPL2-4	GTCGTCCTAGAGGTAGTTCGtTGTTGCTCCCGGATTACACGttgtttcagatcgttaggcagt GAGCATGAATTCTCGCCAAT
EPL2-5	GTCGTCCTAGAGGTAGTTCGtTCGTTAGAGGTATGTCGGACtctctctctgttgcaattcattT GTTGCTCCCGGATTACACG
EPL2-6	GTCGTCCTAGAGGTAGTTCGtGAGCATGAATTCTCGCCAATtacaccagtttcgatctcaac tTCGTTAGAGGTATGTCGGAC
EPL2-7	GTCGTCCTAGAGGTAGTTCGtTGTTGCTCCCGGATTACACGtaaatggacctccttttcttct GAGCATGAATTCTCGCCAAT
EPL2-8	GTCGTCCTAGAGGTAGTTCGtTCGTTAGAGGTATGTCGGACtttgtgctttgtatgaccagat TGTTGCTCCCGGATTACACG
EPL2-9	GTCGTCCTAGAGGTAGTTCGtGAGCATGAATTCTCGCCAATttccaagtcatagaagcatc ctTCGTTAGAGGTATGTCGGAC
EPL2-10	GTCGTCCTAGAGGTAGTTCGtTGTTGCTCCCGGATTACACGttagttggtaccacagcaat ctGAGCATGAATTCTCGCCAAT
EPL2-11	GTCGTCCTAGAGGTAGTTCGtTCGTTAGAGGTATGTCGGACttctcatctctttcatccatatT GTTGCTCCCGGATTACACG
EPL2-12	GTCGTCCTAGAGGTAGTTCGtGAGCATGAATTCTCGCCAATtacctttgttgacttgttcattT CGTTAGAGGTATGTCGGAC
EPL2-13	GTCGTCCTAGAGGTAGTTCGtTGTTGCTCCCGGATTACACGtgaatggttgacgctcgtga atGAGCATGAATTCTCGCCAAT
EPL2-14	GTCGTCCTAGAGGTAGTTCGtTCGTTAGAGGTATGTCGGACtgattcagctggtttcttagat TGTTGCTCCCGGATTACACG
EPL2-15	GTCGTCCTAGAGGTAGTTCGtGAGCATGAATTCTCGCCAATtgagatacggggtcgaattg ttTCGTTAGAGGTATGTCGGAC
EPL2-16	GTCGTCCTAGAGGTAGTTCGtTGTTGCTCCCGGATTACACGtttttagagccgaacttctctt GAGCATGAATTCTCGCCAAT
EPL2-17	GTCGTCCTAGAGGTAGTTCGtTCGTTAGAGGTATGTCGGACttcgtacccgttaacttcaatt TGTTGCTCCCGGATTACACG
EPL2-18	GTCGTCCTAGAGGTAGTTCGtGAGCATGAATTCTCGCCAATtcgtagggatcaatctcttctt TCGTTAGAGGTATGTCGGAC
EPL2-19	GTCGTCCTAGAGGTAGTTCGtTGTTGCTCCCGGATTACACGttctatacgtcttgttttccgtG AGCATGAATTCTCGCCAAT
EPL2-20	GTCGTCCTAGAGGTAGTTCGtTCGTTAGAGGTATGTCGGACttcaattcttgatgcaacgcc tTGTTGCTCCCGGATTACACG
EPL2-21	GTCGTCCTAGAGGTAGTTCGtGAGCATGAATTCTCGCCAATtacgtttagcaacaagcag ggtTCGTTAGAGGTATGTCGGAC
EPL2-22	GTCGTCCTAGAGGTAGTTCGtTGTTGCTCCCGGATTACACGtcatcgtcttctccactaatgt GAGCATGAATTCTCGCCAAT

Continued on following page

Table 3.2: *continued from previous page*

EPL2-23	GTCGTCCTAGAGGTAGTTCGtTCGTTAGAGGTATGTCGGACtttcgaccgtaacaatcgtg gtTGTTGCTCCCGGATTACACG
EPL2-24	GTCGTCCTAGAGGTAGTTCGtGAGCATGAATTCTCGCCAATtaagttcagctttccttagtttT CGTTAGAGGTATGTCGGAC
EPL2-25	GTCGTCCTAGAGGTAGTTCGtTGTTGCTCCCGGATTACACGttttattgttctttgccttcgtGA GCATGAATTCTCGCCAAT
EPL2-26	GTCGTCCTAGAGGTAGTTCGtTCGTTAGAGGTATGTCGGACtgtcttcaagttggttattcct TGTTGCTCCCGGATTACACG
EPL2-27	GTCGTCCTAGAGGTAGTTCGtGAGCATGAATTCTCGCCAATtcttggtgagcctagaagatt tTCGTTAGAGGTATGTCGGAC
EPL2-28	GTCGTCCTAGAGGTAGTTCGtTGTTGCTCCCGGATTACACGttgtaacagttgctgctgttgt GAGCATGAATTCTCGCCAAT
EPL2-29	GTCGTCCTAGAGGTAGTTCGtTCGTTAGAGGTATGTCGGACttgctgttgttgttgttgtT GTTGCTCCCGGATTACACG
EPL2-30	GTCGTCCTAGAGGTAGTTCGtGAGCATGAATTCTCGCCAATtgttttcagtcttaagggcatt TCGTTAGAGGTATGTCGGAC
EPL2-31	GTCGTCCTAGAGGTAGTTCGtTGTTGCTCCCGGATTACACGttccacgtcttccaatacaat tGAGCATGAATTCTCGCCAAT
EPL2-32	GTCGTCCTAGAGGTAGTTCGtTCGTTAGAGGTATGTCGGACtcctgaacgaactttcttgca tTGTTGCTCCCGGATTACACG
EPL2-33	GTCGTCCTAGAGGTAGTTCGtGAGCATGAATTCTCGCCAATtcgtcttcaattttccgtttctT CGTTAGAGGTATGTCGGAC
EPL2-34	GTCGTCCTAGAGGTAGTTCGtTGTTGCTCCCGGATTACACGtgattaaagggatcgtccgtt tGAGCATGAATTCTCGCCAAT
EPL2-35	GTCGTCCTAGAGGTAGTTCGtTCGTTAGAGGTATGTCGGACtagatatccccttcaagtattt TGTTGCTCCCGGATTACACG
EPL2-36	GTCGTCCTAGAGGTAGTTCGtGAGCATGAATTCTCGCCAATttcgaacggccatttgaatc atTCGTTAGAGGTATGTCGGAC
EPL2-37	GTCGTCCTAGAGGTAGTTCGtTGTTGCTCCCGGATTACACGtttggaatgggtcgtacagtt tGAGCATGAATTCTCGCCAAT
EPL2-38	GTCGTCCTAGAGGTAGTTCGtTCGTTAGAGGTATGTCGGACttaccaactctcttcctgaatt TGTTGCTCCCGGATTACACG
EPL2-39	GTCGTCCTAGAGGTAGTTCGtGAGCATGAATTCTCGCCAATtaacatgcagacttggtcga ctTCGTTAGAGGTATGTCGGAC
EPL2-40	GTCGTCCTAGAGGTAGTTCGtTGTTGCTCCCGGATTACACGtatcgttactaccttctcttgt GAGCATGAATTCTCGCCAAT
EPL2-41	GTCGTCCTAGAGGTAGTTCGtTCGTTAGAGGTATGTCGGACtccacttgtcgtaaagtctga tTGTTGCTCCCGGATTACACG
EPL2-42	GTCGTCCTAGAGGTAGTTCGtGAGCATGAATTCTCGCCAATtcccatattcattttgtggagt TCGTTAGAGGTATGTCGGAC
EPL2-43	GTCGTCCTAGAGGTAGTTCGtTGTTGCTCCCGGATTACACGtcttgccggttcatctgaaaa tGAGCATGAATTCTCGCCAAT
EPL2-44	GTCGTCCTAGAGGTAGTTCGtTCGTTAGAGGTATGTCGGACtccgaatctaatcacctgag ttTGTTGCTCCCGGATTACACG
EPL2-45	GTCGTCCTAGAGGTAGTTCGtGAGCATGAATTCTCGCCAATtttgttcgtaggacttcgtact TCGTTAGAGGTATGTCGGAC

Continued on following page

Table 3.2: *continued from previous page*

EPL2-46	GTCGTCCTAGAGGTAGTTCGtTGTTGCTCCCGGATTACACGtcgatactttatggtggcttct GAGCATGAATTCTCGCCAAT
EPL2-47	GTCGTCCTAGAGGTAGTTCGtTCGTTAGAGGTATGTCGGACtgttctgtgatttctgcttttT GTTGCTCCCGGATTACACG
EPL2-48	GTCGTCCTAGAGGTAGTTCGtGAGCATGAATTCTCGCCAATtgaagagttctgtttcgcttct TCGTTAGAGGTATGTCGGAC

Table 3.4: Secondary readout probes used for seqFISH+ experiments.

Probe name	**Sequence**	**Fluorophore**
prERB1	GAGTGCGGCCTTTGATTAA	A647N
prERB2	CTCCGTTACAACCGTCACG	A565
prERB3	TTTGGTGCAATCACCGCCC	A647N
prERB4	CGTGTAATCCGGGAGCAAC	A565
prERB5	CATCCTGAACACCGCGGGA	A647N
prERB6	ATTGGCGAGAATTCATGCT	A565
prERB7	GTCCGACATACCTCTAACG	A647N
prERB8	AAGTAGGTTCACCCTGCCG	A565
prERB9	AAGCGCGAAGATGCAATTG	A647N
prERB10	AATCACAGGCCGAGCTCAG	A565
prERB11	TTACGAAATTCCACCCTCG	A647N
prERB12	TGTTTCACTCAGTAAGCCC	A565
prERB13	GACGACCTGCGGATGAATG	A488

References

Abraham J., K. A. Nasmyth, J. N. Strathern, A. J. S. Klar, and J. B. Hicks, 1984 Regulation of mating-type information in yeast: Negative control requiring sequences both 5′ and 3′ to the regulated region. Journal of Molecular Biology 176: 307–331. https://doi.org/10.1016/0022-2836(84)90492-3

Albuquerque C. P., M. B. Smolka, S. H. Payne, V. Bafna, J. Eng, *et al.*, 2008 A Multidimensional Chromatography Technology for In-depth Phosphoproteome Analysis. Mol Cell Proteomics 7: 1389–1396. https://doi.org/10.1074/mcp.M700468-MCP200

Allfrey V. G., R. Faulkner, and A. E. Mirsky, 1964 ACETYLATION AND METHYLATION OF HISTONES AND THEIR POSSIBLE ROLE IN THE REGULATION OF RNA SYNTHESIS*. Proc Natl Acad Sci U S A 51: 786–794.

Andersson R., and A. Sandelin, 2020 Determinants of enhancer and promoter activities of regulatory elements. Nat Rev Genet 21: 71–87. https://doi.org/10.1038/s41576-019-0173-8

Andreev I., K. M. E. Laidlaw, S. M. Giovanetti, G. Urtecho, D. Shriner, *et al.*, 2023 Discovery of a rapidly evolving yeast defense factor, KTD1, against the secreted killer toxin K28. Proceedings of the National Academy of Sciences 120: e2217194120. https://doi.org/10.1073/pnas.2217194120

Ansari A., and M. R. Gartenberg, 1999 Persistence of an alternate chromatin structure at silenced loci in vitro. Proc Natl Acad Sci U S A 96: 343–348.

Aparicio O. M., B. L. Billington, and D. E. Gottschling, 1991 Modifiers of position effect are shared between telomeric and silent mating-type loci in S. cerevisiae. Cell 66: 1279–1287. https://doi.org/10.1016/0092-8674(91)90049-5

Audergon P. N. C. B., S. Catania, A. Kagansky, P. Tong, M. Shukla, *et al.*, 2015 Epigenetics. Restricted epigenetic inheritance of H3K9 methylation. Science 348: 132–135. https://doi.org/10.1126/science.1260638

Azad G. K., and R. S. Tomar, 2016 The multifunctional transcription factor Rap1: a regulator of yeast physiology. Front Biosci (Landmark Ed) 21: 918–930. https://doi.org/10.2741/4429

Badis G., E. T. Chan, H. van Bakel, L. Pena-Castillo, D. Tillo, *et al.*, 2008 A new library of yeast transcription factor motifs reveals a widespread function for Rsc3 in targeting nucleosome exclusion at promoters. Mol Cell 32: 878–887. https://doi.org/10.1016/j.molcel.2008.11.020

Bailey L. T., S. J. Northall, and T. Schalch, 2021 Breakers and amplifiers in chromatin circuitry: acetylation and ubiquitination control the heterochromatin machinery. Current Opinion in Structural Biology 71: 156–163. https://doi.org/10.1016/j.sbi.2021.06.012

Baker R. E., M. Fitzgerald-Hayes, and T. C. O'Brien, 1989 Purification of the Yeast Centromere Binding Protein CP1 and a Mutational Analysis of Its Binding Site.

Journal of Biological Chemistry 264: 10843–10850. https://doi.org/10.1016/S0021-9258(18)81697-0

Barry R. M., O. Sacco, A. Mameri, M. Stojaspal, W. Kartsonis, *et al.*, 2022 Rap1 regulates TIP60 function during fate transition between two-cell-like and pluripotent states. Genes Dev 36: 313–330. https://doi.org/10.1101/gad.349039.121

Bell S. P., R. Kobayashi, and B. Stillman, 1993 Yeast origin recognition complex functions in transcription silencing and DNA replication. Science 262: 1844–1849. https://doi.org/10.1126/science.8266072

Berger S. L., T. Kouzarides, R. Shiekhattar, and A. Shilatifard, 2009 An operational definition of epigenetics. Genes Dev 23: 781–783. https://doi.org/10.1101/gad.1787609

Berger F., 2019 Emil Heitz, a true epigenetics pioneer. Nat Rev Mol Cell Biol 20: 572–572. https://doi.org/10.1038/s41580-019-0161-z

Bhagwat N. R., S. N. Owens, M. Ito, J. V. Boinapalli, P. Poa, *et al.*, 2021 SUMO is a pervasive regulator of meiosis, (A. L. Marston, P. A. Cole, A. L. Marston, F. Pelisch, J. Matos, *et al.*, Eds.). eLife 10: e57720. https://doi.org/10.7554/eLife.57720

Bhagwat N. R., S. N. Owens, M. Ito, J. V. Boinapalli, P. Poa, *et al.*, SUMO is a pervasive regulator of meiosis. eLife 10: e57720. https://doi.org/10.7554/eLife.57720

Bitterman K. J., R. M. Anderson, H. Y. Cohen, M. Latorre-Esteves, and D. A. Sinclair, 2002 Inhibition of silencing and accelerated aging by nicotinamide, a putative negative regulator of yeast sir2 and human SIRT1. J Biol Chem 277: 45099–45107. https://doi.org/10.1074/jbc.M205670200

Bonetti D., C. Rinaldi, J. Vertemara, M. Notaro, P. Pizzul, *et al.*, 2020 DNA binding modes influence Rap1 activity in the regulation of telomere length and MRX functions at DNA ends. Nucleic Acids Research 48: 2424–2441. https://doi.org/10.1093/nar/gkz1203

Bonnell E., E. Pasquier, and R. J. Wellinger, 2021 Telomere Replication: Solving Multiple End Replication Problems. Frontiers in Cell and Developmental Biology 9.

Bosio M. C., B. Fermi, and G. Dieci, 2017a Transcriptional control of yeast ribosome biogenesis: A multifaceted role for general regulatory factors. Transcription 8: 254–260. https://doi.org/10.1080/21541264.2017.1317378

Bosio M. C., B. Fermi, G. Spagnoli, E. Levati, L. Rubbi, *et al.*, 2017b Abf1 and other general regulatory factors control ribosome biogenesis gene expression in budding yeast. Nucleic Acids Res 45: 4493–4506. https://doi.org/10.1093/nar/gkx058

Bourns B. D., M. K. Alexander, A. M. Smith, and V. A. Zakian, 1998 Sir proteins, Rif proteins, and Cdc13p bind Saccharomyces telomeres in vivo. Mol Cell Biol 18: 5600–5608. https://doi.org/10.1128/MCB.18.9.5600

Boyle P., and C. Després, 2010 Dual-function transcription factors and their entourage. Plant Signal Behav 5: 629–634.

Brakhage A. A., 2013 Regulation of fungal secondary metabolism. Nat Rev Microbiol 11: 21–32. https://doi.org/10.1038/nrmicro2916

Bram R. J., and R. D. Kornberg, 1987 Isolation of a Saccharomyces cerevisiae centromere DNA-binding protein, its human homolog, and its possible role as a transcription factor. Mol Cell Biol 7: 403–409.

Brand A. H., L. Breeden, J. Abraham, R. Sternglanz, and K. Nasmyth, 1985 Characterization of a “silencer” in yeast: A DNA sequence with properties opposite to those of a transcriptional enhancer. Cell 41: 41–48. https://doi.org/10.1016/0092-8674(85)90059-5

Brindle P. K., J. P. Holland, C. E. Willett, M. A. Innis, and M. J. Holland, 1990 Multiple factors bind the upstream activation sites of the yeast enolase genes ENO1 and ENO2: ABFI protein, like repressor activator protein RAP1, binds cis-acting sequences which modulate repression or activation of transcription. Mol Cell Biol 10: 4872–4885.

Brothers M., and J. Rine, 2019 Mutations in the PCNA DNA Polymerase Clamp of Saccharomyces cerevisiae Reveal Complexities of the Cell Cycle and Ploidy on Heterochromatin Assembly. Genetics 213: 449–463. https://doi.org/10.1534/genetics.119.302452

Brothers M., and J. Rine, 2022 Distinguishing between recruitment and spread of silent chromatin structures in Saccharomyces cerevisiae, (W. Dang, and J. K. Tyler, Eds.). eLife 11: e75653. https://doi.org/10.7554/eLife.75653

Brown S. W., 1966 Heterochromatin. Science 151: 417–425. https://doi.org/10.1126/science.151.3709.417

Brown C. A., A. W. Murray, and K. J. Verstrepen, 2010 Rapid Expansion and Functional Divergence of Subtelomeric Gene Families in Yeasts. Current Biology 20: 895–903. https://doi.org/10.1016/j.cub.2010.04.027

Buchman A. R., W. J. Kimmerly, J. Rine, and R. D. Kornberg, 1988a Two DNA-binding factors recognize specific sequences at silencers, upstream activating sequences, autonomously replicating sequences, and telomeres in Saccharomyces cerevisiae. Molecular and Cellular Biology 8: 210–225. https://doi.org/10.1128/mcb.8.1.210-225.1988

Buchman A. R., N. F. Lue, and R. D. Kornberg, 1988b Connections between transcriptional activators, silencers, and telomeres as revealed by functional analysis of a yeast DNA-binding protein. Mol Cell Biol 8: 5086–5099.

Burke D., D. Dawson, and T. Stearns, 2000 *Methods in yeast genetics: a Cold Spring Harbor Laboratory course manual*. Cold Spring Harbor Laboratory Press, Plainview, N.Y.

Carmen A. A., L. Milne, and M. Grunstein, 2002 Acetylation of the Yeast Histone H4 N Terminus Regulates Its Binding to Heterochromatin Protein SIR3*. Journal of Biological Chemistry 277: 4778–4781. https://doi.org/10.1074/jbc.M110532200

Chadwick B. P., and H. F. Willard, 2004 Multiple spatially distinct types of facultative heterochromatin on the human inactive X chromosome. Proc Natl Acad Sci U S A 101: 17450–17455. https://doi.org/10.1073/pnas.0408021101

Challal D., M. Barucco, S. Kubik, F. Feuerbach, T. Candelli, *et al.*, 2018 General Regulatory Factors Control the Fidelity of Transcription by Restricting Non-coding and Ectopic Initiation. Molecular Cell 72: 955-969.e7. https://doi.org/10.1016/j.molcel.2018.11.037

Chen L., and J. Widom, 2005 Mechanism of Transcriptional Silencing in Yeast. Cell 120: 37–48. https://doi.org/10.1016/j.cell.2004.11.030

Chereji R. V., S. Ramachandran, T. D. Bryson, and S. Henikoff, 2018 Precise genome-wide mapping of single nucleosomes and linkers in vivo. Genome Biol 19: 19. https://doi.org/10.1186/s13059-018-1398-0

Chymkowitch P., A. Nguéa P, and J. M. Enserink, 2015a SUMO-regulated transcription: Challenging the dogma. BioEssays 37: 1095–1105. https://doi.org/10.1002/bies.201500065

Chymkowitch P., A. Nguéa P, H. Aanes, C. J. Koehler, B. Thiede, *et al.*, 2015b Sumoylation of Rap1 mediates the recruitment of TFIID to promote transcription of ribosomal protein genes. Genome Res 25: 897–906. https://doi.org/10.1101/gr.185793.114

Clark-Adams C. D., D. Norris, M. A. Osley, J. S. Fassler, and F. Winston, 1988 Changes in histone gene dosage alter transcription in yeast. Genes Dev 2: 150–159. https://doi.org/10.1101/gad.2.2.150

Cockell M., F. Palladino, T. Laroehe, G. Kyrion, C. Liu, *et al.*, 1995 The Carboxy Termini of Sir4 and Rapl Affect Sir3 Localization: Evidence for a Multicomponent Complex Required for Yeast Telomeric Silencing. The Journal of Cell Biology 129.

Cockell M., M. Gotta, F. Palladino, S. G. Martin, and S. M. Gasser, 1998 Targeting Sir Proteins to Sites of Action: A General Mechanism for Regulated Repression. Cold Spring Harb Symp Quant Biol 63: 401–412. https://doi.org/10.1101/sqb.1998.63.401

Conrad M. N., J. H. Wright, A. J. Wolf, and V. A. Zakian, 1990 RAP1 protein interacts with yeast telomeres in vivo: Overproduction alters telomere structure and decreases chromosome stability. Cell 63: 739–750. https://doi.org/10.1016/0092-8674(90)90140-A

Conrad T., F. M. G. Cavalli, J. M. Vaquerizas, N. M. Luscombe, and A. Akhtar, 2012 Drosophila Dosage Compensation Involves Enhanced Pol II Recruitment to Male X-Linked Promoters. Science 337: 742–746. https://doi.org/10.1126/science.1221428

Couvillion M., K. M. Harlen, K. C. Lachance, K. L. Trotta, E. Smtih, *et al.*, 2022 Transcription elongation is finely tuned by dozens of regulatory factors. eLife.

Deng W., and S. G. E. Roberts, 2007 TFIIB and the regulation of transcription by RNA polymerase II. Chromosoma 116: 417–429. https://doi.org/10.1007/s00412-007-0113-9

Devlin C., K. Tice-Baldwin, D. Shore, and K. T. Arndt, 1991 RAP1 is required for BAS1/BAS2- and GCN4-dependent transcription of the yeast HIS4 gene. Mol Cell Biol 11: 3642–3651.

Dodson A. E., and J. Rine, 2015 Heritable capture of heterochromatin dynamics in Saccharomyces cerevisiae, (D. E. Gottschling, Ed.). eLife 4: e05007. https://doi.org/10.7554/eLife.05007

Donovan B. T., H. Chen, C. Jipa, L. Bai, and M. G. Poirier, 2019 Dissociation rate compensation mechanism for budding yeast pioneer transcription factors, (T. Formosa, J. K. Tyler, T. Formosa, and M. Spies, Eds.). eLife 8: e43008. https://doi.org/10.7554/eLife.43008

Dunn M. J., S. U. A. Shazib, E. Simonton, J. C. Slot, and M. Z. Anderson, 2022 Architectural groups of a subtelomeric gene family evolve along distinct paths in Candida albicans. G3 Genes|Genomes|Genetics 12: jkac283. https://doi.org/10.1093/g3journal/jkac283

Eissenberg J. C., T. C. James, D. M. Foster-Hartnett, T. Hartnett, V. Ngan, *et al.*, 1990 Mutation in a heterochromatin-specific chromosomal protein is associated with suppression of position-effect variegation in Drosophila melanogaster. Proc Natl Acad Sci U S A 87: 9923–9927. https://doi.org/10.1073/pnas.87.24.9923

Elgin S. C. R., and G. Reuter, 2013 Position-Effect Variegation, Heterochromatin Formation, and Gene Silencing in Drosophila. Cold Spring Harb Perspect Biol 5: a017780. https://doi.org/10.1101/cshperspect.a017780

Ellahi A., D. M. Thurtle, and J. Rine, 2015 The Chromatin and Transcriptional Landscape of Native Saccharomyces cerevisiae Telomeres and Subtelomeric Domains. Genetics 200: 505–521. https://doi.org/10.1534/genetics.115.175711

Ellahi A., and J. Rine, 2016 Evolution and Functional Trajectory of Sir1 in Gene Silencing. Mol Cell Biol 36: 1164–1179. https://doi.org/10.1128/MCB.01013-15

Endoh M., T. A. Endo, T. Endoh, Y. Fujimura, O. Ohara, *et al.*, 2008 Polycomb group proteins Ring1A/B are functionally linked to the core transcriptional regulatory circuitry to maintain ES cell identity. Development 135: 1513–1524. https://doi.org/10.1242/dev.014340

Eng C.-H. L., M. Lawson, Q. Zhu, R. Dries, N. Koulena, *et al.*, 2019 Transcriptome-scale super-resolved imaging in tissues by RNA seqFISH+. Nature 568: 235–239. https://doi.org/10.1038/s41586-019-1049-y

Feeser E. A., and C. Wolberger, 2008 Structural and Functional Studies of the Rap1 C-Terminus Reveal Novel Separation-of-Function Mutants. Journal of Molecular Biology 380: 520–531. https://doi.org/10.1016/j.jmb.2008.04.078

Feldman J. B., J. B. Hicks, and J. R. Broach, 1984 Identification of sites required for repression of a silent mating type locus in yeast. Journal of Molecular Biology 178: 815–834. https://doi.org/10.1016/0022-2836(84)90313-9

Feldmann E. A., and R. Galletto, 2014 The DNA-Binding Domain of Yeast Rap1 Interacts with Double-Stranded DNA in Multiple Binding Modes. Biochemistry 53: 7471–7483. https://doi.org/10.1021/bi501049b

Fermi B., M. C. Bosio, and G. Dieci, 2016 Promoter architecture and transcriptional regulation of Abf1-dependent ribosomal protein genes in Saccharomyces cerevisiae. Nucleic Acids Res 44: 6113–6126. https://doi.org/10.1093/nar/gkw194

Ferrell J. E., 2012 Bistability, bifurcations, and Waddington's epigenetic landscape. Curr Biol 22: R458–R466. https://doi.org/10.1016/j.cub.2012.03.045

Foss M., F. J. McNally, P. Laurenson, and J. Rine, 1993 Origin Recognition Complex (ORC) in Transcriptional Silencing and DNA Replication in S. cerevisiae. Science 262: 1838–1844. https://doi.org/10.1126/science.8266071

Fouet M., and J. Rine, 2023 Limits to transcriptional silencing in Saccharomyces cerevisiae. Genetics 223: iyac180. https://doi.org/10.1093/genetics/iyac180

Fourel G., E. Lebrun, and E. Gilson, 2002 Protosilencers as building blocks for heterochromatin. BioEssays 24: 828–835. https://doi.org/10.1002/bies.10139

Fox C. A., A. E. Ehrenhofer-Murray, S. Loo, and J. Rine, 1997 The origin recognition complex, SIR1, and the S phase requirement for silencing. Science 276: 1547–1551. https://doi.org/10.1126/science.276.5318.1547

Fujiwara R., N. Damodaren, J. E. Wilusz, and K. Murakami, 2019 The capping enzyme facilitates promoter escape and assembly of a follow-on preinitiation complex for reinitiation. Proc Natl Acad Sci U S A 116: 22573–22582. https://doi.org/10.1073/pnas.1905449116

Ganapathi M., M. J. Palumbo, S. A. Ansari, Q. He, K. Tsui, *et al.*, 2011 Extensive role of the general regulatory factors, Abf1 and Rap1, in determining genome-wide chromatin structure in budding yeast. Nucleic Acids Res 39: 2032–2044. https://doi.org/10.1093/nar/gkq1161

Gao L., and D. S. Gross, 2008 Sir2 Silences Gene Transcription by Targeting the Transition between RNA Polymerase II Initiation and Elongation. Mol Cell Biol 28: 3979–3994. https://doi.org/10.1128/MCB.00019-08

Garbett K. A., M. K. Tripathi, B. Cencki, J. H. Layer, and P. A. Weil, 2007 Yeast TFIID Serves as a Coactivator for Rap1p by Direct Protein-Protein Interaction. Mol Cell Biol 27: 297–311. https://doi.org/10.1128/MCB.01558-06

Gardner K. A., J. Rine, and C. A. Fox, 1999 A region of the Sir1 protein dedicated to recognition of a silencer and required for interaction with the Orc1 protein in saccharomyces cerevisiae. Genetics 151: 31–44. https://doi.org/10.1093/genetics/151.1.31

Gartenberg M. R., and J. S. Smith, 2016 The Nuts and Bolts of Transcriptionally Silent Chromatin in Saccharomyces cerevisiae. Genetics 203: 1563–1599. https://doi.org/10.1534/genetics.112.145243

Gaskill M., and M. Harrison, 2022 Tethering gene regulation to chromatin organization. Science 375: 491–492. https://doi.org/10.1126/science.abn6380

Gelbart M. E., T. Rechsteiner, T. J. Richmond, and T. Tsukiyama, 2001 Interactions of Isw2 Chromatin Remodeling Complex with Nucleosomal Arrays: Analyses Using Recombinant Yeast Histones and Immobilized Templates. Mol Cell Biol 21: 2098–2106. https://doi.org/10.1128/MCB.21.6.2098-2106.2001

Giesman D., L. Best, and K. Tatchell, 1991 The role of RAP1 in the regulation of the MAT alpha locus. Mol Cell Biol 11: 1069–1079.

Gietz R. D., and R. H. Schiestl, 2007 High-efficiency yeast transformation using the LiAc/SS carrier DNA/PEG method. Nat Protoc 2: 31–34. https://doi.org/10.1038/nprot.2007.13

Goldstein A. L., and J. H. McCusker, 1999 Three new dominant drug resistance cassettes for gene disruption in Saccharomyces cerevisiae. Yeast 15: 1541–1553. https://doi.org/10.1002/(SICI)1097-0061(199910)15:14<1541::AID-YEA476>3.0.CO;2-K

Goodnight D., and J. Rine, 2020 S-phase-independent silencing establishment in Saccharomyces cerevisiae, (T. Formosa, K. Struhl, T. Formosa, R. T. Kamakaka, and D. Moazed, Eds.). eLife 9: e58910. https://doi.org/10.7554/eLife.58910

Gottschling D. E., O. M. Aparicio, B. L. Billington, and V. A. Zakian, 1990 Position effect at S. cerevisiae telomeres: Reversible repression of Pol II transcription. Cell 63: 751–762. https://doi.org/10.1016/0092-8674(90)90141-Z

Gottschling D. E., 1992 Telomere-proximal DNA in Saccharomyces cerevisiae is refractory to methyltransferase activity in vivo. Proc Natl Acad Sci U S A 89: 4062–4065.

Goutte C., and A. D. Johnson, 1993 Yeast a1 and alpha 2 homeodomain proteins form a DNA-binding activity with properties distinct from those of either protein. J Mol Biol 233: 359–371. https://doi.org/10.1006/jmbi.1993.1517

Grunstein M., and S. M. Gasser, 2013 Epigenetics in Saccharomyces cerevisiae. Cold Spring Harbor Perspectives in Biology 5: a017491–a017491. https://doi.org/10.1101/cshperspect.a017491

Gueldener U., J. Heinisch, G. J. Koehler, D. Voss, and J. H. Hegemann, 2002 A second set of loxP marker cassettes for Cre-mediated multiple gene knockouts in budding yeast. Nucleic Acids Research 30: e23. https://doi.org/10.1093/nar/30.6.e23

Haber J. E., 2012 Mating-Type Genes and *MAT* Switching in *Saccharomyces cerevisiae*. Genetics 191: 33–64. https://doi.org/10.1534/genetics.111.134577

Haig D., 2012 Commentary: The epidemiology of epigenetics. International Journal of Epidemiology 41: 13–16. https://doi.org/10.1093/ije/dyr183

Hantsche M., and P. Cramer, 2017 Conserved RNA polymerase II initiation complex structure. Current Opinion in Structural Biology 47: 17–22. https://doi.org/10.1016/j.sbi.2017.03.013

Hartley P. D., and H. D. Madhani, 2009 Mechanisms that specify promoter nucleosome location and identity. Cell 137: 445–458. https://doi.org/10.1016/j.cell.2009.02.043

Haruki H., J. Nishikawa, and U. K. Laemmli, 2008 The Anchor-Away Technique: Rapid, Conditional Establishment of Yeast Mutant Phenotypes. Molecular Cell 31: 925–932. https://doi.org/10.1016/j.molcel.2008.07.020

Harvey C. J. B., M. Tang, U. Schlecht, J. Horecka, C. R. Fischer, *et al.*, 2018 HEx: A heterologous expression platform for the discovery of fungal natural products. Science Advances 4: eaar5459. https://doi.org/10.1126/sciadv.aar5459

He S., L.-H. Wang, Y. Liu, Y.-Q. Li, H.-T. Chen, *et al.*, 2020 Single-cell transcriptome profiling of an adult human cell atlas of 15 major organs. Genome Biology 21: 294. https://doi.org/10.1186/s13059-020-02210-0

Hecht A., T. Laroche, S. Strahl-Bolsinger, S. M. Gasser, and M. Grunstein, 1995 Histone H3 and H4 N-termini interact with SIR3 and SIR4 proteins: A molecular model for the formation of heterochromatin in yeast. Cell 80: 583–592. https://doi.org/10.1016/0092-8674(95)90512-X

Herskowitz I., 1989 A regulatory hierarchy for cell specialization in yeast. Nature 342: 749–757. https://doi.org/10.1038/342749a0

Herskowitz I., J. Rine, and J. Strathern, 1992 Mating-type Determination and Mating-type Interconversion in Saccharomyces cerevisiae. Cold Spring Harbor Monograph Archive 21: 583–656. https://doi.org/10.1101/0.583-656

Hicks J., J. N. Strathern, and A. J. S. Klar, 1979 Transposable mating type genes in Saccharomyces cerevisiae. Nature 282: 478–483. https://doi.org/10.1038/282478a0

Ho J. J. D., K. L. Dunbar, B. Naughton, and C. J. B. Harvey, 2022 Turning the world's DNA into new medicines. Trends in Biotechnology 40: 766–767. https://doi.org/10.1016/j.tibtech.2022.01.014

Holt L. J., B. B. Tuch, J. Villén, A. D. Johnson, S. P. Gygi, *et al.*, 2009 Global analysis of Cdk1 substrate phosphorylation sites provides insights into evolution. Science 325: 1682. https://doi.org/10.1126/science.1172867

Hoppe G. J., J. C. Tanny, A. D. Rudner, S. A. Gerber, S. Danaie, *et al.*, 2002 Steps in Assembly of Silent Chromatin in Yeast: Sir3-Independent Binding of a Sir2/Sir4 Complex to Silencers and Role for Sir2-Dependent Deacetylation. Molecular and Cellular Biology 22: 4167–4180. https://doi.org/10.1128/MCB.22.12.4167-4180.2002

Imai S., C. M. Armstrong, M. Kaeberlein, and L. Guarente, 2000 Transcriptional silencing and longevity protein Sir2 is an NAD-dependent histone deacetylase. Nature 403: 795–800. https://doi.org/10.1038/35001622

Irie H., I. Yamamoto, Y. Tarumoto, S. Tashiro, K. W. Runge, *et al.*, 2019 Telomere-binding proteins Taz1 and Rap1 regulate DSB repair and suppress gross chromosomal rearrangements in fission yeast. PLOS Genetics 15: e1008335. https://doi.org/10.1371/journal.pgen.1008335

Ivessa A. S., J.-Q. Zhou, V. P. Schulz, E. K. Monson, and V. A. Zakian, 2002 Saccharomyces Rrm3p, a 5′ to 3′ DNA helicase that promotes replication fork progression through telomeric and subtelomeric DNA. Genes Dev. 16: 1383–1396. https://doi.org/10.1101/gad.982902

Iyer L. M., S. Abhiman, and L. Aravind, 2011 Chapter 2 - Natural History of Eukaryotic DNA Methylation Systems, pp. 25–104 in *Progress in Molecular Biology and Translational Science*, Modifications of Nuclear DNA and its Regulatory Proteins. edited by Cheng X., Blumenthal R. M. Academic Press.

Jackson V., and R. Chalkley, 1985 Histone segregation on replicating chromatin. Biochemistry 24: 6930–6938. https://doi.org/10.1021/bi00345a027

Jackson V., 1988 Deposition of newly synthesized histones: hybrid nucleosomes are not tandemly arranged on daughter DNA strands. Biochemistry 27: 2109–2120. https://doi.org/10.1021/bi00406a044

Jackson J. C., and J. M. Lopes, 1996 The Yeast UME6 Gene Is Required for Both Negative and Positive Transcriptional Regulation of Phospholipid Biosynthetic Gene Expression. Nucleic Acids Research 24: 1322–1329. https://doi.org/10.1093/nar/24.7.1322

Janapala Y., T. Preiss, and N. E. Shirokikh, 2019 Control of Translation at the Initiation Phase During Glucose Starvation in Yeast. Int J Mol Sci 20: 4043. https://doi.org/10.3390/ijms20164043

Janke R., G. A. King, M. Kupiec, and J. Rine, 2018 Pivotal roles of PCNA loading and unloading in heterochromatin function. Proc Natl Acad Sci U S A 115: E2030–E2039. https://doi.org/10.1073/pnas.1721573115

Jenuwein T., and C. D. Allis, 2001 Translating the Histone Code. Science 293: 1074–1080. https://doi.org/10.1126/science.1063127

Johnson L. M., P. S. Kayne, E. S. Kahn, and M. Grunstein, 1990 Genetic evidence for an interaction between SIR3 and histone H4 in the repression of the silent mating loci in Saccharomyces cerevisiae. Proc Natl Acad Sci U S A 87: 6286–6290.

Johnson A., G. Li, T. W. Sikorski, S. Buratowski, C. L. Woodcock, *et al.*, 2009 Reconstitution of Heterochromatin-Dependent Transcriptional Gene Silencing. Molecular Cell 35: 769–781. https://doi.org/10.1016/j.molcel.2009.07.030

Johnson A., R. Wu, M. Peetz, S. P. Gygi, and D. Moazed, 2013 Heterochromatic Gene Silencing by Activator Interference and a Transcription Elongation Barrier. Journal of Biological Chemistry 288: 28771–28782. https://doi.org/10.1074/jbc.M113.460071

Johnson A. N., and P. A. Weil, 2017 Identification of a transcriptional activation domain in yeast repressor activator protein 1 (Rap1) using an altered DNA-binding specificity variant. J Biol Chem 292: 5705–5723. https://doi.org/10.1074/jbc.M117.779181

Jonge W. J. de de, M. Brok, P. Lijnzaad, P. Kemmeren, and F. C. Holstege, 2020 Genome-wide off-rates reveal how DNA binding dynamics shape transcription factor function. Molecular Systems Biology 16: e9885. https://doi.org/10.15252/msb.20209885

Jumper J., R. Evans, A. Pritzel, T. Green, M. Figurnov, *et al.*, 2021 Highly accurate protein structure prediction with AlphaFold. Nature 596: 583–589. https://doi.org/10.1038/s41586-021-03819-2

Kachroo A. H., J. M. Laurent, C. M. Yellman, A. G. Meyer, C. O. Wilke, *et al.*, 2015 Systematic humanization of yeast genes reveals conserved functions and genetic modularity. Science 348: 921–925. https://doi.org/10.1126/science.aaa0769

Kayne P. S., U. J. Kim, M. Han, J. R. Mullen, F. Yoshizaki, *et al.*, 1988 Extremely conserved histone H4 N terminus is dispensable for growth but essential for repressing the silent mating loci in yeast. Cell 55: 27–39. https://doi.org/10.1016/0092-8674(88)90006-2

Kent N. A., S. M. Eibert, and J. Mellor, 2004 Cbf1p Is Required for Chromatin Remodeling at Promoter-proximal CACGTG Motifs in Yeast*. Journal of Biological Chemistry 279: 27116–27123. https://doi.org/10.1074/jbc.M403818200

Khattar E., and V. Tergaonkar, 2020 Role of Rap1 in DNA damage response: implications in stem cell homeostasis and cancer. Experimental Hematology 90: 12–17. https://doi.org/10.1016/j.exphem.2020.08.009

Kimmerly W., A. Buchman, R. Kornberg, and J. Rine, 1988 Roles of two DNA-binding factors in replication, segregation and transcriptional repression mediated by a yeast silencer. The EMBO Journal 7: 2241–2253. https://doi.org/10.1002/j.1460-2075.1988.tb03064.x

Knight B., S. Kubik, B. Ghosh, M. J. Bruzzone, M. Geertz, *et al.*, 2014 Two distinct promoter architectures centered on dynamic nucleosomes control ribosomal protein gene transcription. Genes Dev. 28: 1695–1709. https://doi.org/10.1101/gad.244434.114

Kothiwal D., and S. Laloraya, 2019 A SIR-independent role for cohesin in subtelomeric silencing and organization. Proceedings of the National Academy of Sciences 116: 5659–5664. https://doi.org/10.1073/pnas.1816582116

Kruglyak L., 2008 The road to genome-wide association studies. Nat Rev Genet 9: 314–318. https://doi.org/10.1038/nrg2316

Kubik S., M. J. Bruzzone, P. Jacquet, J.-L. Falcone, J. Rougemont, *et al.*, 2015 Nucleosome Stability Distinguishes Two Different Promoter Types at All Protein-Coding Genes in Yeast. Molecular Cell 60: 422–434. https://doi.org/10.1016/j.molcel.2015.10.002

Kubik S., M. J. Bruzzone, and D. Shore, 2017 Establishing nucleosome architecture and stability at promoters: Roles of pioneer transcription factors and the RSC chromatin remodeler. BioEssays 39: 1600237. https://doi.org/10.1002/bies.201600237

Kurtz S., and D. Shore, 1991 RAP1 protein activates and silences transcription of mating-type genes in yeast. Genes Dev. 5: 616–628. https://doi.org/10.1101/gad.5.4.616

Kuzdere T., V. Flury, T. Schalch, V. Iesmantavicius, D. Hess, *et al.*, 2022 Differential phosphorylation of Clr4SUV39H by Cdk1 accompanies a histone H3 methylation switch that is essential for gametogenesis. EMBO Rep 24: e55928. https://doi.org/10.15252/embr.202255928

Kyrion G., K. Liu, C. Liu, and A. J. Lustig, 1993 RAP1 and telomere structure regulate telomere position effects in Saccharomyces cerevisiae. Genes & Development 7: 1146–1159. https://doi.org/10.1101/gad.7.7a.1146

Landry J., A. Sutton, S. T. Tafrov, R. C. Heller, J. Stebbins, *et al.*, 2000 The silencing protein SIR2 and its homologs are NAD-dependent protein deacetylases. Proceedings of the National Academy of Sciences 97: 5807–5811. https://doi.org/10.1073/pnas.110148297

Lange T. de, 2018 Shelterin-Mediated Telomere Protection. Annual Review of Genetics 52: 223–247. https://doi.org/10.1146/annurev-genet-032918-021921

Langmead B., and S. L. Salzberg, 2012 Fast gapped-read alignment with Bowtie 2. Nat Methods 9: 357–359. https://doi.org/10.1038/nmeth.1923

Lanz M. C., K. Yugandhar, S. Gupta, E. J. Sanford, V. M. Faça, *et al.*, 2021 In-depth and 3-dimensional exploration of the budding yeast phosphoproteome. EMBO reports 22: e51121. https://doi.org/10.15252/embr.202051121

Larson E. D., A. J. Marsh, and M. M. Harrison, 2021 Pioneering the developmental frontier. Molecular Cell 81: 1640–1650. https://doi.org/10.1016/j.molcel.2021.02.020

Lascaris R. F., E. Groot, P. B. Hoen, W. H. Mager, and R. J. Planta, 2000 Different roles for abf1p and a T-rich promoter element in nucleosome organization of the yeast RPS28A gene. Nucleic Acids Res 28: 1390–1396. https://doi.org/10.1093/nar/28.6.1390

Latchman D. S., 2001 Transcription factors: bound to activate or repress. Trends in Biochemical Sciences 26: 211–213. https://doi.org/10.1016/S0968-0004(01)01812-6

Laurenson P., and J. Rine, 1992 Silencers, silencing, and heritable transcriptional states. Microbiol Rev 56: 543–560.

Layer J. H., S. G. Miller, and P. A. Weil, 2010 Direct Transactivator-Transcription Factor IID (TFIID) Contacts Drive Yeast Ribosomal Protein Gene Transcription. J Biol Chem 285: 15489–15499. https://doi.org/10.1074/jbc.M110.104810

Lebrun É., E. Revardel, C. Boscheron, R. Li, E. Gilson, *et al.*, 2001 Protosilencers in Saccharomyces cerevisiae Subtelomeric Regions. Genetics 158: 167–176. https://doi.org/10.1093/genetics/158.1.167

Levine M., and R. Tjian, 2003 Transcription regulation and animal diversity. Nature 424: 147–151. https://doi.org/10.1038/nature01763

Li X.-Y., S. R. Bhaumik, X. Zhu, L. Li, W.-C. Shen, *et al.*, 2002 Selective Recruitment of TAFs by Yeast Upstream Activating Sequences: Implications for Eukaryotic Promoter Structure. Current Biology 12: 1240–1244. https://doi.org/10.1016/S0960-9822(02)00932-6

Li H., B. Handsaker, A. Wysoker, T. Fennell, J. Ruan, *et al.*, 2009 The Sequence Alignment/Map format and SAMtools. Bioinformatics 25: 2078–2079. https://doi.org/10.1093/bioinformatics/btp352

Liao Y., G. K. Smyth, and W. Shi, 2014 featureCounts: an efficient general purpose program for assigning sequence reads to genomic features. Bioinformatics 30: 923–930. https://doi.org/10.1093/bioinformatics/btt656

Lickwar C. R., F. Mueller, S. E. Hanlon, J. G. McNally, and J. D. Lieb, 2012 Genome-wide protein–DNA binding dynamics suggest a molecular clutch for transcription factor function. Nature 484: 251–255. https://doi.org/10.1038/nature10985

Lieb J. D., X. Liu, D. Botstein, and P. O. Brown, 2001 Promoter-specific binding of Rap1 revealed by genome-wide maps of protein–DNA association. Nat Genet 28: 327–334. https://doi.org/10.1038/ng569

Liou G.-G., J. C. Tanny, R. G. Kruger, T. Walz, and D. Moazed, 2005 Assembly of the SIR Complex and Its Regulation by O-Acetyl-ADP-Ribose, a Product of NAD-Dependent Histone Deacetylation. Cell 121: 515–527. https://doi.org/10.1016/j.cell.2005.03.035

Liu C., X. Mao, and A. J. Lustig, 1994 Mutational Analysis Defines a C-Terminal Tail Domain of Rap1 Essential for Telomeric Silencing in Saccharomyces Cerevisiae. Genetics 138: 1025–1040.

Liu C., and A. J. Lustig, 1996 Genetic Analysis of Rap1p/Sir3p Interactions in Telomeric and Hml Silencing in Saccharomyces Cerevisiae. Genetics 143: 81–93.

Liu W., L. Li, H. Ye, H. Chen, W. Shen, *et al.*, 2017 From Saccharomyces cerevisiae to human: The important gene co-expression modules. Biomed Rep 7: 153–158. https://doi.org/10.3892/br.2017.941

Longtine M. S., N. M. Wilson, M. E. Petracek, and J. Berman, 1989 A yeast Telomere Binding Activity binds to two related telomere sequence motifs and is indistinguishable from RAPT. Curr Genet 16: 225–239. https://doi.org/10.1007/BF00422108

Loo S., and J. Rine, 1994 Silencers and Domains of Generalized Repression. Science, New Series 264: 1768–1771.

Love M. I., M. R. Huska, M. Jurk, R. Schöpflin, S. R. Starick, *et al.*, 2017 Role of the chromatin landscape and sequence in determining cell type-specific genomic glucocorticoid receptor binding and gene regulation. Nucleic Acids Res 45: 1805–1819. https://doi.org/10.1093/nar/gkw1163

Lubeck E., A. F. Coskun, T. Zhiyentayev, M. Ahmad, and L. Cai, 2014 Single cell in situ RNA profiling by sequential hybridization. Nat Methods 11: 360–361. https://doi.org/10.1038/nmeth.2892

Luo K., M. A. Vega-Palas, and M. Grunstein, 2002 Rap1-Sir4 binding independent of other Sir, yKu, or histone interactions initiates the assembly of telomeric heterochromatin in yeast. Genes Dev 16: 1528–1539. https://doi.org/10.1101/gad.988802

Luo Y., J. A. North, S. D. Rose, and M. G. Poirier, 2014 Nucleosomes accelerate transcription factor dissociation. Nucleic Acids Res 42: 3017–3027. https://doi.org/10.1093/nar/gkt1319

Lustig A. J., S. Kurtz, and D. Shore, 1990 Involvement of the Silencer and UAS Binding Protein RAP1 in Regulation of Telomere Length. Science 250: 549–553.

Lustig A. J., C. Liu, C. Zhang, and J. P. Hanish, 1996 Tethered Sir3p nucleates silencing at telomeres and internal loci in Saccharomyces cerevisiae. Mol Cell Biol 16: 2483–2495.

Lyon M. F., 1961 Gene Action in the X-chromosome of the Mouse (Mus musculus L.). Nature 190: 372–373. https://doi.org/10.1038/190372a0

Ma J., 2005 Crossing the line between activation and repression. Trends in Genetics 21: 54–59. https://doi.org/10.1016/j.tig.2004.11.004

Madsen C. T., K. B. Sylvestersen, C. Young, S. C. Larsen, J. W. Poulsen, *et al.*, 2015 Biotin starvation causes mitochondrial protein hyperacetylation and partial rescue by the SIRT3-like deacetylase Hst4p. Nat Commun 6: 7726. https://doi.org/10.1038/ncomms8726

Mager W. H., and R. J. Planta, 1990 Multifunctional DNA-binding proteins mediate concerted transcription activation of yeast ribosomal protein genes. Biochimica et Biophysica Acta (BBA) - Gene Structure and Expression 1050: 351–355. https://doi.org/10.1016/0167-4781(90)90193-6

Mahoney D. J., and J. R. Broach, 1989 The HML mating-type cassette of Saccharomyces cerevisiae is regulated by two separate but functionally equivalent silencers. Mol Cell Biol 9: 4621–4630.

Makovets S., I. Herskowitz, and E. H. Blackburn, 2004 Anatomy and Dynamics of DNA Replication Fork Movement in Yeast Telomeric Regions. Molecular and Cellular Biology 24: 4019–4031. https://doi.org/10.1128/MCB.24.9.4019-4031.2004

Marshall M., D. Mahoney, A. Rose, J. B. Hicks, and J. R. Broach, 1987 Functional domains of SIR4, a gene required for position effect regulation in Saccharomyces cerevisiae. Mol Cell Biol 7: 4441–4452. https://doi.org/10.1128/mcb.7.12.4441-4452.1987

Martienssen R., and D. Moazed, 2015 RNAi and Heterochromatin Assembly. Cold Spring Harb Perspect Biol 7: a019323. https://doi.org/10.1101/cshperspect.a019323

Martinez P., M. Thanasoula, A. R. Carlos, G. Gómez-López, A. M. Tejera, *et al.*, 2010 Mammalian Rap1 controls telomere function and gene expression through binding to telomeric and extratelomeric sites. Nat Cell Biol 12: 768–780. https://doi.org/10.1038/ncb2081

Mayran A., and J. Drouin, 2018 Pioneer transcription factors shape the epigenetic landscape. Journal of Biological Chemistry 293: 13795–13804. https://doi.org/10.1074/jbc.R117.001232

Medema M. H., R. Kottmann, P. Yilmaz, M. Cummings, J. B. Biggins, *et al.*, 2015 Minimum Information about a Biosynthetic Gene cluster. Nat Chem Biol 11: 625–631. https://doi.org/10.1038/nchembio.1890

Mellor J., W. Jiang, M. Funk, J. Rathjen, C. A. Barnes, *et al.*, 1990 CPF1, a yeast protein which functions in centromeres and promoters. EMBO J 9: 4017–4026.

Metz C. W., 1938 Chromosome Behavior, Inheritance and Sex Determination in Sciara. The American Naturalist 72: 485–520. https://doi.org/10.1086/280803

Meyer B. J., and L. P. Casson, 1986 Caenorhabditis elegans compensates for the difference in X chromosome dosage between the sexes by regulating transcript levels. Cell 47: 871–881. https://doi.org/10.1016/0092-8674(86)90802-0

Mirdita M., K. Schütze, Y. Moriwaki, L. Heo, S. Ovchinnikov, *et al.*, 2022 ColabFold: making protein folding accessible to all. Nat Methods 19: 679–682. https://doi.org/10.1038/s41592-022-01488-1

Mivelaz M., A.-M. Cao, S. Kubik, S. Zencir, R. Hovius, *et al.*, 2020 Chromatin Fiber Invasion and Nucleosome Displacement by the Rap1 Transcription Factor. Molecular Cell 77: 488-500.e9. https://doi.org/10.1016/j.molcel.2019.10.025

Mo X., E. Kowenz-Leutz, H. Xu, and A. Leutz, 2004 Ras induces mediator complex exchange on C/EBP beta. Mol Cell 13: 241–250. https://doi.org/10.1016/s1097-2765(03)00521-5

Moazed D., A. Kistler, A. Axelrod, J. Rine, and A. D. Johnson, 1997 Silent information regulator protein complexes in Saccharomyces cerevisiae: A SIR2/SIR4 complex and evidence for a regulatory domain in SIR4 that inhibits its interaction with SIR3. Proceedings of the National Academy of Sciences 94: 2186–2191. https://doi.org/10.1073/pnas.94.6.2186

Monaco G., H. Chen, M. Poidinger, J. Chen, J. P. de Magalhães, *et al.*, 2016 flowAI: automatic and interactive anomaly discerning tools for flow cytometry data. Bioinformatics 32: 2473–2480. https://doi.org/10.1093/bioinformatics/btw191

Moreau J.-L., M. Lee, N. Mahachi, J. Vary, J. Mellor, *et al.*, 2003 Regulated Displacement of TBP from the PHO8 Promoter In Vivo Requires Cbf1 and the Isw1 Chromatin Remodeling Complex. Molecular Cell 11: 1609–1620. https://doi.org/10.1016/S1097-2765(03)00184-9

Moretti P., K. Freeman, L. Coodly, and D. Shore, 1994 Evidence that a complex of SIR proteins interacts with the silencer and telomere- binding protein RAP

Moretti P., and D. Shore, 2001 Multiple Interactions in Sir Protein Recruitment by Rap1p at Silencers and Telomeres in Yeast. Molecular and Cellular Biology 21: 8082–8094. https://doi.org/10.1128/MCB.21.23.8082-8094.2001

Moser B. A., and T. M. Nakamura, 2009 Protection and replication of telomeres in fission yeastThis paper is one of a selection of papers published in this Special Issue, entitled 30th Annual International Asilomar Chromatin and Chromosomes Conference, and has undergone the Journal's usual peer review process. Biochem. Cell Biol. 87: 747–758. https://doi.org/10.1139/O09-037

Mueller F., A. Senecal, K. Tantale, H. Marie-Nelly, N. Ly, *et al.*, 2013 FISH-quant: automatic counting of transcripts in 3D FISH images. Nat Methods 10: 277–278. https://doi.org/10.1038/nmeth.2406

Muller H. J., 1930 Types of visible variations induced by X-rays inDrosophila. Journ. of Gen. 22: 299–334. https://doi.org/10.1007/BF02984195

Murray K., 1964 The Occurrence of iε-N-Methyl Lysine in Histones. Biochemistry 3: 10–15. https://doi.org/10.1021/bi00889a003

Nanney D. L., 1958 EPIGENETIC CONTROL SYSTEMS*

Nasmyth K. A., 1982 The regulation of yeast mating-type chromatin structure by SIR: An action at a distance affecting both transcription and transposition. Cell 30: 567–578. https://doi.org/10.1016/0092-8674(82)90253-7

Ohno S., W. D. Kaplan, and R. Kinosita, 1959 Formation of the sex chromatin by a single X-chromosome in liver cells of Rattus norvegicus. Experimental Cell Research 18: 415–418. https://doi.org/10.1016/0014-4827(59)90031-X

Ono J., and D. Greig, 2020 A Saccharomyces paradox: chromosomes from different species are incompatible because of anti-recombination, not because of differences in number or arrangement. Curr Genet 66: 469–474. https://doi.org/10.1007/s00294-019-01038-x

Oppikofer M., S. Kueng, and S. M. Gasser, 2013 SIR–nucleosome interactions: Structure–function relationships in yeast silent chromatin. Gene 527: 10–25. https://doi.org/10.1016/j.gene.2013.05.088

Osborne E. A., Y. Hiraoka, and J. Rine, 2011 Symmetry, asymmetry, and kinetics of silencing establishment in Saccharomyces cerevisiae revealed by single-cell

optical assays. Proc Natl Acad Sci U S A 108: 1209–1216. https://doi.org/10.1073/pnas.1018742108

Papai G., M. K. Tripathi, C. Ruhlmann, J. H. Layer, P. A. Weil, *et al.*, 2010 TFIIA and the transactivator Rap1 cooperate to commit TFIID for transcription initiation. Nature 465: 956–960. https://doi.org/10.1038/nature09080

Park P. J., 2009 ChIP-Seq: advantages and challenges of a maturing technology. Nat Rev Genet 10: 669–680. https://doi.org/10.1038/nrg2641

Passarge E., 1979 Emil Heitz and the concept of heterochromatin: longitudinal chromosome differentiation was recognized fifty years ago. Am J Hum Genet 31: 106–115.

Pelechano V., W. Wei, and L. M. Steinmetz, 2013 Extensive transcriptional heterogeneity revealed by isoform profiling. Nature 497: 127–131. https://doi.org/10.1038/nature12121

Phillips D., 1963 The presence of acetyl groups in histones - PMC

Pillus L., and J. Rine, 1989 Epigenetic inheritance of transcriptional states in S. cerevisiae. Cell 59: 637–647. https://doi.org/10.1016/0092-8674(89)90009-3

Piña B., J. Fernández-Larrea, N. García-Reyero, and F.-Z. Idrissi, 2003 The different (sur)faces of Rap1p. Mol Gen Genomics 268: 791–798. https://doi.org/10.1007/s00438-002-0801-3

Pombo A., and N. Dillon, 2015 Three-dimensional genome architecture: players and mechanisms. Nat Rev Mol Cell Biol 16: 245–257. https://doi.org/10.1038/nrm3965

Power P., D. Jeffery, M. A. Rehman, A. Chatterji, and K. Yankulov, 2011 Sub-Telomeric core X and Y' Elements in S.cerevisiae Suppress Extreme Variations in Gene Silencing. PLOS ONE 6: e17523. https://doi.org/10.1371/journal.pone.0017523

Pryde F. E., and E. J. Louis, 1999 Limitations of silencing at native yeast telomeres. The EMBO Journal 18: 2538–2550. https://doi.org/10.1093/emboj/18.9.2538

Radman-Livaja M., G. Ruben, A. Weiner, N. Friedman, R. Kamakaka, *et al.*, 2011a Dynamics of Sir3 spreading in budding yeast: secondary recruitment sites and euchromatic localization. EMBO J 30: 1012–1026. https://doi.org/10.1038/emboj.2011.30

Radman-Livaja M., K. F. Verzijlbergen, A. Weiner, T. van Welsem, N. Friedman, *et al.*, 2011b Patterns and mechanisms of ancestral histone protein inheritance in budding yeast. PLoS Biol 9: e1001075. https://doi.org/10.1371/journal.pbio.1001075

Ragunathan K., G. Jih, and D. Moazed, 2015 Epigenetics. Epigenetic inheritance uncoupled from sequence-specific recruitment. Science 348: 1258699. https://doi.org/10.1126/science.1258699

Rando O. J., and F. Winston, 2012 Chromatin and Transcription in Yeast. Genetics 190: 351–387. https://doi.org/10.1534/genetics.111.132266

Ravindra A., K. Weiss, and R. T. Simpson, 1999 High-Resolution Structural Analysis of Chromatin at Specific Loci: Saccharomyces cerevisiae Silent Mating-Type Locus HMRa. Molecular and Cellular Biology 19: 7944–7950. https://doi.org/10.1128/MCB.19.12.7944

Rehman M. A., G. Fourel, A. Mathews, D. Ramdin, M. Espinosa, *et al.*, 2006 Differential Requirement of DNA Replication Factors for Subtelomeric ARS Consensus Sequence Protosilencers in Saccharomyces cerevisiae. Genetics 174: 1801–1810. https://doi.org/10.1534/genetics.106.063446

Reinberg D., G. Orphanides, R. Ebright, S. Akoulitchev, J. Carcamo, *et al.*, 1998 The RNA Polymerase II General Transcription Factors: Past, Present, and Future. Cold Spring Harb Symp Quant Biol 63: 83–105. https://doi.org/10.1101/sqb.1998.63.83

Reja R., V. Vinayachandran, S. Ghosh, and B. F. Pugh, 2015 Molecular mechanisms of ribosomal protein gene coregulation. Genes Dev 29: 1942–1954. https://doi.org/10.1101/gad.268896.115

Renauld H., O. M. Aparicio, P. D. Zierath, B. L. Billington, S. K. Chhablani, *et al.*, 1993 Silent domains are assembled continuously from the telomere and are defined by promoter distance and strength, and by SIR3 dosage. Genes Dev. 7: 1133–1145. https://doi.org/10.1101/gad.7.7a.1133

Reuter G., and P. Spierer, 1992 Position effect variegation and chromatin proteins. BioEssays 14: 605–612. https://doi.org/10.1002/bies.950140907

Reverón-Gómez N., C. González-Aguilera, K. R. Stewart-Morgan, N. Petryk, V. Flury, *et al.*, 2018 Accurate Recycling of Parental Histones Reproduces the Histone Modification Landscape during DNA Replication. Mol Cell 72: 239-249.e5. https://doi.org/10.1016/j.molcel.2018.08.010

Rine J., J. N. Strathern, J. B. Hicks, and I. Herskowitz, 1979 A SUPPRESSOR OF MATING-TYPE LOCUS MUTATIONS IN SACCHAROMYCES CEREVISIAE: EVIDENCE FOR AND IDENTIFICATION OF CRYPTIC MATING-TYPE LOCI. Genetics 93: 877–901. https://doi.org/10.1093/genetics/93.4.877

Rine J., and I. Herskowitz, 1987 Four Genes Responsible for a Position Effect on Expression From *HML* and *HMR* in *Saccharomyces cerevisiae*. Genetics 116: 9–22. https://doi.org/10.1093/genetics/116.1.9

Romano G. H., Y. Harari, T. Yehuda, A. Podhorzer, L. Rubinstein, *et al.*, 2013 Environmental Stresses Disrupt Telomere Length Homeostasis. PLoS Genet 9: e1003721. https://doi.org/10.1371/journal.pgen.1003721

Rosenfeld M. G., V. V. Lunyak, and C. K. Glass, 2006 Sensors and signals: a coactivator/corepressor/epigenetic code for integrating signal-dependent programs of transcriptional response. Genes Dev. 20: 1405–1428. https://doi.org/10.1101/gad.1424806

Rossmann M. P., W. Luo, O. Tsaponina, A. Chabes, and B. Stillman, 2011 A common telomeric gene silencing assay is affected by nucleotide metabolism. Mol Cell 42: 127–136. https://doi.org/10.1016/j.molcel.2011.03.007

Rusche L. N., A. L. Kirchmaier, and J. Rine, 2003 The Establishment, Inheritance, and Function of Silenced Chromatin in Saccharomyces cerevisiae. Annual Review of Biochemistry 72: 481–516. https://doi.org/10.1146/annurev.biochem.72.121801.161547

Ryu H.-Y., and M. Hochstrasser, 2021 Histone sumoylation and chromatin dynamics. Nucleic Acids Research 49: 6043–6052. https://doi.org/10.1093/nar/gkab280

Saunders A., J. Werner, E. D. Andrulis, T. Nakayama, S. Hirose, *et al.*, 2003 Tracking FACT and the RNA Polymerase II Elongation Complex Through Chromatin in Vivo. Science 301: 1094–1096. https://doi.org/10.1126/science.1085712

Saxton D. S., and J. Rine, 2019 Epigenetic memory independent of symmetric histone inheritance, (T. Formosa, K. Struhl, T. Formosa, and M. Gartenberg, Eds.). eLife 8: e51421. https://doi.org/10.7554/eLife.51421

Saxton D. S., and J. Rine, 2022 Distinct silencer states generate epigenetic states of heterochromatin. Molecular Cell 82: 3566-3579.e5. https://doi.org/10.1016/j.molcel.2022.08.002

Schindelin J., I. Arganda-Carreras, E. Frise, V. Kaynig, M. Longair, *et al.*, 2012 Fiji: an open-source platform for biological-image analysis. Nat Methods 9: 676–682. https://doi.org/10.1038/nmeth.2019

Schlissel G., 2019 Nucleosomes as carriers of epigenetic memory

Schlissel G., and J. Rine, 2019 The nucleosome core particle remembers its position through DNA replication and RNA transcription. Proceedings of the National Academy of Sciences 116: 20605–20611. https://doi.org/10.1073/pnas.1911943116

Scully K. M., E. M. Jacobson, K. Jepsen, V. Lunyak, H. Viadiu, *et al.*, 2000 Allosteric Effects of Pit-1 DNA Sites on Long-Term Repression in Cell Type Specification. Science 290: 1127–1131. https://doi.org/10.1126/science.290.5494.1127

Sekinger E. A., and D. S. Gross, 2001 Silenced Chromatin Is Permissive to Activator Binding and PIC Recruitment. Cell 105: 403–414. https://doi.org/10.1016/S0092-8674(01)00329-4

Shen W.-C., S. R. Bhaumik, H. C. Causton, I. Simon, X. Zhu, *et al.*, 2003 Systematic analysis of essential yeast TAFs in genome-wide transcription and preinitiation complex assembly. EMBO J 22: 3395–3402. https://doi.org/10.1093/emboj/cdg336

Shi T., R. D. Bunker, S. Mattarocci, C. Ribeyre, M. Faty, *et al.*, 2013 Rif1 and Rif2 shape telomere function and architecture through multivalent Rap1 interactions. Cell 153: 1340–1353. https://doi.org/10.1016/j.cell.2013.05.007

Shore D., D. J. Stillman, A. H. Brand, and K. A. Nasmyth, 1987 Identification of silencer binding proteins from yeast: possible roles in SIR control and DNA replication.

The EMBO Journal 6: 461–467. https://doi.org/10.1002/j.1460-2075.1987.tb04776.x

Shore D., and K. Nasmyth, 1987a Purification and cloning of a DNA binding protein from yeast that binds to both silencer and activator elements. Cell 51: 721–732. https://doi.org/10.1016/0092-8674(87)90095-X

Shore D., and K. Nasmyth, 1987b Purification and cloning of a DNA binding protein from yeast that binds to both silencer and activator elements. Cell 51: 721–732. https://doi.org/10.1016/0092-8674(87)90095-X

Siliciano P. G., and K. Tatchell, 1986 Identification of the DNA sequences controlling the expression of the MAT alpha locus of yeast. Proceedings of the National Academy of Sciences 83: 2320–2324. https://doi.org/10.1073/pnas.83.8.2320

Singh J., and A. J. Klar, 1992 Active genes in budding yeast display enhanced in vivo accessibility to foreign DNA methylases: a novel in vivo probe for chromatin structure of yeast. Genes Dev. 6: 186–196. https://doi.org/10.1101/gad.6.2.186

Sjöstrand J. O. O., A. Kegel, and S. U. Åström, 2002 Functional Diversity of Silencers in Budding Yeasts. Eukaryot Cell 1: 548–557. https://doi.org/10.1128/EC.1.4.548-557.2002

Smith J. S., C. B. Brachmann, I. Celic, M. A. Kenna, S. Muhammad, *et al.*, 2000 A phylogenetically conserved NAD+-dependent protein deacetylase activity in the Sir2 protein family. Proc Natl Acad Sci U S A 97: 6658–6663. https://doi.org/10.1073/pnas.97.12.6658

Snoek T., K. Voordeckers, and K. J. Verstrepen, 2014 Subtelomeric Regions Promote Evolutionary Innovation of Gene Families in Yeast, pp. 39–70 in *Subtelomeres*, edited by Louis E. J., Becker M. M. Springer, Berlin, Heidelberg.

Stavenhagen J. B., and V. A. Zakian, 1998 Yeast telomeres exert a position effect on recombination between internal tracts of yeast telomeric DNA. Genes Dev 12: 3044–3058. https://doi.org/10.1101/gad.12.19.3044

Steakley D. L., and J. Rine, 2015 On the Mechanism of Gene Silencing in Saccharomyces cerevisiae. G3 (Bethesda) 5: 1751–1763. https://doi.org/10.1534/g3.115.018515

Strahl B. D., and C. D. Allis, 2000 The language of covalent histone modifications. Nature 403: 41–45. https://doi.org/10.1038/47412

Strathern J. N., A. J. S. Klar, J. B. Hicks, J. A. Abraham, J. M. Ivy, *et al.*, 1982 Homothallic switching of yeast mating type cassettes is initiated by a double-stranded cut in the MAT locus. Cell 31: 183–192. https://doi.org/10.1016/0092-8674(82)90418-4

Sussel L., and D. Shore, 1991 Separation of transcriptional activation and silencing functions of the RAP1-encoded repressor/activator protein 1: isolation of viable mutants affecting both silencing and telomere length. Proc Natl Acad Sci U S A 88: 7749–7753.

Swaney D. L., P. Beltrao, L. Starita, A. Guo, J. Rush, *et al.*, 2013 Global analysis of phosphorylation and ubiquitylation crosstalk in protein degradation. Nat Methods 10: 10.1038/nmeth.2519. https://doi.org/10.1038/nmeth.2519

Swygert S. G., S. Senapati, M. F. Bolukbasi, S. A. Wolfe, S. Lindsay, *et al.*, 2018 SIR proteins create compact heterochromatin fibers. Proceedings of the National Academy of Sciences 115: 12447–12452. https://doi.org/10.1073/pnas.1810647115

Taddei A., and S. M. Gasser, 2012 Structure and Function in the Budding Yeast Nucleus. Genetics 192: 107–129. https://doi.org/10.1534/genetics.112.140608

Takahashi K., and S. Yamanaka, 2006 Induction of Pluripotent Stem Cells from Mouse Embryonic and Adult Fibroblast Cultures by Defined Factors. Cell 126: 663–676. https://doi.org/10.1016/j.cell.2006.07.024

Takahashi Y.-H., J. M. Schulze, J. Jackson, T. Hentrich, C. Seidel, *et al.*, 2011 Dot1 and Histone H3K79 Methylation in Natural Telomeric and HM Silencing. Mol Cell 42: 118–126. https://doi.org/10.1016/j.molcel.2011.03.006

Talbert P. B., M. P. Meers, and S. Henikoff, 2019 Old cogs, new tricks: the evolution of gene expression in a chromatin context. Nat Rev Genet 20: 283–297. https://doi.org/10.1038/s41576-019-0105-7

Teytelman L., E. A. O. Nishimura, B. Özaydin, M. B. Eisen, and J. Rine, 2012 The Enigmatic Conservation of a Rap1 Binding Site in the Saccharomyces cerevisiae HMR-E Silencer. G3 (Bethesda) 2: 1555–1562. https://doi.org/10.1534/g3.112.004077

Teytelman L., D. M. Thurtle, J. Rine, and A. van Oudenaarden, 2013 Highly expressed loci are vulnerable to misleading ChIP localization of multiple unrelated proteins. Proc Natl Acad Sci U S A 110: 18602–18607. https://doi.org/10.1073/pnas.1316064110

Thurtle D. M., and J. Rine, 2014 The molecular topography of silenced chromatin in *Saccharomyces cerevisiae*. Genes Dev. 28: 245–258. https://doi.org/10.1101/gad.230532.113

Tremethick D. J., 2007 Higher-Order Structures of Chromatin: The Elusive 30 nm Fiber. Cell 128: 651–654. https://doi.org/10.1016/j.cell.2007.02.008

Triolo T., and R. Sternglanz, 1996 Role of interactions between the origin recognition complex and SIR1 in transcriptional silencing. Nature 381: 251–253. https://doi.org/10.1038/381251a0

Vale-Silva L. A., T. E. Markowitz, and A. Hochwagen, 2019 SNP-ChIP: a versatile and tag-free method to quantify changes in protein binding across the genome. BMC Genomics 20: 54. https://doi.org/10.1186/s12864-018-5368-4

Valin A., and G. Gill, 2007 Regulation of the dual-function transcription factor Sp3 by SUMO. Biochemical Society Transactions 35: 1393–1396. https://doi.org/10.1042/BST0351393

Vignais M. L., L. P. Woudt, G. M. Wassenaar, W. H. Mager, A. Sentenac, *et al.*, 1987 Specific binding of TUF factor to upstream activation sites of yeast ribosomal protein genes. EMBO J 6: 1451–1457. https://doi.org/10.1002/j.1460-2075.1987.tb02386.x

Waddington C. H., 2012 The Epigenotype. International Journal of Epidemiology 41: 10–13. https://doi.org/10.1093/ije/dyr184

Wang X., G. Bryant, A. Zhao, and M. Ptashne, 2015 Nucleosome Avidities and Transcriptional Silencing in Yeast. Current Biology 25: 1215–1220. https://doi.org/10.1016/j.cub.2015.03.004

Warfield L., S. Ramachandran, T. Baptista, D. Devys, L. Tora, *et al.*, 2017 Transcription of Nearly All Yeast RNA Polymerase II-Transcribed Genes Is Dependent on Transcription Factor TFIID. Molecular Cell 68: 118-129.e5. https://doi.org/10.1016/j.molcel.2017.08.014

Watson J. D., and F. H. C. Crick, 1953 Molecular Structure of Nucleic Acids: A Structure for Deoxyribose Nucleic Acid. Nature 171: 737–738. https://doi.org/10.1038/171737a0

Weikum E. R., M. T. Knuesel, E. A. Ortlund, and K. R. Yamamoto, 2017 Glucocorticoid receptor control of transcription: precision and plasticity via allostery. Nat Rev Mol Cell Biol 18: 159–174. https://doi.org/10.1038/nrm.2016.152

Weiss K., 1997 Cell type-specific chromatin organization of the region that governs directionality of yeast mating type switching. The EMBO Journal 16: 4352–4360. https://doi.org/10.1093/emboj/16.14.4352

Weiss K., and R. T. Simpson, 1998 High-resolution structural analysis of chromatin at specific loci: Saccharomyces cerevisiae silent mating type locus HMLalpha. Mol Cell Biol 18: 5392–5403. https://doi.org/10.1128/MCB.18.9.5392

Wellinger R. J., and V. A. Zakian, 2012 Everything You Ever Wanted to Know About Saccharomyces cerevisiae Telomeres: Beginning to End. Genetics 191: 1073–1105. https://doi.org/10.1534/genetics.111.137851

Wickham H., 2009 Getting started with qplot, pp. 9–26 in *ggplot2: Elegant Graphics for Data Analysis*, Use R. edited by Wickham H. Springer, New York, NY.

Wickham H., 2016 Getting Started with ggplot2, pp. 11–31 in *ggplot2: Elegant Graphics for Data Analysis*, Use R! edited by Wickham H. Springer International Publishing, Cham.

Woolford J. L., and S. J. Baserga, 2013 Ribosome Biogenesis in the Yeast Saccharomyces cerevisiae. Genetics 195: 643–681. https://doi.org/10.1534/genetics.113.153197

Wotton D., and D. Shore, 1997 A novel Rap1p-interacting factor, Rif2p, cooperates with Rif1p to regulate telomere length in Saccharomyces cerevisiae. Genes Dev 11: 748–760. https://doi.org/10.1101/gad.11.6.748

Wu C., A. Bassett, and A. Travers, 2007 A variable topology for the 30-nm chromatin fibre. EMBO Rep 8: 1129–1134. https://doi.org/10.1038/sj.embor.7401115

Wu A. C. K., H. Patel, M. Chia, F. Moretto, D. Frith, *et al.*, 2018 Repression of Divergent Noncoding Transcription by a Sequence-Specific Transcription Factor. Molecular Cell 72: 942-954.e7. https://doi.org/10.1016/j.molcel.2018.10.018

Yan C., H. Chen, and L. Bai, 2018 Systematic Study of Nucleosome-Displacing Factors in Budding Yeast. Mol Cell 71: 294-305.e4. https://doi.org/10.1016/j.molcel.2018.06.017

Yu L., and R. H. Morse, 1999 Chromatin Opening and Transactivator Potentiation by RAP1 in Saccharomyces cerevisiae. Molecular and Cellular Biology 19: 5279–5288. https://doi.org/10.1128/MCB.19.8.5279

Zaret K. S., 2020 Pioneer Transcription Factors Initiating Gene Network Changes. Annu Rev Genet 54: 367–385. https://doi.org/10.1146/annurev-genet-030220-015007

Zhang Z., K. Shibahara, and B. Stillman, 2000 PCNA connects DNA replication to epigenetic inheritance in yeast. Nature 408: 221–225. https://doi.org/10.1038/35041601

Zhang X., Z. Liu, X. Liu, S. Wang, Y. Zhang, *et al.*, 2019 Telomere-dependent and telomere-independent roles of RAP1 in regulating human stem cell homeostasis. Protein Cell 10: 649–667. https://doi.org/10.1007/s13238-019-0610-7

Appendix: Investigating post-translational modification of Rap1 in relation to its function in silencing and activation.

A1: Background on Rap1 post-translational modification.

The outstanding question that I wished to answer in pursuing this project was *how* the different functions of Rap1 are achieved. One possible explanation of how Rap1 may be able to bind DNA in heterochromatin but not recruit transcription machinery may be the presence of post-translational modifications to the Rap1 protein that alters its ability to bind PIC machinery (or something to finish that thought). Multiple genome-wide mass-spectrometry studies have identified Rap1 residues that are post-translationally modified (Holt *et al.* 2009; Swaney *et al.* 2013; Bhagwat *et al.* 2021; Lanz *et al.* 2021). Furthermore, sumoylation of Rap1 is important for TFIID-mediated activation of ribosomal protein genes (Chymkowitch *et al.* 2015a; b). Many of these modifications lie within the N-terminal 350 amino acids which are dispensable for viability but could still serve a heretofore unappreciated function (**figure A1**). Notably, the C-terminal interaction domain with which the silencing machinery interacts appears to be under-enriched for potential modifications compared to the protein as a whole (**figure A1**). Here, I summarize a variety of experiments I designed in an attempt to discover the underlying mechanism of the duality of Rap1 function.

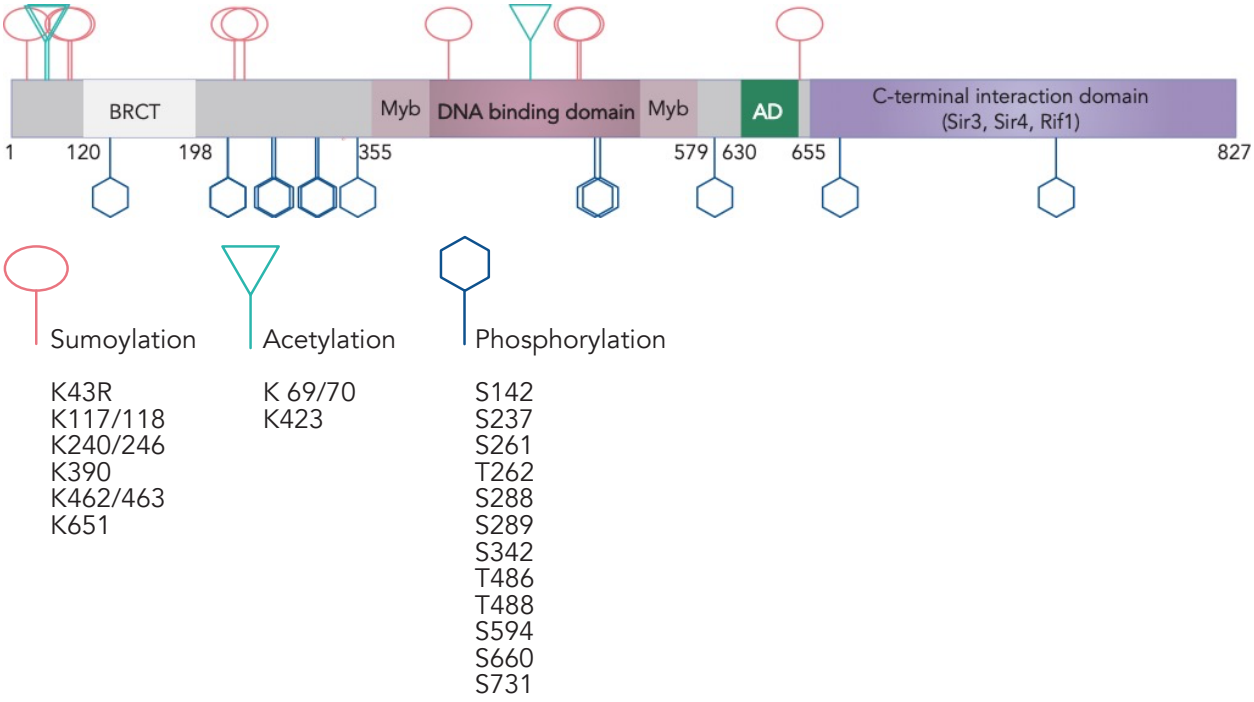

Figure A1: A schematic of the full length Rap1 protein, with reported sites of sumoylation, acetylation, and phosphorylation noted.

A2: Associating sumoylation with Rap1 function

Based on studies showing that sumoylation of Rap1 is important in activating ribosomal protein genes (Chymkowitch *et al.* 2015a; b), we hypothesized that sumoylation of Rap1 may preferentially allow interactions with transcription machinery. Thus, we queried the presence of the ubiquitin-like SUMO protein Supressor of Mif Two 3 (Smt3) at *HML* in the presence and absence of Sir proteins. In *SIR* cells the silent locus was indeed sumoylated, with a greater enrichment of Smt3 in the presence promoter-bound Rap1 (**figure A2.A**). These results indicated that Rap1 could be sumoylated when acting as a silencer. Confoundingly, sumoylation of Sir4 and yKu80 by Siz2 plays a role in the tethering of telomeres to the nuclear membrane. I previously showed that Sir protein enrichment is decreased over the *HML* promoter in the absence of Rap1 (**figure 2.2.D**). Thus, we could not deconvolute whether the decrease in Smt3 in *SIR* rap1 bs mutant cells was reporting on a decrease in Sir4 enrichment or if it was related to the absence of Rap1 in cells with the *HML-p* binding site mutation. In *sir4Δ* cells, we found no evidence of Smt3 enrichment at *HML* in cells with wild-type promoter architecture (**figure A2.A**). Interestingly, we found weak Smt3 enrichment over *HML-p* in rap1 bs mutant cells (figure A2.A). In this context, Rap1 enrichment is significantly diminished (**figure 2.2.A**) and expression of the locus is reduced (**figure 2.3.A**). Sumoylation of histones is known to be associated with gene repression (reviewed in Ryu and Hochstrasser 2021). It is possible that the increase in Smt3 enrichment over *HML-p* suggested the presence of a novel histone at this locus in the absence of Rap1 binding. The presence of such a histone would also convert a canonically nucleosome-depleted promoter to a nucleosome-dense one, which may help to explain the decrease in expression of *HMLα1* and *HMLα2* in the absence of Rap1.

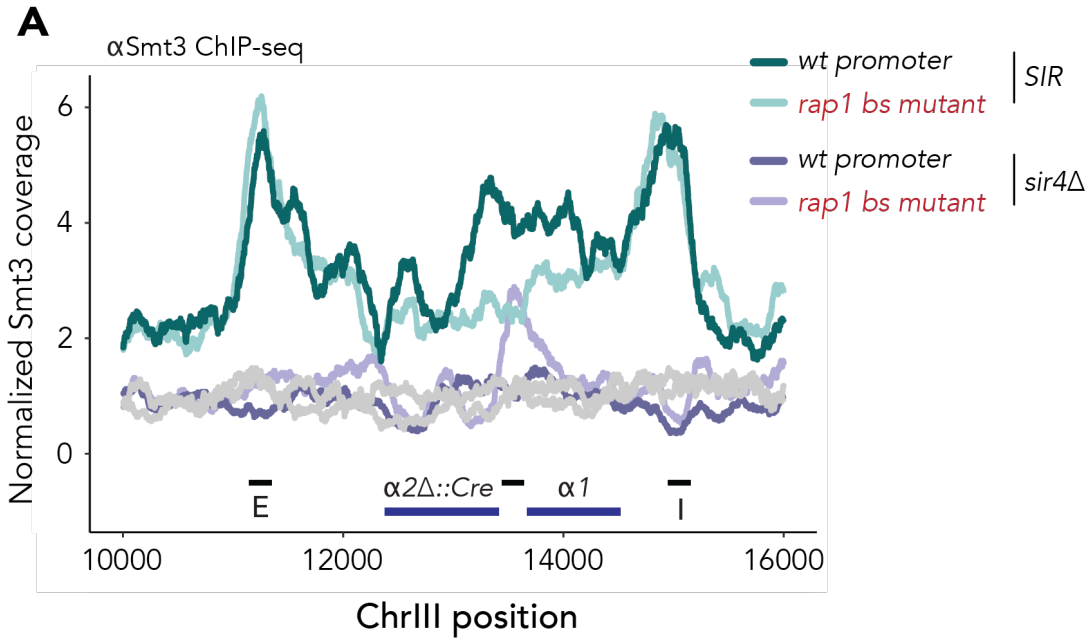

Figure A2.A: Sumoylation signal at *HML-p* was not indicative of post-translational modification of Rap1. Normalized Smt3 enrichment at *HMLα* in *SIR* and *sir4Δ* cells, with and without the rap1 bs mutation. All coverage is normalized to genome-wide median.

We then investigated correlations between Smt3 occupancy and Rap1 apparent dwell-time. To do so, we cross-referenced our Smt3 ChIP-seq enrichment data with the Rap1-bound peaks analyzed in figure 5 to identify overlapping peaks. We assigned overlapping Smt3 peaks to the nearest Rap1 peak and then measured Smt3 enrichment within the defined Rap1 peak region (n = 181). Interestingly, despite reports that sumoylation of Rap1 by TFIID is important for activation of ribosomal protein genes, and our finding that these loci were enriched for longer apparent dwell-times, we did not find a positive correlation between enrichment of Smt3 and Rap1 dwell-time (**figure A2.B**). When we instead plotted Smt3 enrichment as a function of Rap1 occupancy, we found a significant positive correlation between these two measurements (r = 0.53, p = 3.2e-14) (**figure A2.C**). The chromatin remodeler RSC is known to associate preferentially with sumoylated histone H2B (Ryu and Hochstrasser 2021). Although our measurements were not directly measuring sumoylation of Rap1, we thereby inferred that sumoylation of chromatin-associated factors may positively affect recruitment to chromatin thus increasing enrichment in these areas.

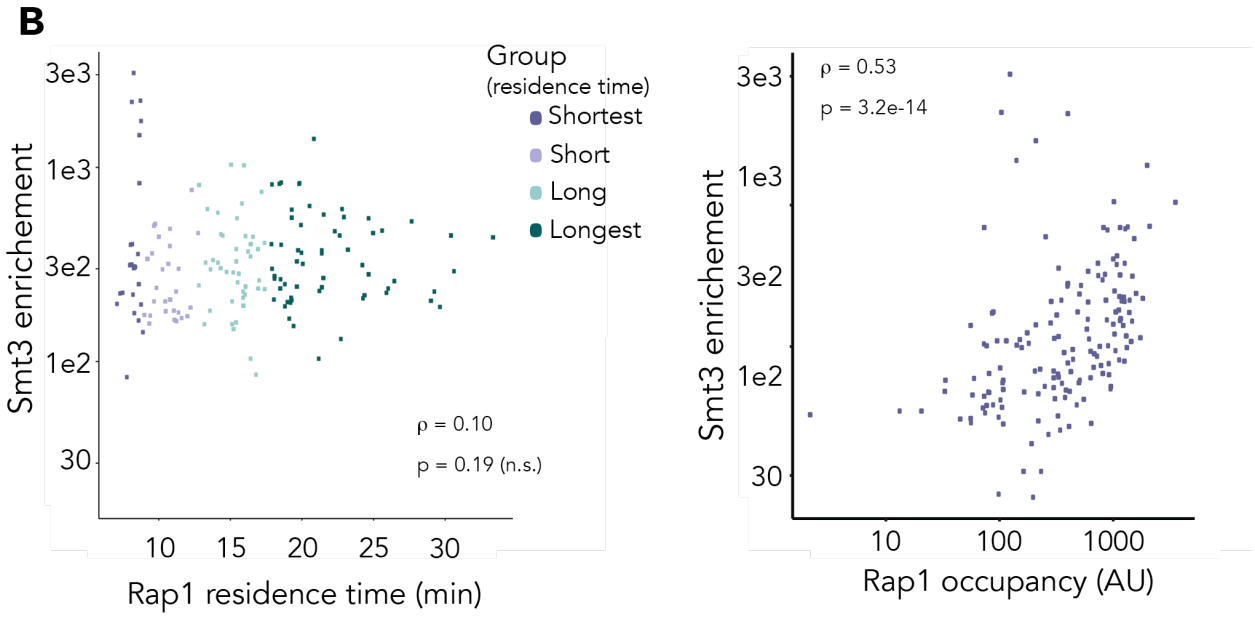

Figure A2.B: Correlations between genome-wide Smt3 enrichment and Rap1 residence time (left) or occupancy (right).

In sum, we found no evidence that one post-translational modification, sumoylation, was defining of the differential functions of Rap1 in silencing and activation (figure A2). However, with our understanding of the competition between silencing and transcription machinery, the idea that post-translational modification of Rap1 may dictate its function in a context-dependent manner is enticing.

A3: Acetylation of Rap1 may cause viability defects but had minimal effects on silencing.

Both Rap1 and Abf1, in addition to being silencer binding proteins, play key roles in the activation of ribosomal protein genes and thus the process of ribosome biogenesis (reviewed in Bosio *et al.* 2017). While almost all RPG promoters are Rap1-dependent, the few that are not are enriched for Abf1 binding sites (Lascaris *et al.* 2000; Knight *et al.* 2014; Fermi *et al.* 2016). There are many known balancing mechanisms between nutrient availability and ribosome biogenesis; protein synthesis is an energetically costly process, and the cell will adapt to slow production when nutrients are not readily available (Janapala *et al.* 2019). In one case study, a glucose-dependent role for Abf1 recruiting the histone deacetylase Rpd3 was revealed to differentially regulate the ribosome biogenesis gene *LTV1* (Bosio *et al.* 2017b). This provides a framework wherein a general regulatory factor is activating a locus under nutrient-rich conditions and is also required for recruiting a chromatin-modifying protein under starvation conditions. Gavin Schlissel investigated the possibility that acetylation of a few key lysines on Abf1 might affect its function as a silencer (Schlissel 2019). He introduced non-acetylatable K-to-R and acetyl-mimic K-to-Q mutations at a few residues. Measuring the changes to silencing stability with the CRASH assay revealed no silencing defects in these mutants.

A separate study looked at changes to the proteome in response to biotin starvation (Madsen *et al.* 2015). Increased mitochondrial acetylation is associated with biotin deficiency while the same condition induces accumulation of the deacetylase Homolog of Sir2 4 (Hst4) in the mitochondria (Madsen *et al.* 2015). This study included proteome-wide changes in acetylation following deletion of *SIR2, HST2,* and *HST4.* Based on their supplementary data, I found a set of three Rap1 residues that exhibited differential acetylation in response to deletion of one of these deacetylases (**figure A3.A**).

									Fold-change in acetylation abundance		
									hst2Δ	*hst4Δ*	*sir2Δ*
DNA repair and recombination protein RAD52	RAD52	NSSNK(1)DTDLK	1.00	246	0.00016	2	582.2806	0.47	1.05		2.57
DNA repair protein RAD7	RAD7	ISENISK(1)WQK	1.00	182	0.000188	2	637.8406	0.65		1.26	
RAT1-interacting protein	RAI1	LDLSSGFQK(1)FK	1.00	65	4.22E-15	2	656.3508	0.12	0.95	1.12	1.11
RAT1-interacting protein	RAI1		0.00	67	4.22E-15	2	656.3508				
DNA-binding protein RAP1	RAP1	VDQTEVEK(1)K	1.00	69	1.31E-05	2	559.2904	0.27	0.86	0.98	1.91
DNA-binding protein RAP1	RAP1	RLEYVYEVDK(1)FGK	1.00	423	0.000173	3	563.2945	0.46			
DNA-binding protein RAP1	RAP1		0.00	70	1.31E-05	2	559.2904				
Ras-like protein 2	RAS2	SDLENEK(1)QVSYQDGLNI	1.00	131	0.00196	3	743.011	-1.05		1.83	
5'-3' exoribonuclease 2	RAT1	QQSDK(1)NNELMK	1.00	478	0.000916	2	696.8248	0.13	1.29	1.31	3.27
5'-3' exoribonuclease 2	RAT1	HRLEK(1)DNEEEEIAK	1.00	522	2.29E-210	3	594.627	-0.08	1.12	1.21	2.28
5'-3' exoribonuclease 2	RAT1	NNELMK(1)DISK	1.00	484	2.49E-07	2	625.3083	-0.34	0.62	1.16	3.42

Figure A3.A: Sites of differential acetylation in each deletion background. Fold-change is calculated relative to wild-type. These data are adapted from Supplementary Data 4 in (Madsen *et al.* 2015).

Encouraged by the near 2-fold increase in Rap1 acetylation in the absence of Sir2, I took a similar approach to Gavin and made K-to-Q and K-to-R mutations at Rap1 residues 69/70 and 423. I then analyzed silencing stability in a CRASH background. On first-pass, it appeared that introduction of neither the acetyl-mimic nor the non-acetylatable residues robustly affected silencing stability (**figure A3.B**). In a few representative colonies, I found increased sectoring indicative of increased loss-of-silencing events. Unfortunately, introduction of these mutations led to scalloping of the colonies indicating viability defects. Scalloping like this is analogous to sectors of death rather than loss-of-silencing events and indicative of potential genome instability.

Alternatively, it is possible that modification of these residues shifted Rap1 interactions in a way that promoted its action as a repressor rather than as an activator. If this were the case, the increased scalloping would suggest that modifying these residues induced Rap1-mediated repression of essential genes. If that were the case, however, I would expect the acetyl-mimic and un-acetylatable mutations to behave in opposite ways. On the other hand, since the colonies had non-canonical morphologies, I could not confidently say whether the sectors that were missing would have been un-silenced or not. Thus, I was unable to rigorously deconvolute the results.

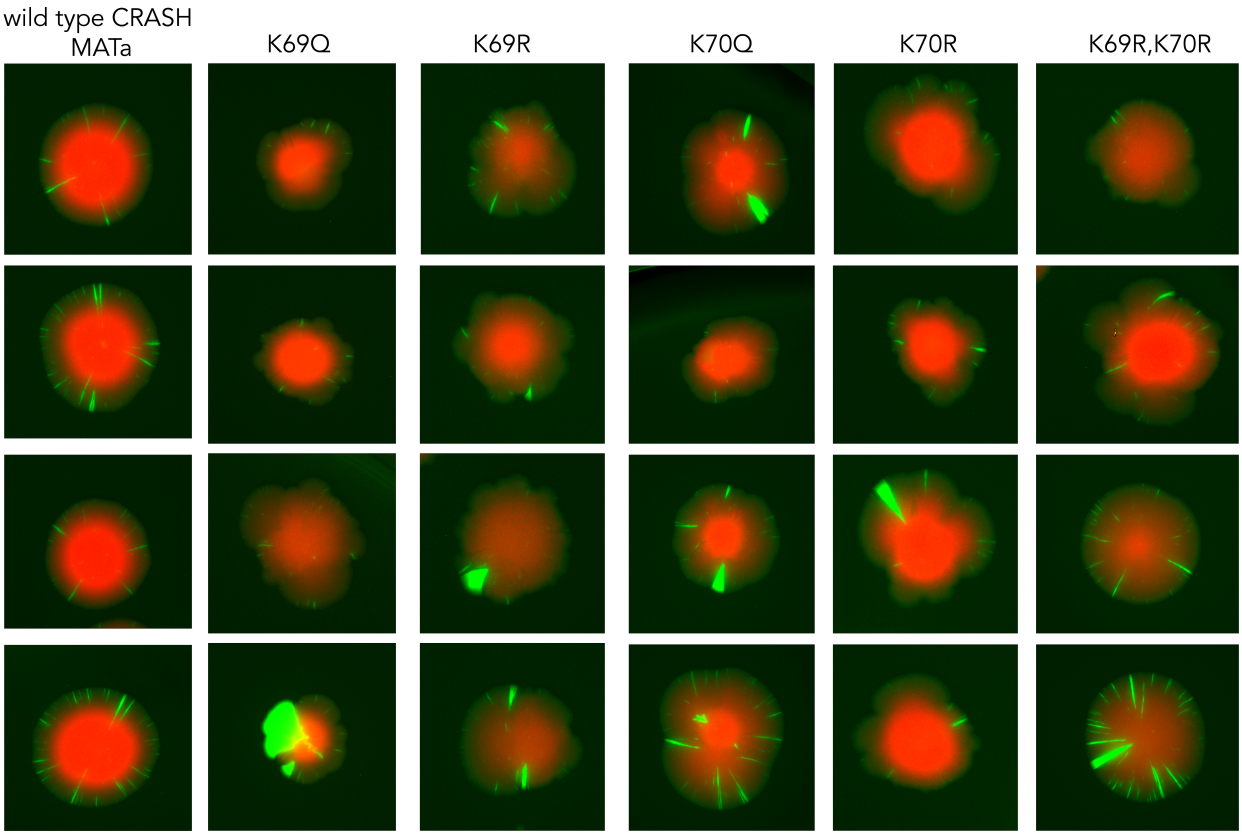

Figure A3.B: Representative CRASH colony images for various acetyl-mimic and non-acetylatable residues of Rap1.

A4: Structure-informed investigation of steric occlusion of transcription machinery from Rap1's activation domain in the presence of Sir proteins.

In Chapter 2, I dissected the context-dependent function of Rap1 at *HML* and tested multiple models of Sir-based silencing. It has continued to irk me that while I narrowed down the mechanism to somewhere between "Rap1 binds" and "pre-initiation machinery is occluded" I have no clear mechanism of the differentiation between the two. To try to understand better how this might be occurring, I used ColabFold (Mirdita *et al.* 2022), a multimer structure prediction model from based on AlphaFold (Jumper *et al.* 2021). This program allows you to feed in amino acid sequences of multiple proteins and predicts their structures as a complex. Early genetic studies of the Rap1 C-terminal domain identify regions important for interaction with Sir3 and Sir4 (Moretti and Shore 2001). This paper identifies the C-terminus of Sir3 to interact with Rap1. I began by looking at the predicted structure of a Rap1-Sir3 complex (**figure A4.A**). As both proteins are quite large, and the N-terminus of Rap1 is largely unstructured, I trimmed the Rap1 protein sequence that I was using to exclude the first 329 amino acids. For the same reason, I focused only on amino acids 356-978 of Sir3.

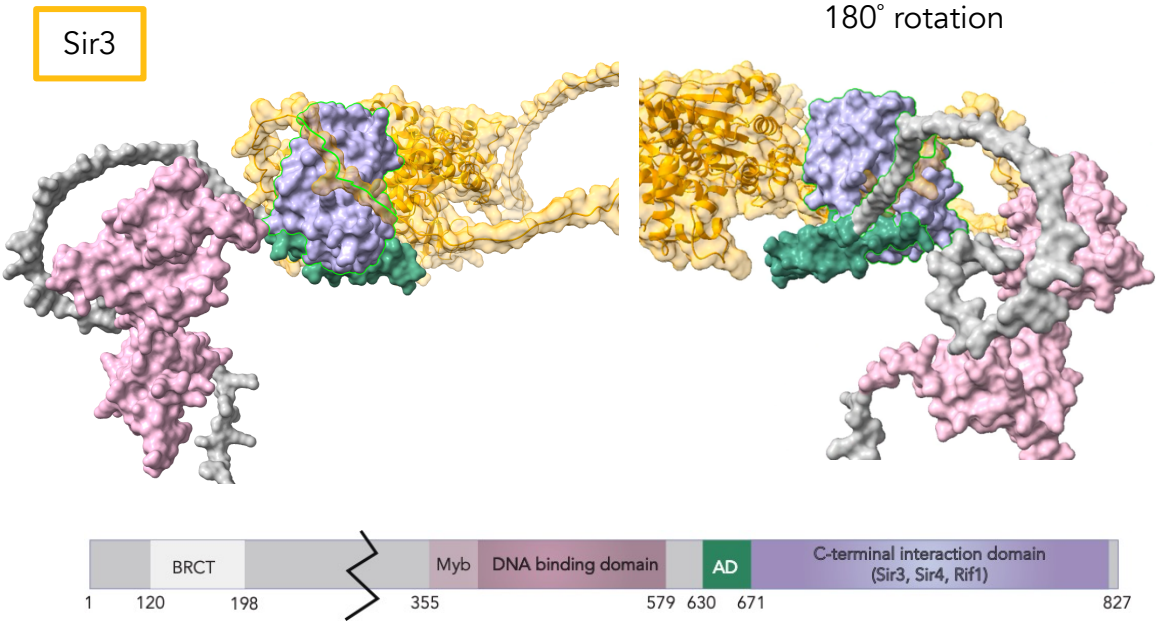

Figure A4.A: ColabFold multimer prediction using Rap1 amino acids 330-827 and Sir3 amino acids 356-978. Cartoon below models color codes domains of Rap1 as they appear in the predicted structure. Sir3 protein is indicated in yellow. The image on the right is a 180˚ rotated view of the structure on the left.

Based on this predicted structure, I can see that, while the Rap1 C-terminus is the domain most closely in contact with Sir3, interactions between these two proteins appear to bring the CTD into a conformation where the Activation Domain (AD) is occluded by both Sir3 and the Rap1 CTD. Notably, this prediction does not take into account the presence of the rest of the Sir complex, so it is possible that when in complex with Sir2 and Sir4, the Rap1 AD is even further occluded.

The activation domain of Rap1 is known to interact with multiple TFIID subunits (Garbett *et al.* 2007). Using the same multimer prediction algorithm, I looked at the interactions between the portion of Taf12 identified as binding Rap1 which included amino acids 130-530. TFIID is a 15-subunit complex, so looking at just one Rap1 interaction partner is obviously a simplistic view. However, the predicted structure reveals a clear interaction between Taf12 and the Rap1 AD (figure A4.B). Keeping the large DNA-binding domain in approximately the same position for reference, I find speculative evidence for a competitive interaction between Sir proteins and TFIID for the Rap1 activation domain. In Chapter 2, I show that recruitment of Rap1 to the promoter of *HML* in *SIR* cells is not accidental but is instead an active participant in stabilizing the silent domain (figure 2.2). If these predicted models were correct, they imply that Sir-based silencing acts not at the level of protein occlusion (as I showed to be the case), but that specifically the interaction between the Rap1 CTD and Sir proteins induces a conformational change that occludes transcription machinery from the Rap1 activation domain.

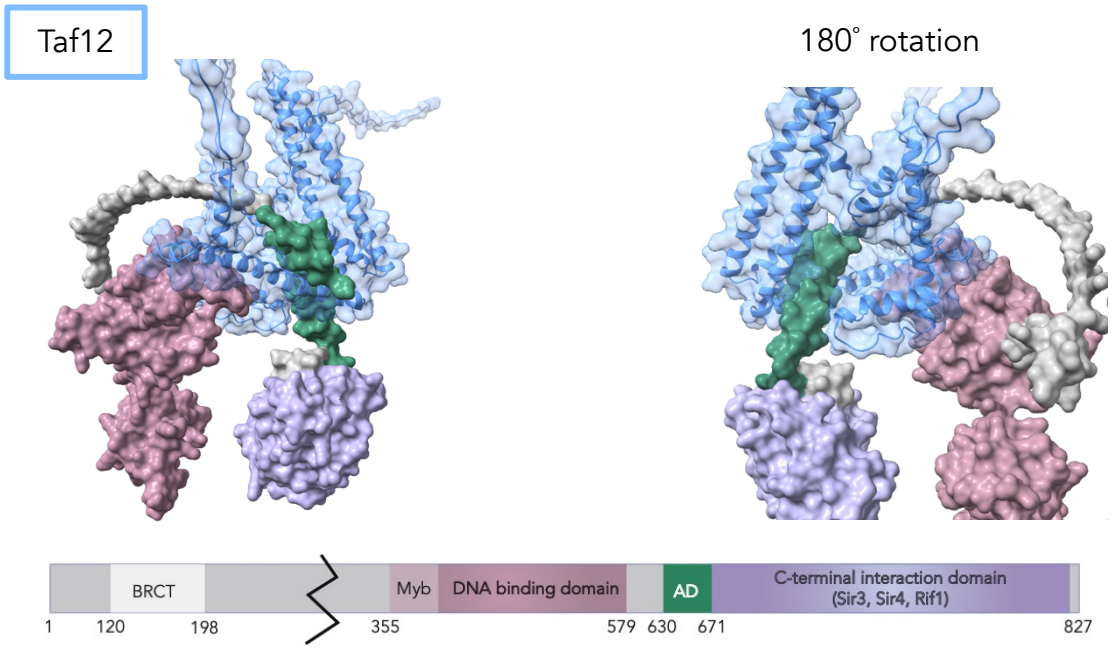

Figure A4.B: ColabFold predicted structure of the Rap1-Taf12 complex using amino acids 330-827 of Rap1 and amino acids 130-540 of Taf12. Cartoon below models color codes domains of Rap1 as they appear in the predicted structure. Taf12 protein is indicated in blue. The image on the right is a 180˚ rotated view of the structure on the left.

As I mentioned at the beginning of this appendix, multiple genome-wide mass spectrometry studies reveal at least 13 sites of potential phosphorylation on Rap1 (**figure A1**) (Albuquerque *et al.* 2008; Holt *et al.* 2009; Lanz *et al.* 2021) including three in or near the C-terminal domain: S594/S660/S731. In the intervening time, a few more residues near the Activation Domain and C-terminal interaction domain of Rap1 have been identified as potentially phosphorylated: S655 and S658. If we zoom in on those residues

in the predicted Sir3-Rap1 structure, there are H-bonds between S658 and the Sir3 interaction domain (**figure A4.C**). While these interactions do not appear to be of particularly high-affinity, I am encouraged by this finding, especially considering that this prediction does not consider any of the other components of the Sir complex. Furthermore, S658 is interacting with a positively charged lysine residue on Sir3. If these serines were in fact phosphorylated, it's possible the negative charge of the modification would increase the affinity of the interaction between the two proteins. To further investigate this possibility, I've optimized a co-IP for differentially tagged Rap1 and Sir3 proteins. Both proteins have large unstructured domains which made capturing the interaction more difficult. I am also integrating the S-to-A and S-to-D mutations into the endogenous Rap1 locus and will monitor the cells for silencing by CRASH and RT-qPCR. In the most ideal setting, introduction of the S-to-D mutations will increase the affinity between Rap1 and Sir3, while the S-to-A mutations would decrease interactions, and I will be able to quantify those changes by densitometry of the co-IP. For comparison I will be doing the same experiment for Rap1 interacting with a TFIID subunit and would expect to see the opposite shift in affinities; if I've increased interactions between Rap1 and Sir proteins my hypothesis would predict that the Rap1 activation domain would more often be occluded when phosphorylated at these residues, while decreasing the likelihood of that interaction by introducing un-phosphorylatable alanines would increase the frequency of interactions with transcription machinery. In support of my hypothesis, I re-ran the ColabFold multimer predictor substituting aspartic acids for serines at residues 655,658, and 660 (S655D/S658D/S660D) (**figure A4.D**). Adding in an analysis of electrostatic potential to the predicted structure of Sir3, I can see that the Sir3 domain predicted to interact with these phosphorylated residues of Rap1 is particularly basic which supports the hypothesis that phosphorylation of Rap1 S655/S658/S660 would increase affinity between the two proteins. While all of this is speculative at the moment, I am excited by the prospect of zeroing in on a mechanism differentiating the two functions of Rap1.

Pioneer-type proteins bind pervasively in the genomes of multicellular eukaryotes and are implicated in restructuring the chromatin landscape during periods of rapid developmental flux. Generally, this is thought to occur through their maintenance of regions of open chromatin and preferential recruitment of certain cofactors (reviewed in Larson *et al.* 2021). Rap1 and Abf1, which share many of the same hallmarks as pioneer factors, could act in a similar fashion. In the case of the single celled organism, however, this dynamic reprogramming of gene expression patterns would be in response to environmental stimuli. Perhaps the reason general regulatory factors exhibit such dichotomous functions and prevalent binding genome-wide is to prime the cell for rapid adaptation via their differential modification and ensuing switch in function based on external cues.

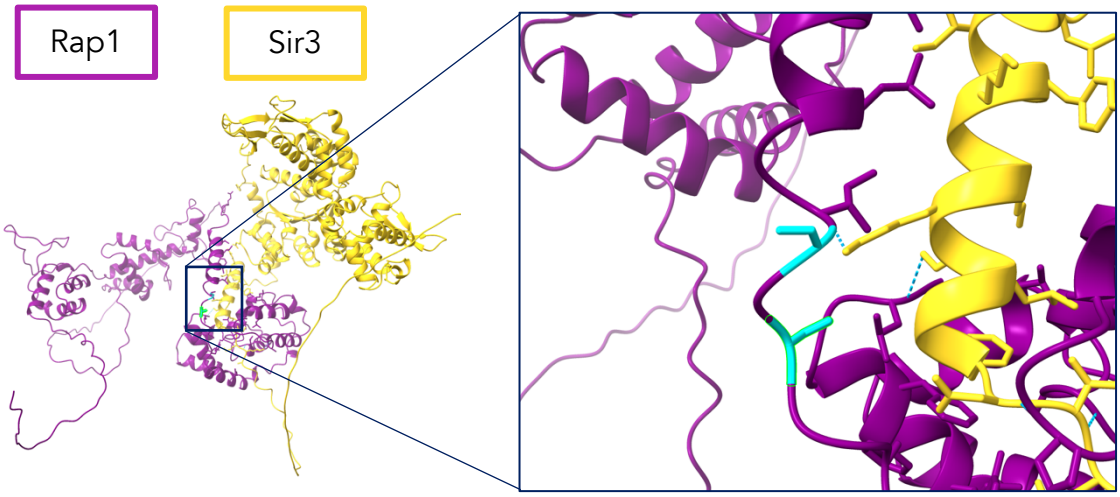

Figure A4.C: Highlighting the potential interactions in a Colab-fold predicted structure of the Rap1-Sir3 complex. Inset shows hydrogen bonds between potentially phosphorylated residue Rap1-S658 and Sir3-K470 (dotted lines). Rap1 S658 and S660 are highlighted in teal.

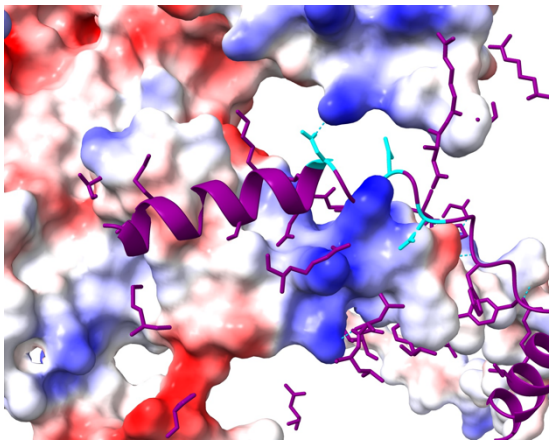

Figure A4.D: Electrostatic potential projection of Sir3 predicted structure with Rap1. Rap1 S655D/S658D/S660D are in teal. The Rap1 AD is the purple helix.